Design and Development of a Phosphoric Acid Fuel Cell

Thapelo Pholo

20214146

A dissertation submitted in fulfillment of the requirements for the Magister Technologiae: Engineering: Electrical

Department: Applied Electronics and Electronic Communication

Faculty of Engineering and Technology

Vaal University of Technology

Vanderbijlpark

Supervisor: Prof HCvZ Pienaar

Date: June 2008

Declaration

I, Thapelo Pholo, hereby declare that the following research information is solely my own work. This is submitted for the requirements of the Magister Technologiae: Engineering: Electrical to the Department of Applied Electronics and Electronic Communication at the Vaal University of Technology, Vanderbijlpark. This work has not previously been accepted in substance for any degree and is not being concurrently submitted in candidature for any degree.

Signed ……..

Date ……..

Acknowledgements

I wish to express my sincere gratitude to the following individuals and institutions that facilitated this research and enabled this document to be completed successfully:

- Prof HCvZ Pienaar

  Your encouragement, contribution and guidance helped me in this new endeavour on Fuel Cells which were previously unknown to me. You generated interest and discipline in me. Your wisdom helped me to rise above and to become a better person.

- Dr JF Janse van Rensburg for his contribution and always encouraging me to surge forward even when the chips were down.

- Personnel of the Department of Applied Electronics and Electronic Communication for support and encouragement.

- Telkom South Africa Ltd, Telkom Centre of Excellence, TFMC Pty Ltd, M-TEC and THRIP.

- Mr J du Toit

- Mr M Rugaju, a fellow student

Dedication

Life is this simple:
We are living in a transparent world,
And God shines through in every moment.
This is not just a fable or a nice story;
It is living truth.

If we remember God, abandon ourselves to God,
And forget ourselves,
We may see this truth:
God manifests everywhere, in everything.
We cannot be without God.
It's impossible.
It's simply impossible.

Thomas Merton

This dissertation is dedicated to the memory of my late father who often said and taught me that: ***'Success is sweet, but it usually has the scent of sweat about it'.***

- *My Mother and family for being my pillar of strength.*

- *To M'e M'atsepo (may her soul rest in peace) and the Sefeane family for giving me courage, will to succeed and showing me the meaning of life and education.*

- *Madibe for always being by my side.*

Abstract

Fuel cells are electrochemical devices that convert chemical energy of a fuel cell into electricity at high efficiency without combustion. They are viewed as viable power sources for many applications including automobiles, distributed power generation and portable electronics. This dissertation presents the design and development of a phosphoric acid fuel cell. It deals with the experimental studies on phosphoric acid fuel cells and possible integration in replacing the conventional sources of electrical energy in stand-by power supply systems, particularly for use in the telecommunications industry. The design of a DC-DC converter system is also incorporated into the system.

The first objective was to establish performance parameters and past studies on phosphoric acid fuel cells and this research revealed that parameters that affect the system's performance include: reactant gas pressures, mass flow rates as well as the operating temperature. Mathematical models in the literature were studied and verified against the simulation models acquired.

The second objective was to design and assemble a single cell in order to analyze the cell's performances as well as the operating parameters in order to obtain a model for predicting and simulating the performance of larger fuel cell stacks.

The next objective was to analyse from a set of design equations and construct a small DC-DC converter. The converter was used to boost a small fuel cell voltage and regulate it at a higher voltage level.

Finally, the performance characteristics of the developed fuel cell, mathematical and simulation models were evaluated and compared. Simulation results for the models and the converter showing a regulated output voltage are presented. Some recommendations for improved system performance and for further studies are suggested.

TABLE OF CONTENTS

List of figures

List of Tables

Annexures

Glossary of abbreviations and symbols

A

A - Amperes

α - Charge transfer coefficient

AC - Alternating current

AFC - Alkaline fuel cell

B

β - Transistor current gain

BJT - Bipolar junction transistor

BP - Bipolar plate

C

° C - Degrees Celsius

C - Coulomb

C - Carbon

cm - Centimetre

D

ΔG_f - Change in Gibbs free energy of formation

Δg_f - Per mole change in Gibbs free energy of formation

ΔV_{act} - Activation loss

ΔV_{omic} - Ohmic loss

ΔV_{trans} - Mass transfer loss

DC - Direct current

DG - Distributed generation

DMFC - Digital mass flow controller

DMFM - Digital mass flow meter

E

E - Theoretical fuel cell electromotive force

E_{OC} - Practical fuel cell open circuit voltage

EMF - Electromotive force

F

F - Farad

F - Faraday's constant, 96 485 Coulombs

FC - Fuel cell

G

G_f - Gibbs free energy of formation

GDE - Gas diffusion electrode

GDL - Gas diffusion layer

H

H - Henry

H - Hydrogen atom

H^+- Hydrogen proton

H_2 - Hydrogen molecule

H_2O - Water

I

i - Fuel cell stack output current density

i_o - Exchange current density

I_D - Current through a diode

I_O - Fuel cell stack output current

I_S - Saturation current of a transistor

I_{SD} - Saturation current of a diode

ICE - Internal combustion engine

J

J - Joule

K

K - Boltzmann's constant, 1.38 x 10^{-23} $J.K^{-1}$

K - Kelvin

KW - Kilowatts

L

λ - Flow stoichiometry

M

m - Mass transfer overvoltage constant

m - Metre

m - Milli, 10^{-3}

mA - Milliamps

mm - Millimetre

MEA - Membrane electrode assembly

MOSFET - Metal-oxide semiconductor field effect transistor

Mol - Mole

N

η - Efficiency

n - Mass transfer overvoltage coefficient

N - Avogadro's number, 6.022×10^{23}

N - Newton

N_C - Number of cells in a fuel cell stack

NASA - National Aeronautical and Space Administration

O

Ω - Ohm

O - Oxygen

-OH- Hydroxyl ions

P

P_1, P_2 - Pressure

P_{H2} - Hydrogen pressure

P_{H2O} - Water pressure

P_{O2} - Oxygen pressure

PAFC - Phosphoric acid fuel cell

PEM - Proton exchange membrane

PTFE - Polytetrafluoroethelyne

PWM - Pulse-width modulation

Q

q - Charge of an electron, 1.062×10^{-19}

R

R - Resistance

R_D - Ohmic resistance of a diode

r - Area specific resistance

S

S - Second

SLMP - Standard litres per minute

T

T - Temperature

t_{OFF} - Off-time of a switch

t_{ON} - On-time of a switch

U

μ - Micro, 10^{-6}

V

V - Volt

V_D - Voltage across a diode

V_{DC} - Direct current voltage

V_{IN} - Input voltage

V_O - Output voltage

V_{OUT} - Output voltage

V_S - Direct current source voltage

V_{STACK} - Output voltage of a fuel cell stack

V_T - Terminal voltage

W

W - Watt

XYZ

Definition of terms

Air: The mixture of oxygen, nitrogen and other gases which, with varying amounts of water vapour, forms the atmosphere of the earth.

Anion: A negatively charged ion; an ion that is attracted to the anode.

Anode: The electrode at which oxidation takes place. For fuel cells and other galvanic cells, the anode is the negative terminal; for electrolytic cells, the anode is the positive terminal.

Bipolar plates: Conductive plates in a fuel cell stack that act as an anode for one cell and a cathode for the adjacent cell.

Carbon: An atom and primary constituent of hydrocarbon fuels.

Catalyst: A chemical substance that increases the rate of a reaction by lowering the amount of energy needed to cause the reaction without itself being consumed.

Cathode: The electrode at which reduction occurs. For fuel cells and other galvanic cells, the cathode is the positive terminal; for electrolytic cells, the cathode is the negative terminal.

Cation: A positively charged ion.

Current collector: Term used to describe the conductive material in a fuel cell that collects electrons.

Electrode: A conductor through which electrons enter or leave an electrolyte.

Electrolysis: A process that uses electricity, passing through an electrolytic solution or other appropriate medium, to cause a reaction that breaks chemical bonds.

Electrolyte: A substance that conducts charged ions from one electrode to the other in a fuel cell, battery or electrolyser.

Electron: A stable atomic particle that has a negative charge.

Energy: The quantity of work a system or substance is capable of doing.

Enthalpy: measure of the heat content of a chemical or physical system; the enthalpy change is the amount of heat released or absorbed when a chemical reaction occurs at a constant pressure.

Entropy: The degree of randomness or disorder of a system on the molecular level.

Fuel: A material used to create heat or power through conversion in such processes as combustion or electrochemistry.

Fuel cell: A device that produces electricity through an electrochemical process, usually from hydrogen and oxygen.

Fuel cell stack: Individual fuel cells connected in series. Fuel cells are stacked to increase voltage.

Gas: Fuel gas, such as natural gas.

Gas diffusion: Mixing of two gases caused by random molecular motions.

Graphite: Mineral consisting of a form of carbon that is soft, black and lustrous and has a greasy feeling.

Greenhouse effect: Warming of the earth's atmosphere owing to gases in the atmosphere that allow solar radiation to reach the earth's atmosphere but do not allow the emitted infrared radiation to pass back out of the earth's atmosphere.

Hydrogen (H_2): Hydrogen (H) is the most abundant element in the universe but it is generally bonded to another element. Hydrogen gas (H_2) is a diatomic gas composed of hydrogen atoms and is colourless and odourless.

Hydrophobic: a property of a material that has aversion to water (repels water).

Internal combustion engine: An engine that converts the energy contained in a fuel inside the engine into motion by combusting the fuel.

Ion: Atom or molecule that carries a positive or negative charge because of the loss or gain of electrons.

Oxidant: A chemical, such as oxygen, that consumes electrons in an electrochemical reaction.

Oxidation: loss of one or more electrons by an atom, molecule or ion.

Oxygen (O_2): A diatomic colourless, tasteless, odourless gas that makes up about 21 percent of air.

Phosphoric acid fuel cell (PAFC): A type of fuel cell in which the electrolyte consists of concentrated phosphoric acid (H_3PO_4).

Proton: A sub - atomic particle in the nucleus of an atom that carries a positive electric charge and is not movable by electric means.

Reactant: A chemical substance that is present at the start of a chemical reaction.

Renewable energy: A form of energy which is never exhausted because it is renewed by nature.

Stoichiometry: The quantitative relationships between the amounts of reactants and products in a chemical reaction.

Chapter 1 Introduction

1.1 Background

As the global energy demands for electricity, heating and transportation increase, the sources of fossil fuels (oil, gas, coal) which have traditionally provided this energy are depleting. The conflicts over scarce fossil fuels such as oil and gas are anticipated to become more common, further jeopardising the security of supply. The global climate changes constantly and it is becoming warmer. Human activity is contributing to this warming causing an unnatural and dangerously rapid level of climatic change to occur (Archant 2004).

By burning fossil fuels, greenhouse gases such as carbon dioxide are released into the atmosphere where they contribute in causing the planet to warm-up like a greenhouse. This increase in heat energy is causing large changes in climatic patterns that are having increasingly adverse effects on the planet and human life (Archant 2004).

In order to mitigate the effects of climatic change, the level of greenhouse gases that humans release into the atmosphere must be reduced and hence the need to find an alternative to fossil fuels for energy and electricity production in order to reduce the negative effects of climatic change (Archant 2004). Renewable energy is energy from inexhaustible sources such as sun, wind and wave power.

Above all this, traditional methods of electricity generation are inherently inefficient. They burn fuel and air to generate a high temperature gas which, in turn, is expanded in a mechanical device like a cylinder or turbine to ultimately drive an electrical generator. For example, a coal-burning power plant transfers heat from this hot gas to boil high pressure water. Gasoline and diesel engines use the hot combustion gas itself at high pressure (ERDC 2007).

Fuel cells (FC) have emerged over the past decade as tantalizing alternatives to conventional power technologies because of their potential to reduce the

environmental impact and geopolitical consequences of the use of fossil fuels. The need for high efficiency, low emission energy conversion devices has attracted attention towards fuel cells the world over.

FCs are electrochemical devices where the chemical energy contained in hydrogen and oxygen is converted directly into electrical energy, water and heat. By definition it is an electrical cell, which unlike storage cells can be continuously fed with a fuel so that the electrical power output is sustained (Counihan 1981:63). Although they were invented some 160 years ago by a UK amateur scientist, Sir William Grove (Acres 2001:60), they have taken long to come to the forefront of energy and environmental considerations. This has arisen, not so much because their environmental attributes were not known or promoted, but more as a result of technical challenges to be met in developing a viable power system.

Competition from the internal combustion engines and steam turbines has been a factor. One other limitation has been the limited current that the FC could produce as a result of the small effective area of the electrodes (Mond and Langer 1889: as quoted by Acres 2001:60). Not until the work of Bacon, starting in 1933 (Adams *et al.* 1963:129) was a fuel cell developed with the capability of delivering power densities of 1000 $mAcm^{-2}$ at 0.8 V.

There are five different types of FCs and they can be classified according to the electrolyte they use and to the operational temperature, i.e. the temperature that is in the cell when they produce electricity. Among these various types, a phosphoric acid fuel cell (PAFC) operates at a relatively low working temperature (150 °C - 220 °C) owing to the higher ionic conductivity of liquid phosphoric acid (Feret 1990:59).

The PAFC is of the most commercially advanced fuel cell technology available. It is a widely used and well-documented type of fuel cell (Sammes *et al.* 2004:373). They use liquid phosphoric acid usually contained in a silicone carbide matrix as the electrolyte. They work at slightly higher temperatures than proton exchange membrane fuel cells or alkaline fuel cells.

The PAFC, at around 40 percent, is the least efficient of the FC varieties but it is still

more efficient than that of fossil power generation (20-25 percent) (Bell 2001:67). The PAFC does not generate poisonous carbon dioxide causing degradation of the cell, and reuses the heat produced by the electrode reactions (Ascoli *et al.* 1989:875).

In spite of the attractive aspects, a PAFC has shown some disadvantages such as high cathodic overpotentials and rapid degradation of cell performance.

1.2 Problem statement

There are several hurdles to be overcome before FCs can become a commercially viable technology on a large scale. Cost is one such factor. The required catalyst, membrane and cell hardware such as bipolar plates are expensive, resulting in a very high initial cost.

Attempts to enhance the performance of PAFCs have mainly been directed to electrodes, electrocatalysts and system engineering (Kordesch and Simader 1996:89). There is a need to increase the power density of the cell and to reduce costs, both of which are inextricably linked (Larminie and Dicks 2000:33).

The purpose of the research is to design and build a PAFC that will culminate in the development of a FC stack that will be able to power remote telecommunication sites and equipment while also being cost-effective. The output voltage of the FC will be boosted to a higher level according to the load if the need arises by a means of a DC-DC boost converter so that it can be at a desirable level ready to be used.

1.3 Methodology

The research included both the practical and theoretical study of the PAFC, the mathematical model, electrical equivalent circuits and the boost converter. The research was divided into four phases in order to have a systematic approach and output.

- The first phase consisted of the literature study of the PAFC, its characteristics, operation and design.

- The second phase consisted of the theory of the general design and mathematical model of the PAFC. This is where the design parameters of the fuel cell system are dealt with systematically.

- The third phase dealt with the actual building and development of the FC hardware and accessories as well as the design and development of a DC-DC converter. This included the acquisition of proprietary materials like the electrolyte retaining matrix.

- The fourth and final stage of the research was the testing of the developed FC. The FC results were then compared with calculated values obtained from mathematical models and equivalent circuits and simulations. Then results, conclusions and recommendations were given.

1.4 Delimitations

The design and development of the PAFC focused only on a single cell i.e. not the stack design. However, certain calculations and extrapolations allowed for a 100 W load based on the proposed single cell. The research did not involve the construction of the electrolyte retaining matrix assembly as its manufacturing and materials are still proprietary.

1.5 Importance of the research

The main objective of this research was to design and develop a PAFC that could be used for telecommunication purposes as a reliable and efficient back-up power mostly for remote sites. Most of the remote telecommunications equipment have a power rating of 100 W.

The output of the research work would be the design principles and prototype for alternative power that could be beneficial to the telecommunications industry to power equipment especially on remote sites. This would also be beneficial for future

studies and as a test set for other students at the Telkom Centre of Excellence at the Vaal University of Technology.

1.6 Overview of the report

The report consists of five chapters relating to the design and development of a PAFC.

Chapter 1 contains an introduction with the background on the study of FCs, the need for the research, as well as the aims and values of the research. The methodology of the research study is outlined and the delimitations and approach are presented.

Chapter 2 starts with the introduction and discussion on the history of FCs, their advantages and disadvantages. The literature review, characteristics and operation of the PAFC follow directly afterwards. This chapter further discusses the FC thermodynamic and electrochemical equations. Losses occurring in the FC and the polarisation curve together with the various parameters affecting the FC behaviour are presented. The chapter concludes with the various components desired and layout for the development of the PAFC together with a discussion on the boost converter.

Chapter 3 deals with the actual design of a PAFC system. The equivalent electronic circuit, the mathematical models and computer simulations are dealt with in detail. The review of the system together with the boost converter concludes the chapter.

Chapter 4 is devoted to the explanation of the setup of the hardware of the PAFC. All the experimental work, analysis and measurements performed on the fuel cell and components are presented. The interaction between the various components and the software and hardware are explained. The operation of the FC and the results conclude the chapter.

In Chapter 5, conclusions are drawn, suggestions for further improvements are also presented and hence recommendations are made regarding the design.

1.7 Summary

This chapter presented the underlying factors and reasons that necessitated the execution of the research as well as its importance and relevance. The background has been provided and also the research methodology used in the research and the overview of the dissertation.

The theoretical study of PAFCs, characteristics, components, operation and modelling are discussed in Chapter 2 and is concluded with a discussion of the DC-DC converter.

Chapter 2 Fundamentals of a PAFC

2.1 Introduction

Although FCs would appear to be a new technology, the idea that reversing the electrolysis process should be possible by reacting hydrogen and oxygen to generate electricity was first recognized by Sir William Grove in 1839 (Grove 1839 14:127-130). Half a century later, in 1889, the first practical device using coal and air to accomplish this was built by Ludwig Mond and Charles Langer.

Francis Bacon developed what was perhaps the first successful FC device in 1932, with a hydrogen-oxygen cell using alkaline electrolyte and nickel electrodes. Since the 1960s, NASA has used FCs in the Apollo and the space shuttle missions to supply crews with electricity and water (Hoogers 2003:2-17).

In today's society there is an enormous demand for energy. Also, the electric utility is struggling to meet the expanding power demands. For these reasons, the application of fuel cell technologies may be one of the most important technological advancements of the next decades.

FCs are electrochemical devices that convert the chemical energy of a gaseous fuel directly into electricity and are widely regarded as a potential alternative to stationary and mobile power sources. They complement heat engines and reduce the over-dependence on fossil fuels and thus have significant environmental implications (Pukrushpan *et al.* 2005:1).

Electrochemical energy conversion is defined as a spontaneous reaction in an electrochemical reactor that consumes a fuel and an oxidant, and such reactions at the anode and cathode that generate electricity, heat and water (Srinivasan 2006:191). The direct conversion of chemical energy into electrical energy is facilitated by the electrode-electrolyte structure of the FC. One of the two electrodes (either anode or electrode) will produce the appropriate ions needed to pass through the electrolyte. These ions which can be thought of as free-moving are either positive

or negative and are attracted to the opposite electrode through the electrolyte to complete the process.

According to Supramaniam Srinivasan (2006: 199), in previous publications, there are as many classifications of FCs as types of fuel cells. The most common classification has been according to the operating temperature, the fuel used for direct utilization and the electrolyte in the FC. However, the most outstanding distinction is the type of electrolyte used. Furthermore, Pukrushpan *et al.* (2005:4) add that the differences in cell characteristics such as cell material, operating temperature and fuel diversity, make each type of FC suitable for different applications.

The essential difference between a FC and a battery is the continuous nature of the energy supply. The fuel and the oxidant are supplied continuously to a FC from an external source. In a battery, the fuel and oxidant are contained within; when the contained reactants have been consumed, the battery must be replaced or recharged (Linden 1984: 41-3). It can also be said that FCs are open systems with fuel and oxidant flowing through the cell, whereas batteries are typically closed systems containing a set amount of fuel and oxidant that is gradually consumed via a chemical reaction.

The PAFCs produced by UTC Fuel Cells were the world's first commercially available FC product (King and Ishikawa 1996:86). The PAFC although the least efficient of the FC varieties, it is still more efficient than the fossil fuel power generation (Bell 2001:12). An inorganic acid of concentrated phosphoric acid (H_3PO_4) is used as the electrolyte, hence the name of the FC. Interest in this system evolved in the mid 1960s because H_3PO_4 could be used in a concentrated form (above 85 percent) in a FC at intermediate temperatures of 150° to 200 °C (Srinivasan 2006:505).

According to Vielstich *et al.* (2003:297), PAFCs were selected over alkaline fuel cells for commercialization because of the ability of H_3PO_4 to reject carbon dioxide and were also selected over Nafion because of H_3PO_4 low cost and ease of water management. Vielstich further goes on to state that, in conjunction with the

development of PAFCs, considerable research was performed to improve performance, reduce cost and increase endurance.

The earliest PAFCs operated at about 80 °C, whereas the current cells operate at about 200 °C. The benefits of such an operating temperature are better electrode kinetics of oxygen reduction, lesser ohmic overpotential losses and higher carbon monoxide (CO) tolerance. This increase in temperature was accomplished by the improvement in the materials of construction used in the FC stack, for example with the evolution from fibreglass to silicon carbide as the matrix material (Vielstich *et al.* 2003:297).

FCs are not limited by the thermodynamic constraints by which typical heat-based combustion processes are limited. There are no thermal and/or mechanical energy conversions taking place throughout the whole cycle. They have a simple construction and have no moving parts, thus resulting in minimal noise production. A major advantage FCs have over internal combustion (IC) engines is that they do not create harmful emissions and hence they are environmentally friendly.

FCs are also very compact, allowing them to be placed in space-restricted areas. Another advantage that FCs have over other power sources is that FCs only require hydrogen and oxygen as energy sources. However, FCs have their disadvantages as well, owing to the difficulty of storage and distribution of hydrogen.

Hydrogen, particularly for use in FC application can be stored in various ways. It can be stored as a compressed gas, liquid, solid or combined with other chemicals. Larger quantities of hydrogen can be stored in natural gas fields, aquifers and salt domes. Automobiles and buses utilizing FCs store hydrogen on a relatively small scale as a compressed gas in stainless steel cylinders at a pressure of about 130-150 bars. Liquid hydrogen is stored cryogenically such as for space storage. Hydrogen is stored as a "solid" in metal hydrides. The application of metal hydrides as a source of hydrogen for portable FCs is the widely used medium nowadays (Srinivasan 2006:421).

To place the scope of the research described in this chapter into context, a brief desc-

tion of the operation of the PAFC together with its various components will firstly be presented. The discussion of electrochemical and thermodynamics principles of FCs will lead the characteristics of the output voltage as well as its underlying factors. The mathematical model, equivalent electronic circuit and the simulation will then be presented. The chapter will conclude with a discussion on the DC-DC converter which is used for the regulation and increase of the relatively low voltage of the FC.

2.2 Operation and thermodynamics of a PAFC

The basic operation of a PAFC is given below, but a more detailed description of each component is given in section 2.3. As shown from the basic schematic representation of a unit (single) cell in Figure 1, a PAFC is composed of two porous gas diffusion electrodes, a cathode, an anode and an electrolyte together with an external load. The active layer on both the porous electrodes contains high surface area platinum (Pt) particles which are finely dispersed and supported on high surface area carbon.

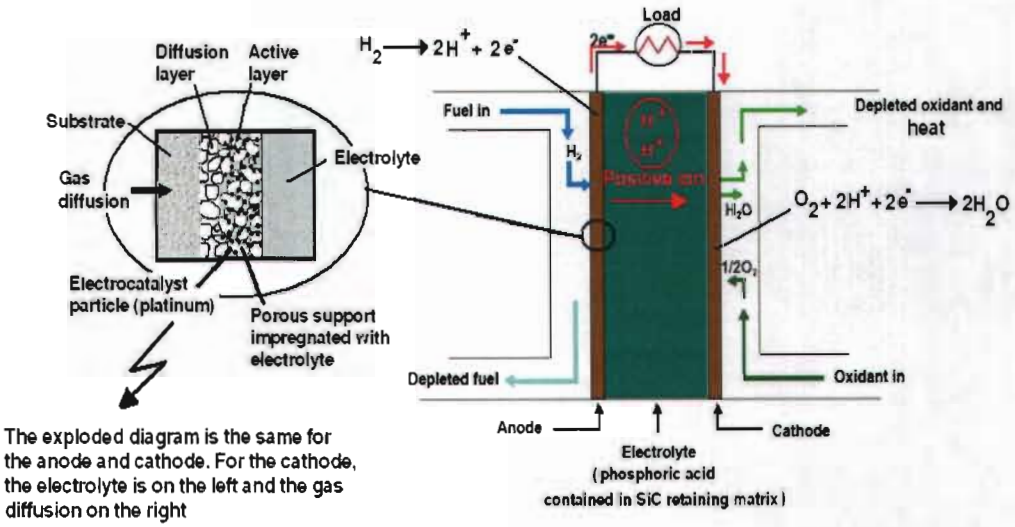

Figure 1 Operation of a unit fuel cell

The electronically insulated (i.e. one that does not conduct free electrons) electrolyte H_3PO_4 which is phosphoric acid, serves as the physical barrier preventing the fuel and oxidant gas streams from directly mixing and allowing only the appropriate ions

to move freely across. This requires that one of the reactant gases must be able to form the ionized specie needed to complete the process and form the primary by-product which is water.

The H_3PO_4 is contained in a retaining matrix (Silicon carbide, SiC) which provides most of the properties that are required by the matrix for retaining H_3PO_4 electrolyte. SiC is readily wettable and can be easily formed into a matrix when filled with the electrolyte. The retaining matrix is shown in Figure 22 on page 46.

In a PAFC, two half cell reactions take place simultaneously, an oxidation reaction at the anode and a reduction reaction at the cathode. Both the reactions make up the oxidation-reduction (redox) reaction of the FC and the formation of water from hydrogen and oxygen gases.

The FC processes can be described in three stages as shown in Figure 2 and Figure 3 respectively. The first two stages discuss the chemical reactions at both the electrodes and the third explains the ion conduction through the electrolyte. The fuel and oxidant are supplied to the anode and cathode, respectively. The stages are as follows:

At the anode:

Hydrogen is oxidised according to the equation:

$$2H_2 \rightarrow 4H^+ + 4e^- \qquad (2.1)$$

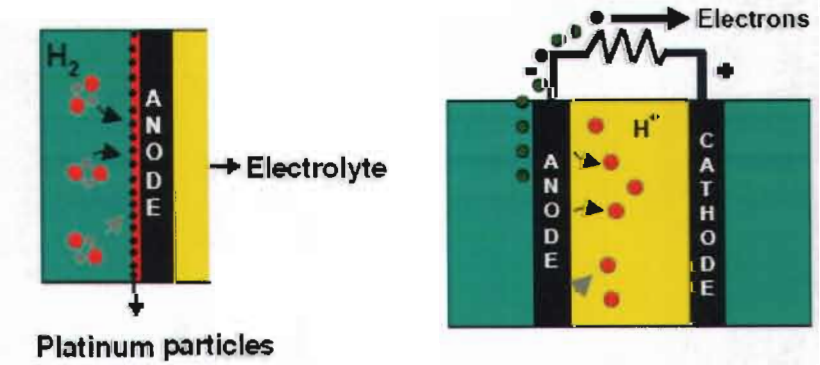

Figure 2 Fuel cell process (anode)

The H_2 is supplied to the anode side where ionization occurs and releases electrons and H^+ ions. The Pt surface helps in forming the weak H-Pt bonds. Each adsorbed hydrogen molecule ionizes into four H_2 protons (H^+) and four electrons (e^-). The electrons are then forced to flow from the anode through an external load before re-entering the FC into the cathode (it is this flow of electrons that is referred to as electrical current).

The remaining hydrogen proton bonds with a water molecule on the membrane surface, forming a hydronium ion (H_3O^+). The H_3O^+ travels through the electrolyte material to the cathode and leaves the Pt catalyst site free for the next hydrogen molecule.

At the cathode:

The reduction reaction is given by:

$$O_2 + 4H^+ + 4e^- \rightarrow 2H_2O \qquad (2.2)$$

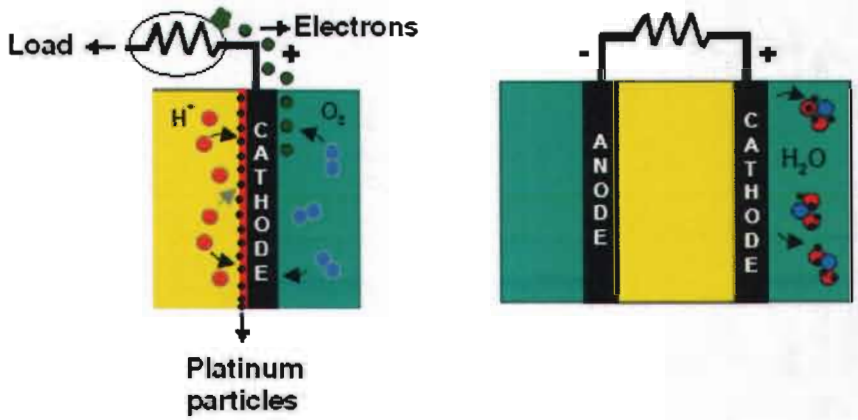

Figure 3 Fuel cell process (cathode)

At this electrode, oxygen molecules diffuse through and come into contact with a Pt catalyst on the electrode surface. The catalytic surface on the active layer of the cathode facilitates the separation of the adsorbed oxygen molecule. After breaking apart, the oxygen molecules bond to the Pt surface and form a weak O-Pt bond, enabling the reduction to proceed. Each oxygen atom then leaves the Pt catalyst site, combining with two electrons (which have travelled through the load) and two

protons (which have travelled through the H_3PO_4 electrolyte) to form one molecule of water. The redox reaction has now been completed. The Pt catalyst on the cathode electrode is again free for the next oxygen molecule.

As earlier mentioned, the only by-products of the FC are water and heat generated by the chemical reaction. The overall reaction of a hydrogen-oxygen FC can be given by:

$$2H_2+O_2 \rightarrow 2H_2O \tag{2.3}$$

The reaction can also be simplified to its equivalent form by:

$$H_2+\frac{1}{2}O_2 \rightarrow H_2O \tag{2.4}$$

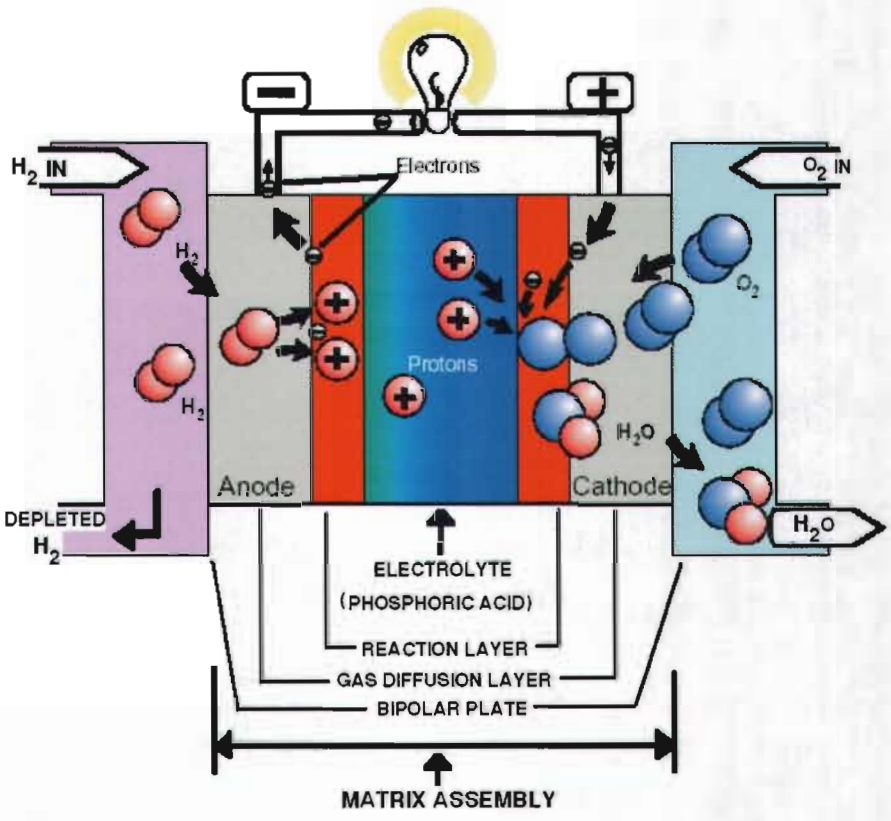

Figure 4 Structure of a PAFC unit stack

The operation of the FC is also shown in Figure 4. In a PAFC the gas diffusion layers, reaction layer, electrolyte retaining matrix and electrodes are all incorporated into one layer known as the matrix assembly. However, owing to the liquid electrolyte, SiC has two separate structures that are put together after being soaked with the electrolyte.

Electrical energy is only obtained from a FC when a reasonable current is drawn. In many electrical power-generating devices, energy conversions to electricity are very clear. However, the energy conversion from chemical inputs and outputs is not as clear. When dealing with chemical energy, the Gibbs free energy and enthalpy are often used. The chemical energy of hydrogen, oxygen and water is considered in calculating the theoretical output voltage of a FC.

The chemical energy of the FC is defined by the enthalpy of formation and Gibbs free energy. Gibbs free energy is defined as the energy available to do external work which involves moving electrons around an external circuit. Enthalpy of formation is the sum of Gibbs free energy and the energy connected with entropy. In FCs, change in Gibbs free energy of formation (ΔG_f) is considered, as this change is responsible for the energy released. This change is the difference between the free energy of the products and the reactants, as shown in equation (2.5) (Larminie and Dicks 2003: 25-29).

$$\Delta G_f = G_f \text{ products} - G_f \text{ reactants} \tag{2.5}$$

Where:

$G_f \equiv$ Gibbs free energy of formation in Joules

These quantities can be expressed in their 'per mole' form to make the comparisons easier. They are indicated by $^-$ over the lower case letter ($\bar{g}_f$) which is given by equation (2.6) below (Larminie and Dicks 2003: 25-29).

$$\Delta \bar{g}_f = \bar{g}_f \text{ products} - \bar{g}_f \text{ reactants} \tag{2.6}$$

Considering the basic reaction for the hydrogen-oxygen FC:

$$H_2 + \frac{1}{2}O_2 \rightarrow H_2O \tag{2.7}$$

The product is one mole of H_2O and the reactants are one mole of H_2 and half a mole of O_2. Thus,

$$\Delta \bar{g}_f = \left(\bar{g}_f\right)_{H_2O} - \left(\bar{g}_f\right)_{H_2} - \frac{1}{2}\left(\bar{g}_f\right)O_2 \tag{2.8}$$

Equation (2.8) above seems straightforward and simple. However, the Gibbs free energy of formation is not constant and changes with temperature and the state of the reactants and products (liquid or gas). If there are no losses in the FC, then all the Gibbs free energy is converted into electrical energy.

For the hydrogen-oxygen fuel cell, the two electrons pass through the external circuit for each water molecule produced and each molecule of hydrogen used, as given in equation (2.1). In a lossless system, electrical work done is equal to the change in Gibbs free energy. Furthermore, electrical work done to move a charge of 2 F for a voltage of E is given by:

$$\text{Electrical work done} = -2FE \quad \text{joules} \tag{2.9}$$

Thus E can be written as shown below in equation (2.10). This fundamental equation gives the open circuit voltage of the FC (Larminie and Dicks 2003: 25-29).

$$E = \frac{-\Delta \bar{g}_f}{2F} \quad V \tag{2.10}$$

Where:

F ≡ Faraday constant (96 485 Coulombs)

The following table shows $\Delta \bar{g}_f$ for the basic hydrogen FC reaction as in equation (2.10).

Table 1. $\Delta \bar{g}_f$ for the reaction $H_2 + \frac{1}{2}O_2 \rightarrow H_2O$ at various temperatures.

FORM OF WATER PRODUCT	TEMPERATURE (°C)	$\Delta \bar{g}_f$ (KJ mol^{-1})
Liquid	25	-237.2
Liquid	80	-228.2
Gas	80	-226.1
Gas	100	-225.2
Gas	200	-220.4
Gas	400	-210.3
Gas	600	-199.6
Gas	800	-188.6
Gas	1000	-177.4

From Table 1 and Table 2, it is evident that a decrease in $\Delta \bar{g}_f$ results in an increase in temperature and hence a decrease in cell voltage. However, at higher temperatures voltage losses are less, resulting in higher cell voltages (Larminie and Dicks 2003: 33).

Table 2 $\Delta \bar{g}_f$, maximum EMF, and efficiency limit (HHV basis)

FORM OF WATER PRODUCT	TEMP (°C)	$\Delta \bar{g}_f$, KJ mol^{-1}	MAX EMF V	EFFICIENCY LIMIT %
Liquid	25	-237.2	1.23	83
Liquid	80	-228.2	1.18	80
Gas	100	-225.2	1.17	79
Gas	200	-220.4	1.14	77
Gas	400	-210.3	1.09	74
Gas	600	-199.6	1.04	70
Gas	800	-188.6	0.98	66
Gas	1000	-177.4	0.92	62

Substituting the standard condition values for hydrogen and oxygen in equation (2.10), gives:

$$E = \frac{-\Delta \bar{g}_f}{2F}$$

$$E = \frac{-\left(-237.2\times10^{3}\right)}{2(96\,485)} \text{ at } 25\ ^{\circ}\text{C}.$$

$$= 1.229\ \text{V}$$

For example, a PAFC operating at 200 °C has $\Delta \bar{g}_f$ = -220.4 KJ, so

$$E = \frac{-\left(-220.4\times10^{3}\right)}{2\times(96\,485)}$$

$$= 1.14\ \text{V}$$

The open circuit voltage given above, assumes no irreversibilities, and assumes pure hydrogen and oxygen at standard temperature and pressure (25 °C and 100 KPa). However, in practice, this voltage would be lower than that because of the losses in voltage as is discussed in section 2.4. The output voltage of a single cell is typically 0.8 V. For a higher voltage value several cells can be connected in series to form a stack.

2.3 PAFC components

One of the main research tasks for FC researchers is the development and characterization of the functional materials in particular, concerning the development of low cost alternatives to commercially available components. In order to realize full commercialization, the cost of manufacturing should be minimised. As part of achieving this, a proper selection of materials for manufacturing should be made but without compromise to quality.

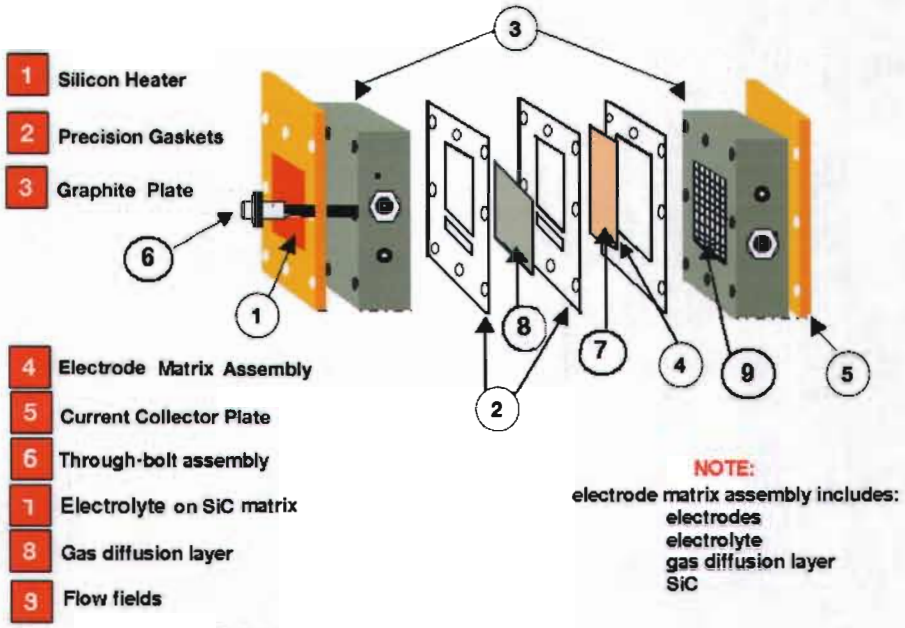

Figure 5 Components of a single fuel cell

The components of a single cell stack in a PAFC electrochemical cell stack are shown in Figure 5. The primary components of a PAFC are an ion conducting electrolyte, a cathode and an anode. The three are often referred to as a unit or single cell. These primary components in a FC also form part of the secondary components of the FC which are discussed below together with their associated functions. The components are listed below:

- Bipolar plate
- Gas diffusion layer and electrodes
- Electrolyte
- Gaskets

2.3.1 Bipolar plates (BP)

Much effort is being expended on the development of cost-effective materials for the bipolar plates. With respect to corrosion resistance, graphite materials are preferred. According to Steele *et al.* (2001:347), the conductivity of graphite materials is much

less than that of metallic materials. The flow fields in the FC design are usually made of graphite into which flow channels are conveniently machined.

According to Hoogers (2003:4-18), these plates have high electronic and good thermal conductivity and are stable in the chemical environment inside the FC. The gas flow fields are machined into the blank plates by a standard milling and engraving process. The flow fields or channels are used to distribute the reactant gases evenly over the entire membrane active surface area. Water management is one other function of the flow fields which assist in getting rid of excess water.

The graphite is easily machined but abrasive. The flow fields are several millimetres thick, mainly to give the mechanical strength and to allow the engraving of the flow channels (Hoogers 2003:4-18). In terms of FC stacks, the flow fields are machined on both sides so that the graphite block forms the anode and the cathode on either side and hence the term, bipolar plate. They are also used to serve as the electrical connection between adjacent cells in fuel cell stacks.

Flow field designs currently in the market and employed by leading stack developers are still proprietary. However, the patent literature gives hints as to what concepts are used (Hoogers 2003:4-19). Figure 6 shows the different flow channel designs mostly employed in FCs. The serpentine flow field described by Ballard researchers is shown in Figure 6(b) below. Hoogers goes on to say that, this design is believed to overcome the blockage of certain channels by product water because the differential pressure between the inlet and outlet forces stagnant water out of the channels.

The parallel gas channels as indicated in Figure 6(a), are a possibility when compression energy is needed to drive the reactants through the flow field structure. This design may lead to pressure imbalances between adjacent channels and gas blockages.

Figure 6(c), looks like a compromise between straight channels and a single serpentine flow field. This is interesting with regard to the materials and the integration of cooling within the bipolar plate.

Structures of the type shown in Figure 6(d) have channels which are no longer continuous, but the gas is forced to flow through some part of the diffusion layer. This design is known as the interdigitated flow structure.

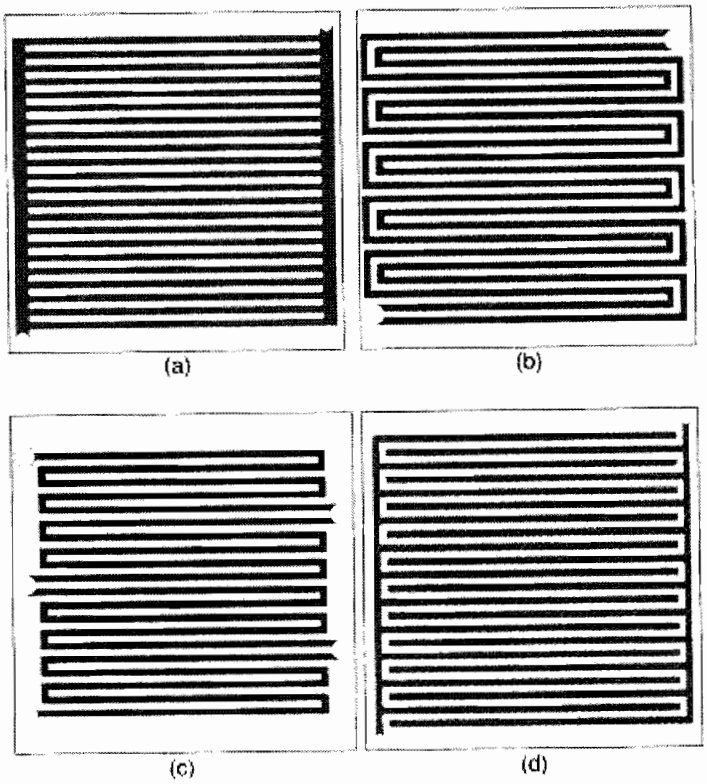

Figure 6 Different flow field designs (Hoogers 2003:4-19).

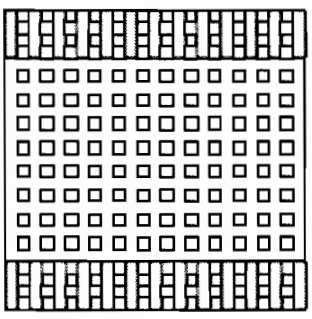

Figure 7 Column flow field pattern (Electrochem Inc.)

The design in Figure 7 is known as a column flow field and is made of squares which are generally known as landing areas. This design is able to tackle many problems encountered by other designs particularly for operation in the portable PAFC. This design has a low pressure drop from inlet to outlet resulting in lower auxiliary power needed to drive the flow of reactants. Even though this results in lower auxiliary power, it helps in preventing the build-up of water in the reactive areas of the flow fields by continuously blowing out the product water through the outlet. This design also facilitates for general coverage of the active area by the reactant gases. The design considerations for the channels of this flow pattern are given in section 3.2.3 on page 48 and the flow pattern is also shown in Figure 25 on page 48.

Another strategy is to use metallic bipolar plates. The gaseous flow structure can be easily fabricated in thin metal foils by pressing, but only a few metals are sufficiently corrosion resistant in the acidic environment of the membrane. The most promising materials are stainless steels, as the other candidate metals such as titanium, niobium, tantalum and gold are too expensive (Steele *et al.* (2001:347).

Stainless steels can provide satisfactory performance for longer times. Furthermore, the steel is protected by a passive layer at the cathode side, but the anode side becomes contaminated by corrosion products. To avoid corrosion, a conductive coating can be applied to the metallic plates. Stacks with metallic bipolar plates have been developed by Nuvera and Siemens (Steele *et al.* (2001:349).

2.3.2 Gas diffusion layer (GDL) and electrodes

Modern fuel cell electrodes are gas diffusion electrodes (GDE) that consist of a gas-porous layer of high surface area catalyst, a gas-porous electrically conducting gas diffusion layer and an electrode substrate (Hoogers 2003:4-16). Electrodes for phosphoric acid fuel cells are generally porous gas diffusion electrodes to ensure the supply of the reactant gases to the active zones where the noble metal catalyst is in contact with the ionic and electronic conductor. The fabrication of gas diffusion electrodes (GDE) is an intricate procedure in which all details of the structure and preparation are important and is beyond the scope of this research.

The reason for this is that the function of the electrodes is far more than just catalyzing a reaction, which is carried out by the catalyst particles. It also protects the catalyst layer and helps with water management by removing the excess water away from the membrane (Larminie and Dicks 2003:72-73). The preferred catalyst is platinum on carbon. Carbon is bonded with polytetrafluoroethelyne (PTFE) to create the catalyst structure. According to Larminie and Dicks (2003:72), the carbon has the following functions:

- To disperse the platinum catalyst to ensure good utilization of the catalytic metal.
- To provide micropores in the electrode for maximum gas diffusion to the catalyst and electrode-electrolyte interface.
- To increase the electrical conductivity of the catalyst.

The porous gas diffusion electrode facilitates the contact between the three phases that are involved in the reaction. This is where the reacting gas, electrode and electrolyte touch each other. According to Weidlich (1989:15), in a porous electrode only the pores where the capillary force and gas pressure are balanced contribute towards the generation of electricity. In order to convert as much gas as possible, the porous electrodes are formed into double layer electrodes, whereby the upper layer with its fine pores is facing towards the electrolyte and the large pored working layer faces the side with the gas. Figure 8 refers.

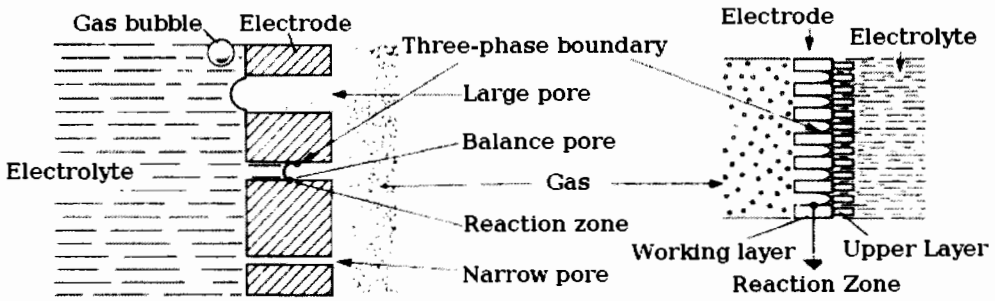

Figure 8 Porous electrodes with large and smaller pores (Weidlich 1989:15)

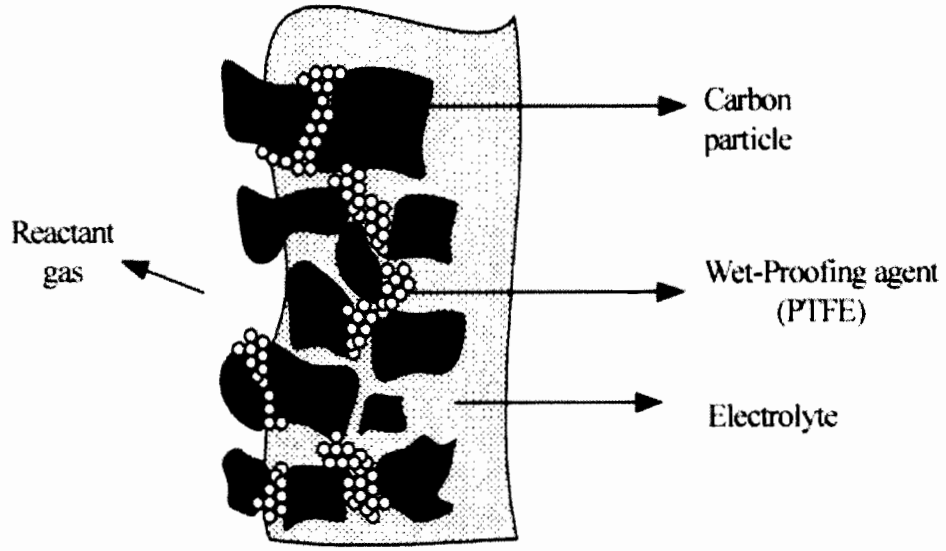

Figure 9 Two-phase hydrophobic GDL (Kordesch and Simader 1996:39)

Figure 9 shows the action of PTFE particles filling the spaces that would have been filled by water through to catalyst sides. As exemplified in Figure 8, the available pores are narrow, allowing only gas molecules through to the catalyst reaction sites.

2.3.3 Electrolyte

The electrolyte permits only the appropriate ions to pass which in this case are positive hydrogen ions. This is why it is mostly referred to as a proton conductor. H_3PO_4 is used as the electrolyte because it is the only inorganic acid that exhibits the required thermal stability, chemical and electrochemical stability and low enough volatility to be effectively used (Larminie and Dicks, 2003:177). H_3PO_4 does not react with CO_2 to form carbonate ions as is the case with alkaline fuel cells; therefore carbonate formation is not a problem with phosphoric acid fuel cells.

Note: The electrolyte does not react with the ions.

The H_3PO_4 is uniquely contained in a SiC particle matrix using capillary action. The electrolyte, since it is in a liquid form, is soaked in a matrix so that it can be contained in the FC. The silicon carbide matrix which holds the electrolyte is

produced with particles approximately 1 micron in size allowing the matrix to be about 0.1-0.2 mm thick (Larminie and Dicks, 2003:178). This thickness allows considerably lower ohmic losses. The structural matrix is thick enough to prevent cross-over of the reactant gases from the anode to the cathode. The SiC matrix has no effect on the chemical reactions of the FC.

In PAFC, the acid serves as the ionic electrolyte as well as the solvent. The ionization reaction of the acid is represented by the equation (Srinivasan 2006:504):

$$H_3PO_4 \rightarrow H^+ + H_2PO_4^- \qquad (2.11)$$

Srinivasan goes on to say that the specific conductivity of the H_3SO_4 is quite low at temperatures less than 100 °C and in order to operate a PAFC at reasonably high temperatures (about 150 °C), the acid strength needs to be about 85 percent.

The electrolyte reservoir is etched on the anode graphite block of the cell so as to replenish the small amounts of electrolyte lost from the SiC matrix by evaporation during the operation of the fuel cell.

2.3.4 Gaskets

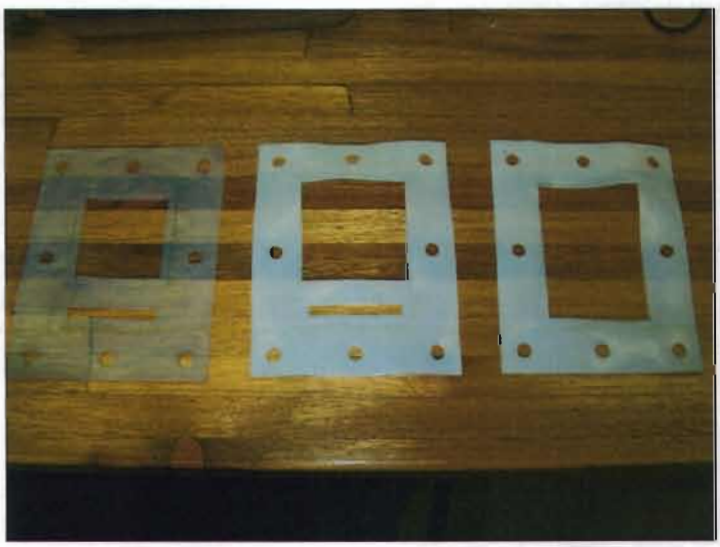

Figure 10 Fuel cell gaskets

The gaskets are used to prevent gaseous exchange or fuel crossover between the reactant gases in a FC. The gasket ensures proper sealing so that it creates a barrier between the reactant gases. The gaskets are made of an incompressible PTFE material with silicon or Teflon with a thickness of 0.25 mm and can withstand the high operational temperatures of up to 200 ˚C.

This ensures that gaskets do not shrink due to high temperatures and as a result leak the reactant gases. A common safety concern for the fuel cell systems are hydrogen leaks. As hydrogen is a combustible material its uncontrolled release can carry risks. Typical silicone gaskets for a PAFC are shown in Figure 10.

2.4 Electrochemical model

The performance of a FC can be summarized with a graph of its current-voltage characteristics called a current-voltage (I-V) (polarisation) curve. It shows the voltage output of the FC for a given current output. An ideal FC would supply the desired or designed amount of current as long as it is supplied with sufficient fuel while maintaining a constant voltage determined by the cell thermodynamics.

As stated earlier, in practice, however, the actual voltage output of a FC is less than the ideal thermodynamically predicted voltage. An example of a typical I-V for a FC is shown in Figure 11. The following section discusses the polarisation curve followed by the performance characteristics of the FC. Note should be taken that the current has been normalized by the area of the FC, giving a current density in amperes per square centimetre because a larger FC can produce more electricity than a smaller FC. Polarisation curves are normalized by the FC area to make results comparable.

As discussed above, FC performance is characterised by its polarisation curve. Three distinct regions of a FC polarisation curve are noticeable from the curve in Figure 11:

- At low current densities, the cell potential drops sharply as a result of the activation polarisation.

- At intermediate current densities, the cell potential drops linearly with current, clearly as a result of ohmic losses (i.e. cell resistance).

- At high current densities, the cell potential drop departs from linear relationship, with current density, as a result of more pronounced concentration polarisation.

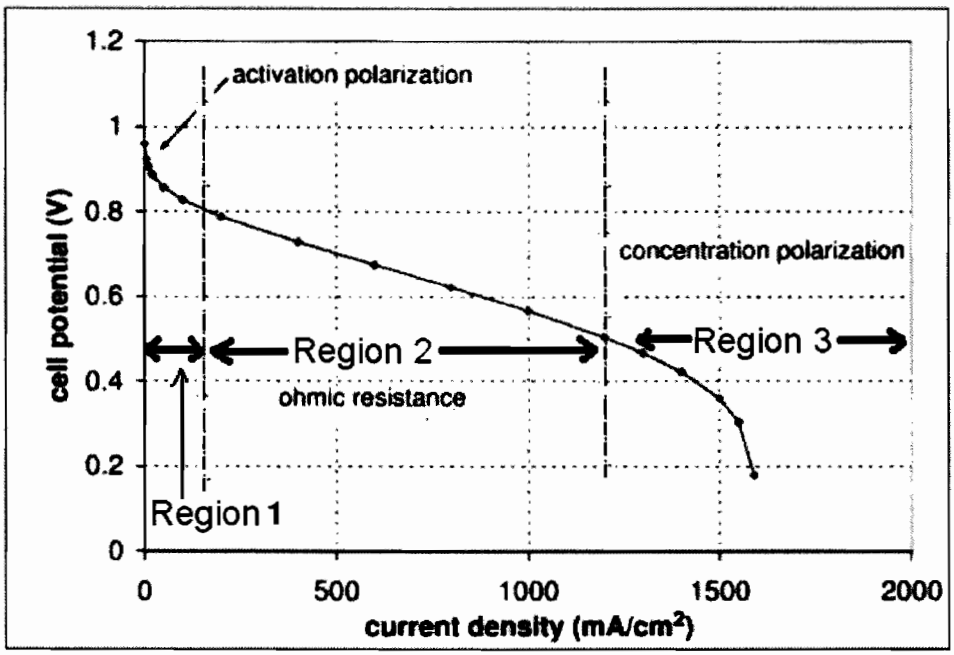

Figure 11 Voltage-current characteristics of a typical FC (Barbir 2005:250)

As mentioned before, an actual FC has a lower efficiency than the ideal one because of the irreversible losses in the cell reaction. The FC terminal voltage drops from the open circuit voltage of which this is proportional to the current drawn by the load. This phenomenon is known as polarisation. There are three main irreversibilities as shown in Figure 11 and are shown as region 1, 2 and 3:

- Activation polarisation: This is caused by the slowness of the reaction taking place on the surface of the electrodes. Some of the electrode potential is used to drive the chemical reaction that transfers the electrons to or from the electrode. In addition, it occurs when the rate of electrochemical reaction at

the electrode surface is influenced by electrode kinetics (Amphlett *et al.* 1995). Raising the cell temperature can reduce the loss due to activation polarisation. This voltage drop contributes mainly in region 1 of the curve in Figure 11. A general equation used to give the values of activation losses is the Tafel equation (Larminie and Dicks 2003:49). It can be expressed in many forms and the simple form is:

$$\Delta V_{act} = A \ln\left(\frac{i}{i_0}\right) \quad \text{V} \tag{2.12}$$

Where:

A ≡ a constant

i ≡ fuel cell current density in $mAcm^{-2}$

i_0 ≡ current density where voltage drop begins to move away from zero in $mAcm^{-2}$

For i_0, this means for example, if i_0 is 100 $mAcm^{-2}$, there will be no voltage drop until the current density i is greater than 100 $mAcm^{-2}$.

A very small amount of electrons will however manage to pass through the electrolyte and not through the external circuit. This is responsible for internal current. Also, some of the hydrogen may diffuse through the electrolyte and react directly with the oxygen at the cathode and hence not produce current from the cell. This is termed fuel crossover and can be combined with the internal current to form internal current density i_n. the activation loss can then be expressed as:

$$\Delta V_{act} = A \ln\left(\frac{i + i_n}{i_0}\right) \quad \text{V} \tag{2.13}$$

Activation losses can be affected factors like cell temperature, catalysts and reactants pressure and concentration.

- Ohmic polarisation: As in any other conductor, this occurs owing to the resistance to proton transfer in the electrolyte, resistance to the flow of

electrons through the electrodes and the contact resistance at the cell terminals. This is the simplest mode of voltage decrease and is proportional to the current. The ohmic polarisation is expressed as:

$$\Delta V_{ohm} = ir \quad \text{V} \tag{2.14}$$

Where:

$i \equiv$ current density in mAcm^{-2}

$r \equiv$ total resistance of individual cell components including electrode electrical resistance, cell interconnects and ionic resistance of electrolyte in Ω.

These losses can be reduced by using electrolytes with high ionic conductivity, electrodes with high electronic conductivity and reducing the space between electrodes to minimise electrolyte resistance. The resistance of the FC is dependent on the current density and the temperature.

- Concentration polarisation: This loss is also called mass transfer loss and occurs owing to the changing concentration of the reactants at the surface of the electrodes. When current is flowing, the surface concentration at the reaction site becomes less than the bulk concentrations as both oxygen and hydrogen are used by the cell.

The extent of this change in concentration will depend on the current being drawn from the FC and the physical factors relating to how well the circulation is around the electrodes as well as how quickly the oxygen can be replenished (Larminie and Dicks 2003:57). This voltage drop can be expressed as:

$$\Delta V_{conc} = \frac{RT}{2F} \ln\left(\frac{C_{surface}}{C_{bulk}}\right) \quad \text{V} \tag{2.15}$$

Where:

$C_{surface} \equiv$ surface concentration

$C_{bulk} \equiv$ bulk concentration

As is evident from equation (2.15) above, the voltage drop is due to the difference in pressure and not due to current or current density. There are limitations with the practical use of equation (2.15) particularly when air rather than pure oxygen is used. Larminie and Dicks (2003:57), however, give an entirely empirical approach that uses equation 2.16. This gives a very good fit to the results, provided the constants m and n are chosen properly.

$$\Delta V_{conc} = me^{ni} \quad \text{V} \tag{2.16}$$

Where:

i ≡ current density in mAcm^{-2}

m and n ≡ constants

The value of m will typically be about 3×10^{-5} V and n about $8\times10^{-3}\text{cm}^2\text{mA}^{-1}$.

These changes in concentration cause the concentration polarisations which are therefore more pronounced at high temperatures, as seen in Figure 11. A steady supply of reactants is required at the electrode-electrolyte interface to maintain the flow of electric current.

In order to obtain the operating voltage of a FC at a current density i, all the losses explained in section 2.5 – activation, ohmic and concentration losses, are combined then the actual operational graph of a FC is produced. The polarisation curve can also be used to determine if the specific FC is operating at high standards. This is depicted by equation (2.17) below.

$$V = E - \Delta V_{ohm} - \Delta V_{act} - \Delta V_{conc} \quad \text{V} \tag{2.17}$$

$$V = E - ir - A\ln\left(\frac{i+i_n}{i_0}\right) - m^{ni} \quad \text{V} \tag{2.18}$$

Where,

E ≡ the reversible OCV given by equation (2.10)

i_n ≡ the internal and fuel crossover equivalent current density

A ≡ the slope of the Tafel line

i_0 ≡ the exchange current density in $mAcm^{-2}$

m and n ≡ constants in the concentration loss equation (2.16)

Equation (2.18) above is always simplified in a useful and practical way and therefore yields equation (2.20) where the crossover current i_n is negligible and is usually used for explaining the initial drop in voltage.

For the part of activation loss, this will yield:

$$\Delta V_{act} = A\ln\left(\frac{i}{i_0}\right) = A\ln(i) - A\ln(i_0) \quad \text{V} \tag{2.19}$$

$$V = E + A\ln(i_0) - ir - A\ln(i) - m^{ni} \quad \text{V} \tag{2.20}$$

Eliminating the constant in the second part of the equation and postulating a real, practical, open circuit voltage E_{oc} given by the equation:

$$E_{oc} = E + A\ln(i_0) \quad \text{V} \tag{2.21}$$

The following equation is produced:

$$V = E_{oc} - ir - A\ln(i) - m^{ni} \quad \text{V} \tag{2.22}$$

Even though equation (2.22) above is simple, it still gives an excellent fit with the results of real FCs (Larminie and Dicks 2003:60). A model of this equation will be discussed using MATLAB modelling software in section 2.5.

2.5 Mathematical model of PAFC with MATLAB

The equation (2.22) can be modelled in MATLAB to give an output resembling the curve in Figure 11. The logarithmic model does not work at very low currents,

especially at zero. A better fit would be to start the plots with a current of about 1.0 $mAcm^{-2}$. The script files below can be used to produce the polarisation curve.

$r = 0.000245,$

$m = 2.11^{-5},$

$n = 0.008$

$i = linspace(1.1000, 200)$

$v = E_{OC} - r \times i - A \times \log(i) - m^{(ni)}$

$plot(i, v)$

$title('polarization - curve - at - T\_f_c = 150\,\mathrm{deg}')$

$xlabel('current\_density(A/cm^2)');$

$ylabel('output\_voltage(volts)');$

$plot(i, v\_out, '*')$

$grid\_on$

$hold\_on$

$disp(v\_out)$

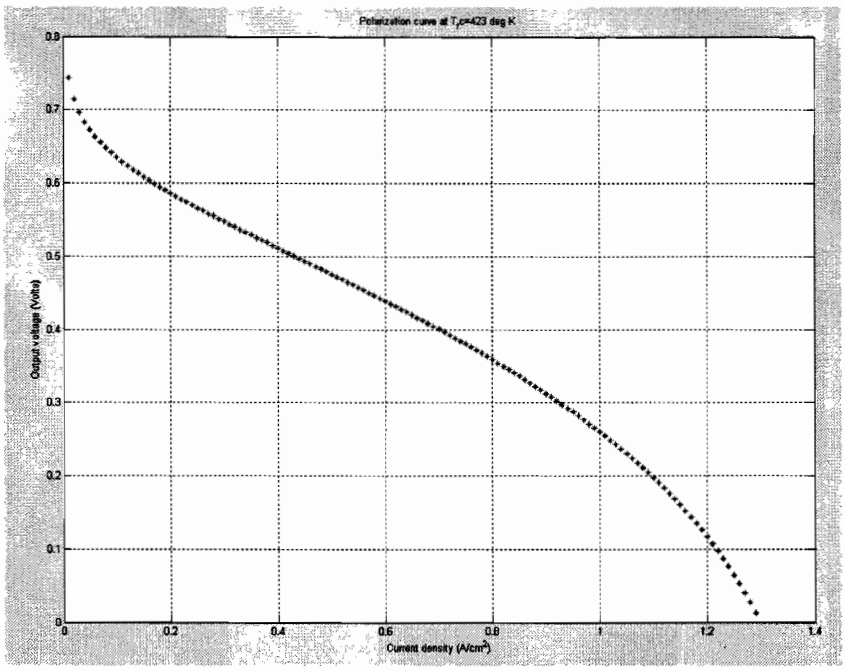

Figure 12 Polarisation curve produced from script in section 2.5

2.6 Electronic circuit model of a PAFC

Fuel cells are usually characterised from their electrochemical perspective and hence this yields many mathematical models that are important for improving the design of membranes, flow fields and catalysts as well as determining the optimal operating conditions such as fuel flow rates, humidity and temperature (Yerramalla *et al.* 2000:82-86). However the drawback is that they are not well-suited for describing the electrical behaviour of the fuel cell or how it will interact with power-conditioning circuits such as converters.

There are two types of FC equivalent circuit models that are mostly discussed: a dynamic model and a passive model. A dynamic model is used to optimise the performance, transient response and efficiency of power converters and inverters whilst a passive model is used to determine the potential performance and degradation of the fuel cell during a stand-by mode. This study deals with the analysis of the FC whilst producing power and therefore, dynamic models will be discussed. The model represents the losses inherent to fuel cells.

Dicks–Larminie model

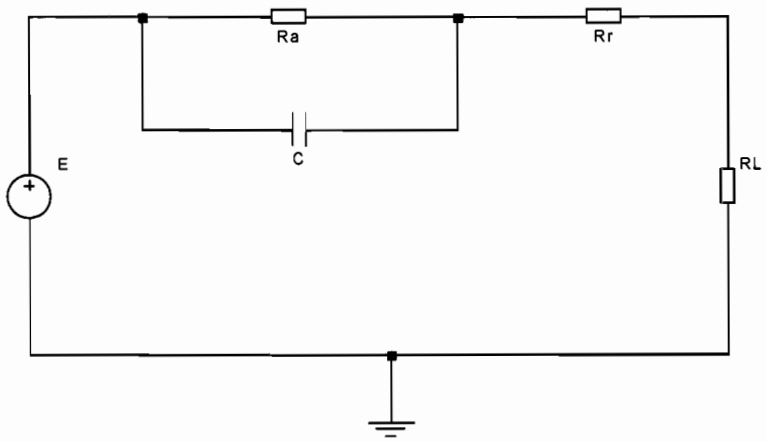

Figure 13 Dicks–Larminie model

The Dicks–Larminie electric model is shown in Figure 13 and models the activation polarisation, the ohmic polarisation and the concentration together with the Nernst voltage. In this model, Ra, the activation and concentration losses are related to the

double layer capacitance. R_{ohmic} is related to the flow of hydrogen and electrons while the capacitor C, is the charge double layer. The Nernst voltage is modelled by the voltage source.

Yu–Yuvarajan model

The Yu–Yuvarajan model in Figure 14 can also be used to model the different operating regions of the polarisation curve. The static model consists of a diode, two transistors and a resistor. The diode models the activation polarisation with its principle of the potential barrier which inhibits the migration of carriers across the PN-junction. The ohmic polarisation of the FC is modelled by the parasitic resistance of the diode. The two transistors and a resistor form a current-limiting circuit that models the concentration polarisation while the dynamic portion of the FC electric circuit model consists of a capacitor and an inductor.

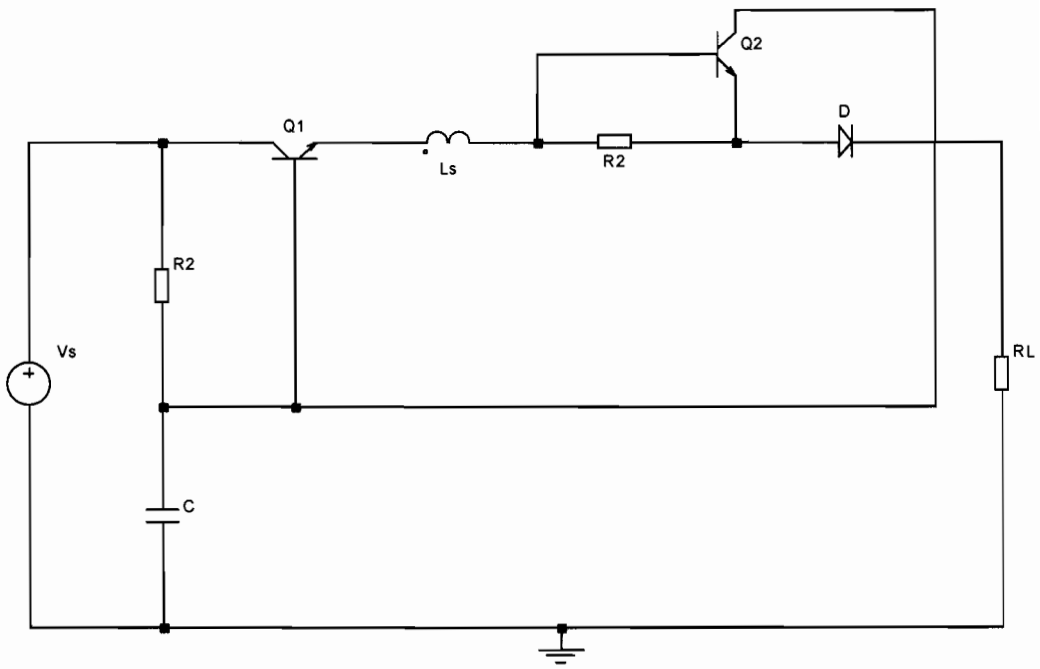

Figure 14 Yu–Yuvarajan model

In this circuit model Figure 14, Vs is the OCV of the stack and the load is depicted by RL. The relationship between the voltage across the diode (V_D) and the current through it (I_D) is given by Yu and Yuvarajan (2005:240):

$$V_D = nV_T \ln\left(\frac{I_D}{I_{SD}}\right) \text{V} \tag{2.23}$$

Where:

$$V_T = \frac{KT}{q} \qquad \text{V} \tag{2.24}$$

Where:

$n \equiv$ the emission coefficient

$I_{SD} \equiv$ saturation current

$V_T \equiv$ thermal voltage in terms of Boltzmann's constant (K)

$T \equiv$ absolute temperature

$q \equiv$ electronic charge

K $\equiv$ Boltzmann's constant

This equation resembles the activation polarisation of a FC in equation (2.12).

From the circuit model in Figure 14, by removing the capacitor, the inductor and the diode, the variation of the output voltage as a function of load current can be determined. The base current of Q1 and Q2 can then be written as:

$$I_{B1} = \frac{I_O - I_{C2}}{1+\beta} \quad \text{A} \tag{2.25}$$

$$I_{C2} \approx I_S e^{\frac{I_O R2}{V_T}} \quad \text{A} \tag{2.26}$$

Where:

$I_S \equiv$ saturation current of Q1 and Q2 in Amperes (A)

$V_T \equiv$ thermal voltage of transistors in Volts (V)

The output voltage is then given by:

$$V_O = V_S - R1\left(I_{B1} + I_{C2}\right) - V_{BE1} - R2\left(I_O - I_{C2} - I_{B2}\right) \text{ V} \tag{2.27}$$

Substituting equations (2.25) and (2.26) into equation (2.27) and assuming a larger value of β, the output voltage can be simplified to:

$$V_O = V_S - R2I_O - R1I_S e^{\frac{R2I_O}{V_T}} - V_{BE1} \qquad \text{V} \tag{2.28}$$

The total FC output voltage is found by combining equations (2.23) and (2.28):

$$V_O = V_S - V_{BE1} - I_O R2 - nV_T \ln\left(\frac{I_O}{I_{SD}}\right) - R1I_S e^{\frac{I_O R2}{V_T}} \qquad \text{V} \tag{2.29}$$

Where:

$R1$ and $R2$ are used to model the concentration losses.

2.7 Factors affecting performance of a PAFC

Fuel cell performance is not only affected by polarisation but also by the design parameters such as cell size, power level, cost and operating variables that include temperature, pressure, fuel composition and current density (Acharya 2004:33).

2.7.1 Temperature

As can be seen from Table 2, with increase in temperature the reversible voltage for a hydrogen fuel cell decreases. In a physical FC, the effect of temperature is different. The improvement in performance at higher temperatures is due to the decrease in polarisation losses. An increase in temperature leads to an increase in reaction rate and lower cell resistance due to improved ionic conductivity of the electrolyte. However, material problems related to electrode degradation and electrolyte loss due to evaporation are accelerated at higher temperatures (Acharya 2004:33).

2.7.2 Pressure

The change in Gibbs free energy owing to pressure can be studied by the Nernst equation (Larminie and Dicks, 2003:36). It shows the effect of pressure on cell voltage as follows:

$$E = E_O + \frac{RT}{2F} \ln \left(\frac{P_{H_2} \left(P_{O_2} \right)^{\frac{1}{2}}}{P_{H_2O}} \right) \quad \text{V} \tag{2.30}$$

Where:

E_O ≡ output voltage at standard pressure and temperature (1.229 V)

F ≡ Faraday constant

P_{H_2} ≡ hydrogen pressure

P_{O_2} ≡ oxygen pressure

P_{H_2O} ≡ water pressure

It can be seen from equation (2.30) that increasing the operating pressure of the FC has a positive impact on the cell voltage.

2.7.3 Reactant utilization and flow rate

As the reactant gases react at the electrodes, their partial pressures decrease and reaction products increase causing the cell potential to fall. The voltage is at its lowest near the fuel exit where the fuel concentration is at its lowest. Lower fuel utilisation leads to a higher cell voltage because voltage cannot change along the electrode and thus the current density drops near the exit where the fuel concentration is lower. These two contrasting factors need to be optimised so that both cell voltage and system efficiency are balanced (Larminie and Dicks, 2003:39).

Also from equation (2.30), it can be seen that an increase in fuel partial pressure leads to an increased cell voltage. Changing the gas composition of hydrogen from

100 percent to 50 percent hydrogen combined with carbon dioxide will reduce the voltage by 0.015 V per cell (Acharya 2004:24).

2.7.4 Current density

The current and voltage in a FC are inversely proportional. When improving the FC efficiency, the FC is operated at higher voltages and this results in low current density as well as lower power densities. To increase the power output, the cell area has to be increased resulting in a larger, heavier and costlier fuel cell. Figure 15 shows the relation between the cell voltage, current density and power density (Hirschenhofer *et al.* 1998:2-10).

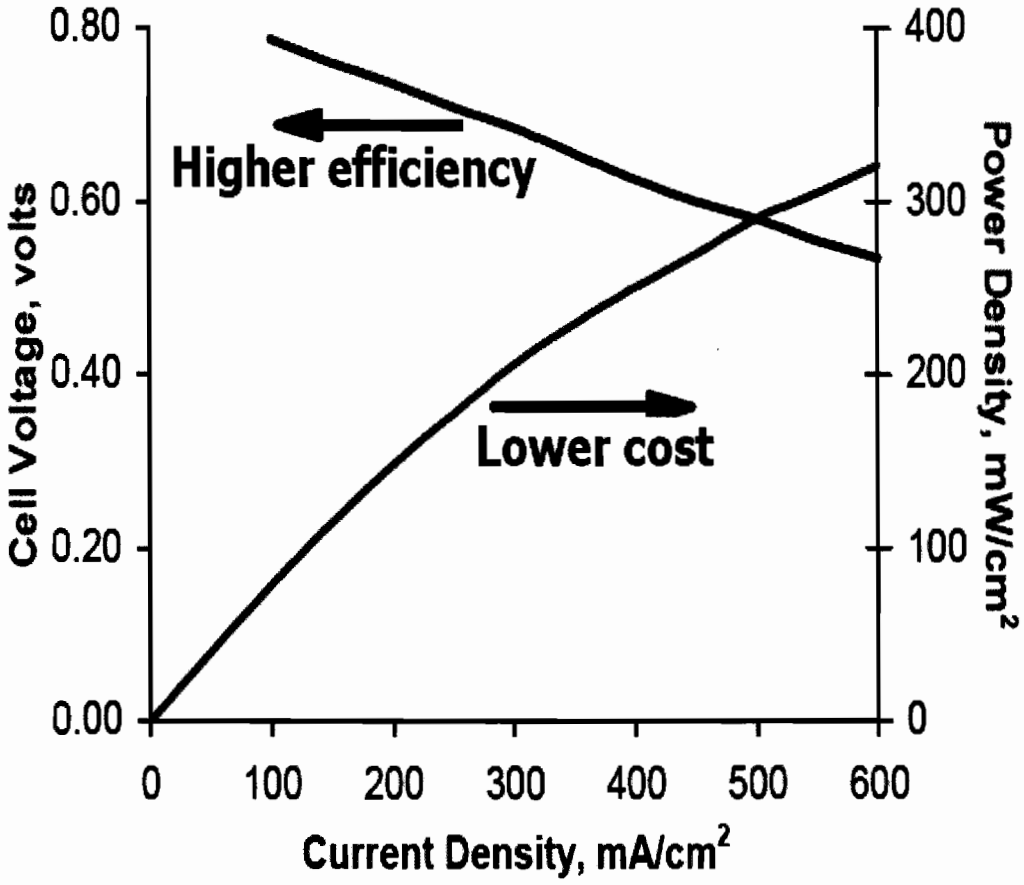

Figure 15 Fuel cell operating point - Efficiency vs Cost

2.8 DC-DC converter

The DC output of the FC is not stable due to the FC electrochemical properties. The unregulated DC voltage of the FC is converted into regulated and controlled DC output and to a desired voltage level by means of a DC-DC converter. From Figure 15, it can be seen that when all the other factors are constant, the actual FC shows a voltage drop with an increase in current density. A switched mode regulator is therefore required to maintain a constant DC output voltage. Depending on the topology of the converter, the output level can either be higher or lower than the input voltage.

Due to the low voltage generated by the FC stack and also its slow response to load changes, a FC stack cannot be connected to a load directly but must be connected through a DC-DC converter. For grid interconnection, the FC stack voltage must be boosted to a higher level for inversion into AC voltage. The purpose of the inverter is to convert DC power to AC power. Most household's applications require 220 V at 50 Hz. Residential FC systems may be employed in stand-alone or grid-connected configurations.

The design of the DC-DC converter is nothing else but the determination of the component values making the converter. For the selection of component values, there are design equations which are normally provided by manufacturer's data sheets. They also provide the limits as well as charging currents and duty cycles.

Apart from choosing the desired topology for the converter to be used, the determination of component values constitutes the design and development of a DC-DC converter. This involves the inductance L and capacitance C.

As stated earlier, the boost converter is a switched mode converter that is capable of producing a DC output voltage higher in amplitude than the input DC voltage. The schematic of the boost converter is shown in Figure 16.

The essential components are an electronic switch with an associated drive circuit, a diode, and an inductor. The drive signal of the switch S_1 usually a MOSFET or IGBT

is a high frequency PWM signal, which produces two operating modes (Erickson and Maksimovic 2001:21).

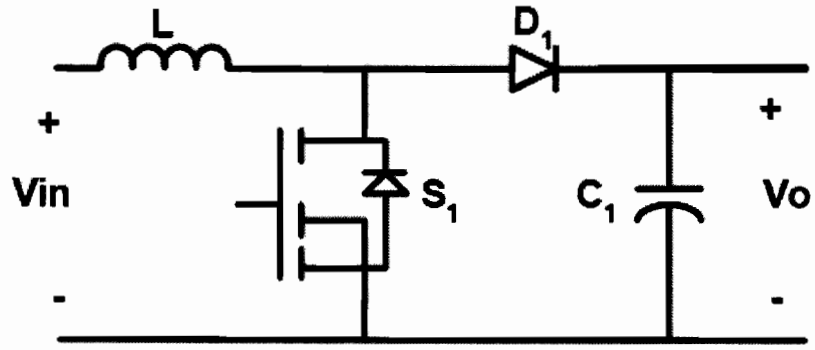

Figure 16 Topology of the boost converter

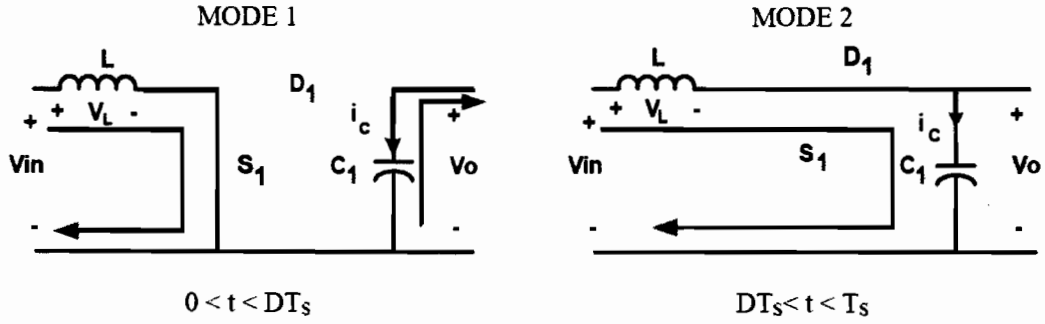

Figure 17 Boost converter operation modes

The first operating mode shown in Figure 17 is when the switch S_1 is on for a time $t_{on} = DT_S$ and the diode D_1 is not conducting. At this instant, the current increases linearly in the inductor L to its peak value. Simultaneously, the energy is stored in the inductor while the output current is supplied entirely from the capacitor C_1, which is chosen to be a large enough value to supply the load current at the time t_{on} with a minimum specified voltage drop.

In the defining equation for t_{on}, D is the duty cycle and represents the fraction of the commutation period T_S or switching period. For this analysis it is assumed that the inductor current always remains flowing (continuous conduction). For this mode,

the inductor voltage and capacitor current can be calculated using the following equations respectively:

$$V_L = V_{IN} \tag{2.31}$$

$$i_C = \frac{V_O}{R} \tag{2.32}$$

The second operating mode of the boost converter is when the switch S_1 is turned off for a time $t_{off} = T_S - t_{on}$. During the off state, the inductor L delivers its stored energy to the capacitor C and charges it up via diode D_1 to a higher voltage than the input voltage V_{IN}. This energy is the one that supplies the load current and replenishes the charge drained away from the capacitor C when it was supplying the load current (Todorovic 2004:34).

It can be established that for a given charge time, t_{on}, and a given input voltage, there is a specific discharge time, t_{off}, for an output voltage. Since the average inductor voltage in steady state must equal zero, the rest of the voltages can be calculated.

$$V_L = V_{IN} - V_O \tag{2.33}$$

$$i_C = i_L - \frac{V_O}{R} \tag{2.34}$$

$$V_{in} \times t_{on} = t_{off} \times V_L \tag{2.35}$$

And because:

$$V_{out} = V_{in} \times V_L \tag{2.36}$$

The V_{out} relationship can be established:

$$V_{out} = V_{in} \times \left(1 + \frac{t_{on}}{t_{off}} \right) \tag{2.37}$$

And using the relationship for duty cycle (D):

$$\frac{t_{on}}{\left(t_{on} + t_{off} \right)} = D \tag{2.38}$$

Then for the boost circuit this yields:

$$V_{out} = \frac{V_{in}}{\left(1 - D \right)} \tag{2.39}$$

The voltage conversion ratio $M(D)$ of the output to the input voltage becomes:

$$M(D) = \frac{V_O}{V_{in}} = \frac{1}{1 - D} \tag{2.40}$$

It is evident from equation (2.40) that the output voltage is controlled by the value of the duty cycle. Also from the above expression it can be seen that the output voltage is always higher than the input voltage. This is why this topology is sometimes referred to as a step-up converter.

An important characteristic of this topology is that it does not need transformers and the voltage stress for the switch is relatively low when compared to other DC-DC step-up converter topologies. The use of this topology to step up the voltage supplied by FCs is feasible when the ratio between the output voltage and the input voltage is not higher than two or three and when no galvanic isolation is required (Todorovic 2004:36).

The DC-DC boost converter mode has been uniformly implemented in the MATLAB/simulink as shown in Figure 18.

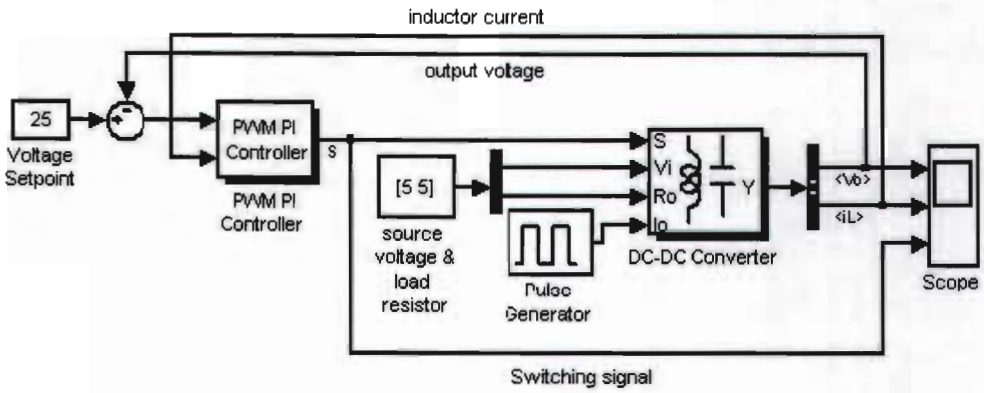

Figure 18 Input and output connections of the DC-DC converter model

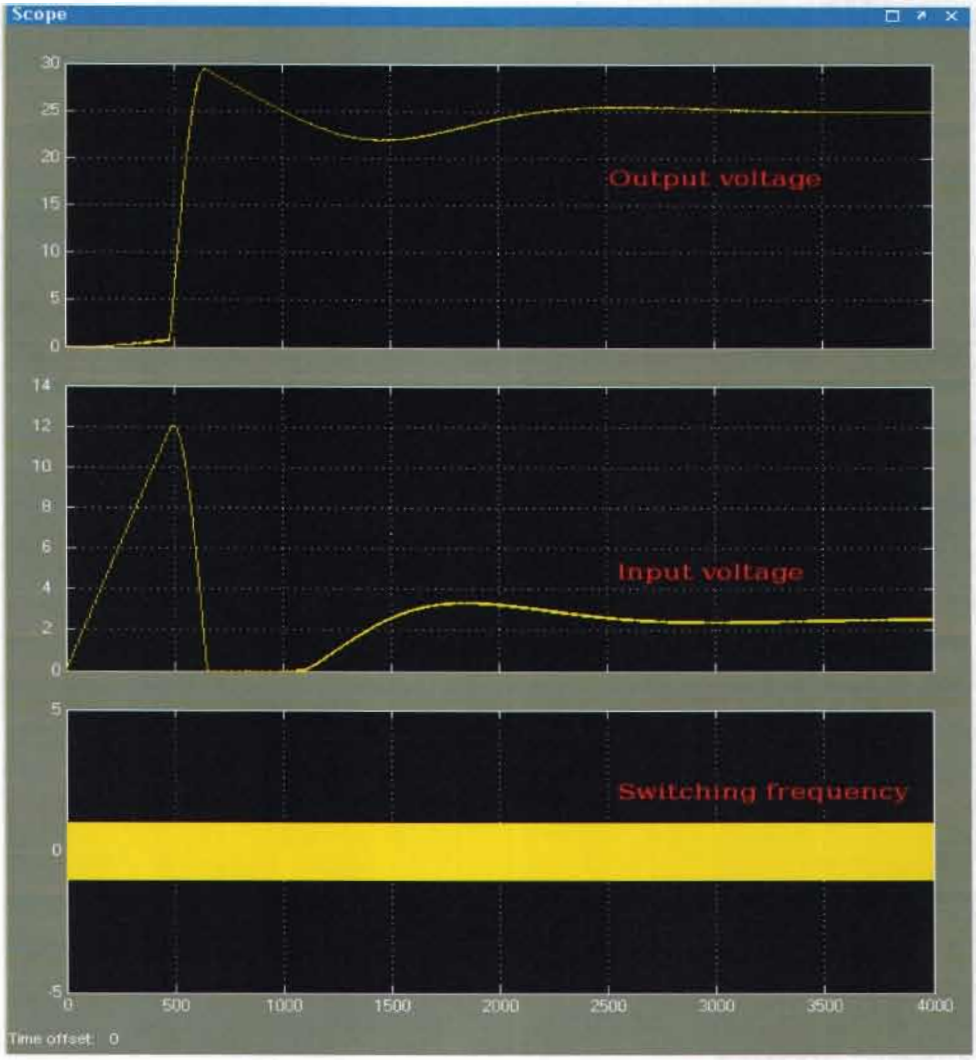

Figure 19 DC-DC simulation result

The input and output connections of the model are shown in Figure 18. The first input to the model is the switch signal. The second one defines the DC source voltage and internal resistance. The third input is used to define the output current. The model has two outputs, the output voltage and the inductor current which are the states of the system.

The model can be configured with a number of parameters. These parameters are: capacitance, C; inductance, L; the internal resistance of the capacitor and the inductor, R_C and R_L respectively. The output result of the simulation is shown in Figure 19.

2.9 Summary

This chapter presented the history and challenges for FCs. The characteristics and operation of the FC were discussed as well as the output voltage influencing factors. FC operation under different operating conditions was considered. The various components that constitute the unit FC were discussed. Then the modelling of the FC using mathematical model simulation of the output voltage using MATLAB was also considered. The chapter concluded with a discussion on the DC-DC boost converter and its models.

The following chapter discusses the physical design of a unit FC and its design parameters. The data from the unit FC is then analysed to model the bigger 100 W stack that can be used for such a load. The chapter will conclude with the design parameters of the DC-DC boost converter.

Chapter 3 Design aspects of a PAFC

3.1 Introduction

In the previous chapter, the operation of the PAFC, its cell characteristics and the underlying factors affecting its performance were considered. The mathematical modelling of the terminal voltage using MATLAB and the power conditioning and regulating through the DC-DC converter were discussed.

This chapter focuses on the practical design of the PAFC device components and additional FC parameters. The unit cell stack is used to characterise the operation of the PAFC and validation of the computer simulations and mathematical model. Suffice to say at this point that the model will then be used to represent a 100 W stack. The design of the DC-DC boost converter concludes the chapter.

3.2 Design of PAFC components

This section presents the design of the unit cell PAFC components from steel end plates, graphite blocks, electrolyte-retaining matrix and gaskets for sealing of the FC. Since the single cell consists of an electrode, electrolyte matrix and bipolar plate, the cell performance is related to a capability of each component. The analysis of these components will in turn result in the physical design of the unit cell.

3.2.1 Bipolar plates

Stated again, much effort is being expended on the cost effectiveness of materials for the manufacturing of bipolar plates. Isotropic graphite offers a good thermal and electronic conductivity and is used for this purpose. The graphite block is 145 mm x 115 mm x 20 mm. The flow fields were designed and drawn using computer-aided drawing (CAD) software and then sent to Electrochem Inc. for machining onto the bipolar plates by a standard milling and engraving process.

The flow field's dimensions have been suggested by many researchers for various reasons. A column flow pattern was chosen for the design and had a width between the squares of 2 mm and a depth of 2 mm. Figure 25 refers. Figure 20 (not to scale), illustrates this principle. The pattern is machined on both the anode and the cathode side. This is further described in section 3.2.3.

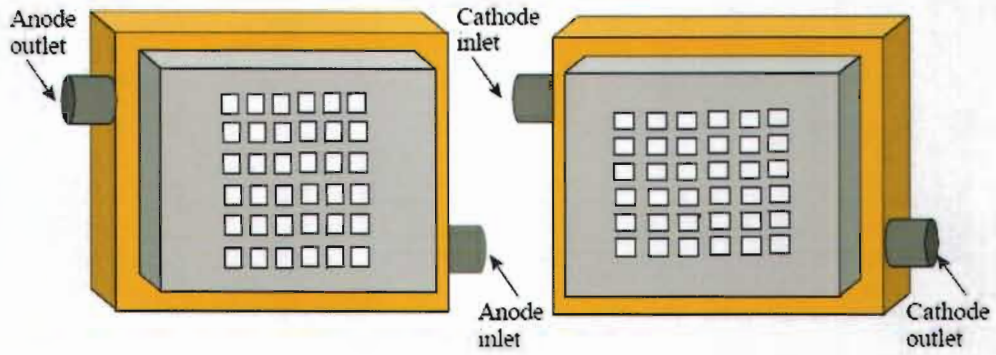

Figure 20 Bipolar plates

As discussed in section 2.3.1, the flow pattern design presents a low pressure drop from the inlet and outlet as the FC will be operating on low pressure of less than 1 bar. Figure 21 shows the machined graphite blocks. The ribs formed from squares protruding on the flow field help in aligning the membrane evenly on the block allowing the same contact pressure throughout.

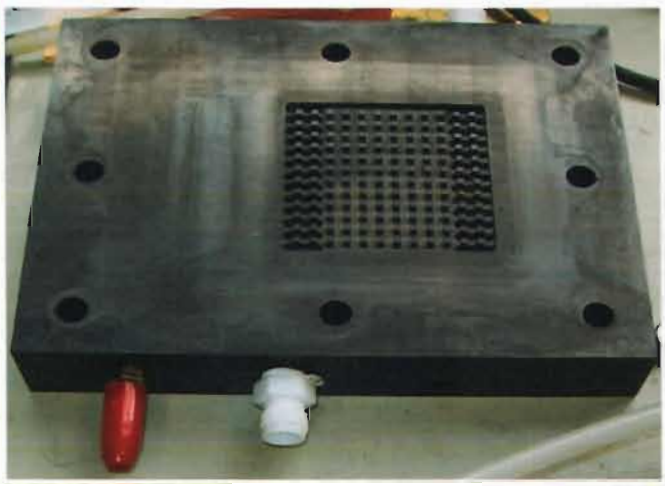

Figure 21 Graphite BP

3.2.2 Electrolyte matrix assembly

One of the most important components of the PAFC in terms of cell performance and lifetime is the electrolyte-retaining matrix layer (Hirschenhofer *et al.* 1998: 3-7). According to Hirschenhofer *et al.* (1998:3-8), the best matrix material for use in PAFCs is silicon carbide (SiC) with a binder, polytetrafluoroethylene (PTFE) content of about 3-15 weighted percent and hence this was used in the design.

For good performance in a FC, the electrolyte matrix must be wettable to an extent to provide good ionic conduction, must be free from cracks in order to prevent gas crossover and must have good structural integrity. The matrix has a thickness of 0.1-0.2 mm. The ionic resistance of the matrix is very low, owing to its thinness while the mechanical properties are somewhat limited. The matrix had an effective area of 25 cm^2 and covered only the active area with the flow field. The maximum pressure difference between the anode and the cathode should not exceed 200 mbar (Barbir 2005:65).

Figure 22 Silicon carbide electrolyte-retaining matrix

The matrix also has porous gas diffusion electrodes attached on the anode side and on the cathode side. Every electrode faces the channel on one side and the electrolyte

on the other side. A platinum electrocatalyst whose function is primarily to favour the gas reaction is placed on the electrolyte side. Since the electrolyte is in a liquid form, for water management purposes the electrodes are hydrophobic. The active area had a platinum loading of 0.6 $mgcm^{-2}$. The electrodes used throughout the measurements were commercially available electrodes with an active area of 25 cm^2.

Figure 23 Matrix material surrounded by gasket with SiC side facing up

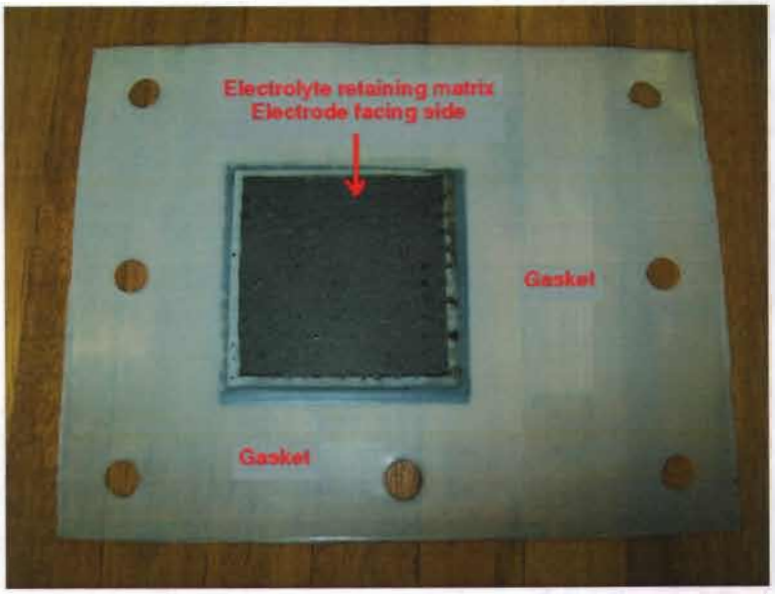

Figure 24 Matrix material surrounded by gasket with electrode side facing up

In this particular FC, the SiC is wetted with a few drops of H_3PO_4 and the reservoir is filled with excess electrolyte. Phosphoric acid was used instead of other acidic electrolyte mediums because as stated in section (2.3.2), it is the only inorganic acid that exhibits the required thermal stability, and low enough volatility to be effectively used.

3.2.3 Cell hardware

All the tests on the PAFC were performed on a unit cell with an active area of 25 cm^2. The electrolyte matrix was sandwiched between the two flow fields, which were clamped together by the outer stainless steel plates and current collector plates. The stainless steel plates were 5 mm thick and pressed together by 8 (eight) bolts with flow-fields plates and the matrix assembly in between. See Figure 31 on page 54. The flow field plates were made of graphite which featured high temperature resistance and low electrical resistivity.

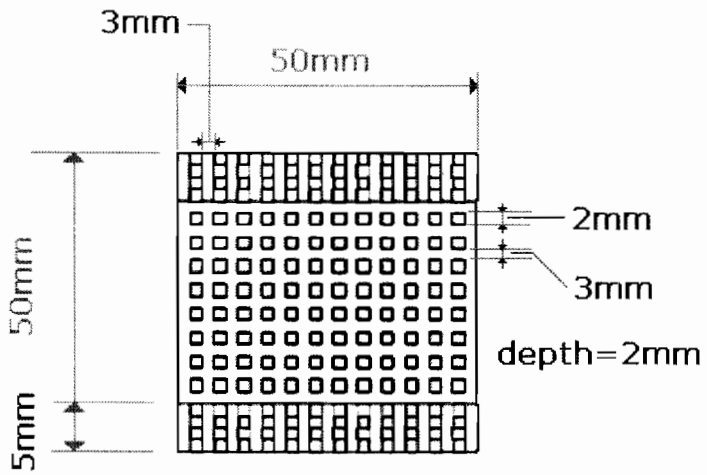

Figure 25 Schematic of the flow field

Flow field channels were machined in column configuration into the graphite plates for the supply of the reactants and the removal of the products. The structure and the dimensions of the flow channels are depicted in Figure 25. The cross-section of the flow channel was 3 mm with 2 mm gap between two adjacent channels. Moreover the flow field plates have a thickness of 25 mm to compensate for the deflection of

the end plates and thus, to achieve a homogenous pressure distribution over the active area.

The flow field pattern was firstly designed and drawn by making use of computer-aided software and then the design was exported and machined or engraved onto the graphite plates using a milling machine. The width of the square rib was 2 mm and the spacing between the ribs was 3 mm. The depth of the rib from surface to its floor was 2 mm and the dimensions of the graphite blocks were 110 mm x 110 mm. The design can be varied in many ways according to the preferred dimensions for better performance of the FC.

3.2.4 Gaskets

A common safety concern for the FC systems is hydrogen leaks. As hydrogen is a combustible material its uncontrolled release can carry risks. For sealing the FC, gaskets made of incompressible PTFE material with a thickness of 0.25 mm were used and a set torque of 5 Nm was used to tighten the bolts. The choice of torque was based on previous work and experiments.

According to Srinivasan (2006:289), the thickness of the gaskets is one of the important parameters in the construction of the FC. The gasket thickness determines how much the flow fields are allowed to pinch into the electrode structure. For a good contact pressure which translates to a low contact resistance, it is essential that the ribs of the flow field bite into the electrode providing good contact. Typical pinch values as suggested by Srinivasan are 0.05 - 0.07 mm for a carbon paper backing and 0.254 - 0.381 mm for a carbon cloth backing.

Since electrode thickness for each anode and cathode may vary, gasket thickness for either side is determined separately using the formula:

$$\textit{Gasket thickness} = \textit{(individual electrode thickness)} - \textit{(desired pinch)} \quad (2.38)$$

A great deal of time was spent on making sure that the FC was completely sealed and thus no reactant gas leakages should occur. In order to ascertain this, pressure-

measuring film was used. Figure 26 shows the lower unshaded side that had less or no pressure exerted on that area and hence reactant gas leakages. Conversely, Figure 27 shows the gas tightness of exerting much more pressure and changing the gasket material.

The thickness of the matrix material and gaskets contribute to the electrical resistance of the cell and hence it is important to maintain a uniform contact pressure and the smallest distance as possible between BPs and GDLs.

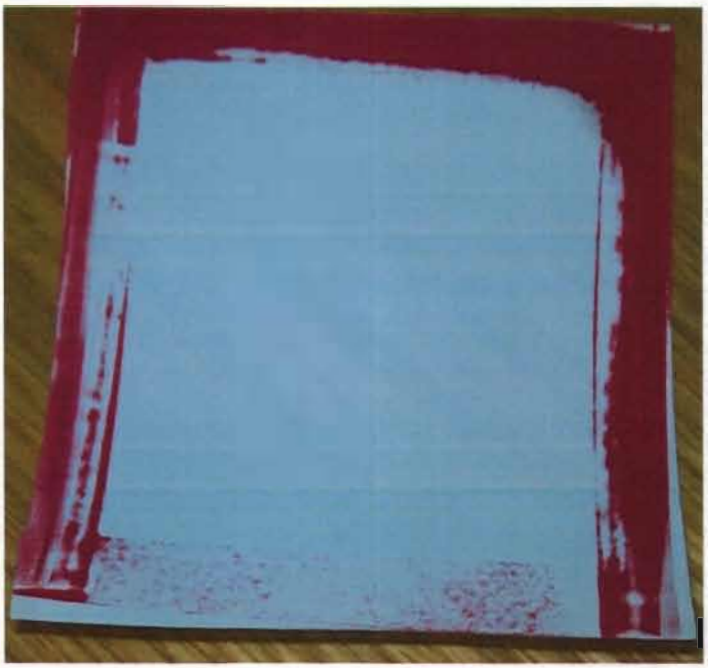

Figure 26 Reactant gases leakage test

A typical pressure distribution obtained for one of the experimental cells with a pressure measuring film is shown in Figure 28. The pressure distribution was measured at room temperature in a cell including the matrix assembly and all the gaskets. The bolts were tightened with a torque of 8 Nm. In general, the intensity of the red coloration of the image in Figure 28 indicates the degree of contact pressure per certain area. The darker areas depict the regions of higher contact pressure. Moreover, the column pattern of the flow field structure can be clearly seen.

As can be seen in Figure 28, the pressure onto the electrode is smaller along the flow channels but however, the darker red coloration shown along the squares is moderately uniform and indicates a reasonably homogeneous pressure distribution over the active area. The exact pressure exerted on a specific location can thus be determined by comparing the colour variations against a predefined index which is obtained together with the pressure film. However, for this study it was not necessary to know the exact pressure values but to observe the pressure patterns and places of lower and higher pressure as well as areas where the cell is not gas tight.

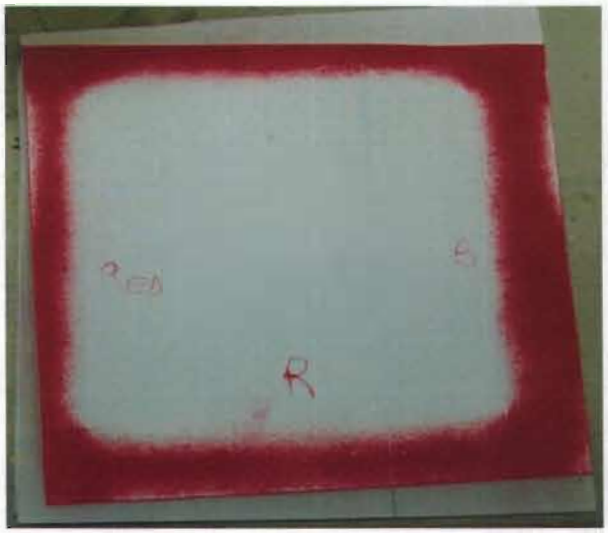

Figure 27 Reactant gases leakage test

Figure 28 Pressure distributions in the experimental cell active area (25 cm^2)

The gaskets employed in the FC should be able to withstand a temperature of up to 200 °C. This ensures that they do not shrink due to high operational temperatures. Initially Teflon material was alternately used with PTFE material for gaskets until ultimately the researcher settled for PTFE towards the last stages of the experiments.

3.2.5 Other parameters

3.2.5.1 Flow configurations

Generally, PAFCs can be operated in two different flow configurations: co-flow and counter-flow as illustrated in Figure 29 and 30 respectively. In co-flow, the hydrogen concentration and hence the hydrogen permeation across the membrane decreases with oxygen concentration along the flow channels. If the hydrogen crossover is high and the air stoichiometry low, total oxygen depletion on the cathode may occur close to the outlet and may result in a very inhomogeneous current distribution (Kordesch and Simader 1996 91:191-205).

In contrast to co-flow, the counter-flow mode could result in a more homogenous current distribution over the active area at low air stoichiometry. At the oxidant inlet, the hydrogen concentration and thus the hydrogen crossover may be the lowest and consequently, less oxygen is consumed. This is the reason why the distribution of oxygen and thus the current distribution over the active area may be more homogenous in counter-flow mode than at a low air stoichiometry.

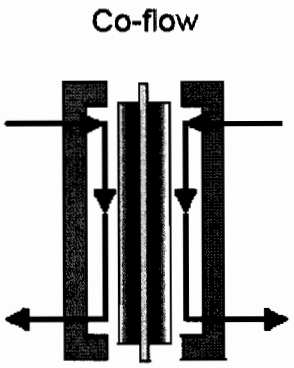

Figure 29 Principal flow concepts in fuel cells (co-flow)

Since this study is characterising the operation of the PAFC under realistic operating conditions which is at low air stoichiometry, the counter-flow operation was chosen for the tests. In addition, water may be easier removed from the cathodic flow field with the help of gravity.

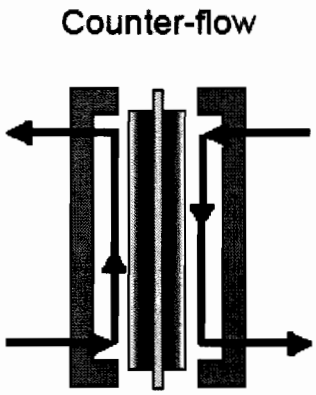

Figure 30 Principal flow concepts in fuel cells (counter-flow)

3.2.5.2 Cell orientation

The position of the cell is an additional parameter which has to be considered. This applies particularly for portable applications. This can either be the upright or horizontal position. The cell position may affect the cell performance because cathodic flooding is affected which limits or enhances the oxygen transport to the active sites. The upright position was chosen for this particular research study as it showed consistency with earlier investigations by other researchers.

3.3 Final stack assembly

Figure 34 shows the photograph of a complete cell assembly while Figure 31 shows the assembly of the PAFC. The illustration in Figure 32 shows the sequence of the individual components within the cell assembly and the components are placed in the order they appear in the Figure.

A single cell is built by stacking in sequence the anode graphite block, anode gasket,

anode facing matrix assembly, the middle gasket, cathode facing matrix, cathode gasket and the cathode graphite block on an end plate fitted with the necessary bolts. This is shown in Figure 31.

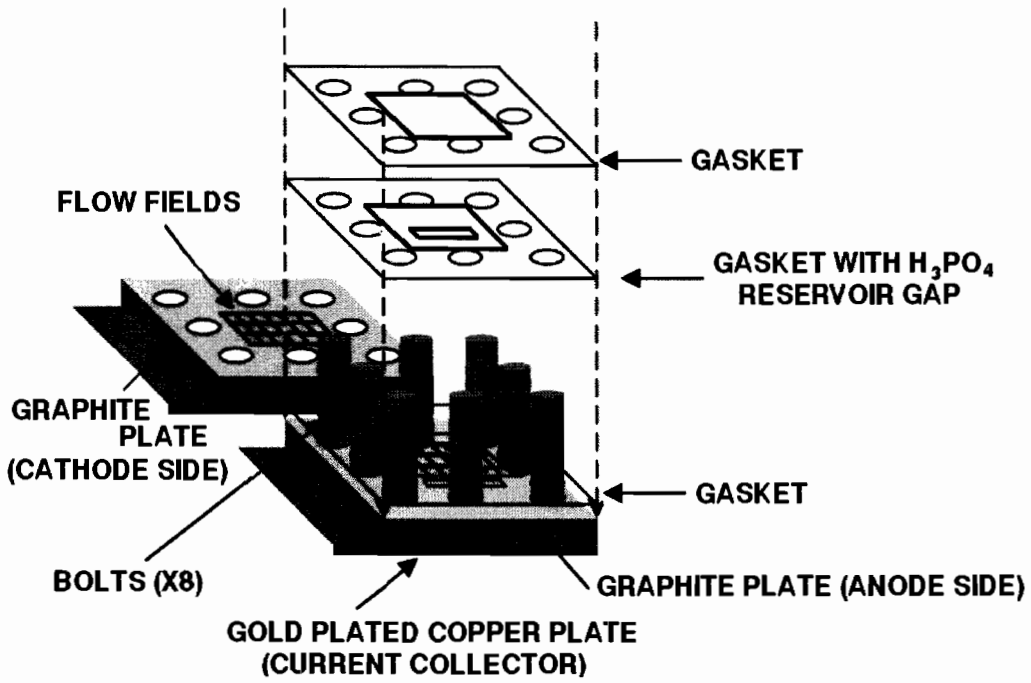

Figure 31 Cell assembly

The steel end plate is placed facing up with the high density graphite flow field block on top with the flow field pattern also facing up. All the bolts insulated with FEP heat shrink are in one set of plates and also serve as alignment pins. The first gasket is placed on the flow field plate (anode side) followed by the matrix assembly. The second gasket then follows and is lined up with the matrix assembly.

The electrode assembly at the cathode side is then placed on the second gasket followed by the final gasket. The graphite block and the copper plates are then placed followed by the insulation washers and nuts. Insulating washers and bushings at either end ensure electrical isolation. The current collector plates are inserted between the graphite blocks and the steel end plates on both sides.

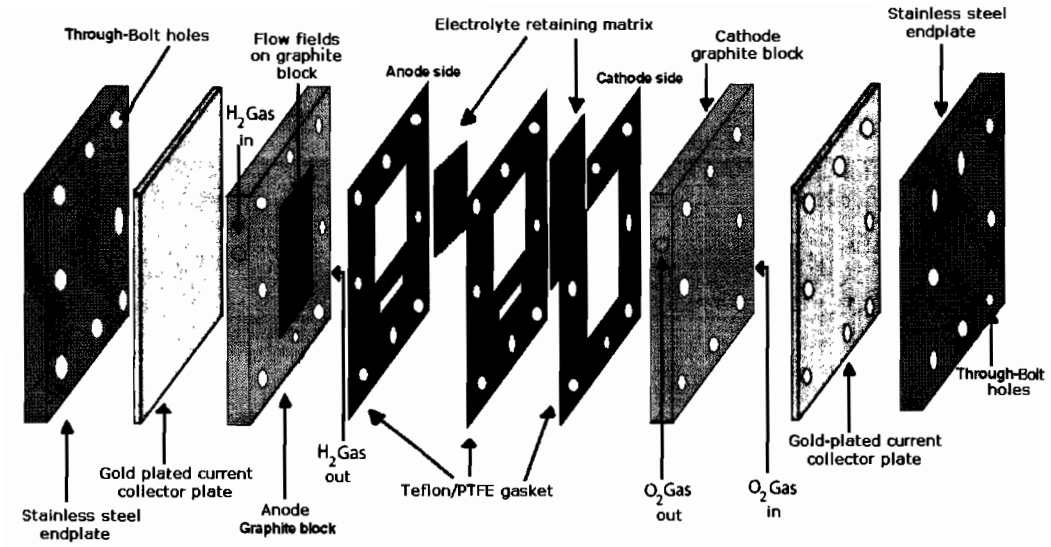

Figure 32 FC component assembly

Once all components are stacked together and proper alignment is attained, the nuts are hand-fastened and the FC is put upright. Compression is then applied by tightening the nuts symmetrically as shown in the sequence diagram in Figure 33. Spring washers provide more uniform force across the assembly. Compression is applied using an adjustable torque wrench at 3 Nm and then to the required 5 Nm. Care is taken in attaining the optimum force so that a balance is found between establishing a good electrical contact while not compromising the porous structure of the matrix assembly.

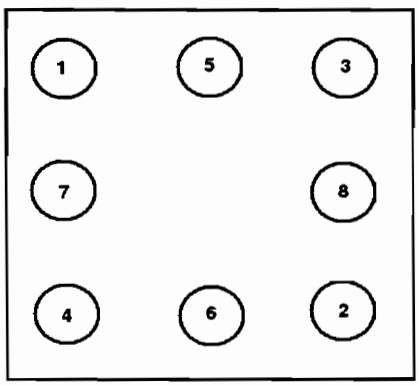

Figure 33 Bolt sequence

The output cell current is collected from solid gold-plated copper plates between the steel plate and graphite blocks while the cell voltage is accomplished by means of leads attached to the banana plugs inserted into the graphite blocks. This is done to eliminate the possibility of current line drop on potential measurements.

The operational temperature of the FC of around 200 °C as earlier stated, is kept constant by means of a temperature controller. Temperature control is achieved with silicon-insulated resistive heating pads bonded to the steel end plate and connected to the controller. Thermocouples which are placed in the thermocouple wells on both graphite blocks are also connected to the controller. Additional heating is accomplished by cartridge heaters which are inserted into the anode and the cathode electrode blocks.

Figure 34 Assembled fuel cell

3.4 100 W PAFC stack model

3.4.1 Mathematical modelling

Mathematical modelling is considered a basic tool in the development of FCs as it provides valuable insight into the electrochemistry of a FC and processes that take

place in the system. Even though there are several models available to describe relevant factors in FCs, the model that focused on simulating the operation of the FC stack utilizing, in several cases, experimental data was adapted.

Table 3 Measured data of a PAFC stack

	Stack voltage (V)	Current (A)	Current ($mA.cm^{-2}$)
1	0.73	0.03	1.2
2	0.64	0.04	1.6
3	0.63	0.05	2.0
4	0.62	0.06	2.4
5	0.60	0.08	3.2
6	0.59	0.1	4
7	0.57	0.2	8
8	0.56	0.3	12
9	0.55	0.4	16
10	0.54	0.5	20
11	0.53	0.6	24
12	0.52	0.7	28
13	0.51	0.8	32
14	0.50	1.0	40
15	0.49	1.5	60
16	0.48	2.0	80
17	0.47	2.5	100
18	0.46	3.0	120
19	0.45	3.5	140
20	0.44	4.0	160
21	0.43	4.5	180
22	0.42	5.5	220

As earlier stated, in order to adopt and simulate for the required 100 W FC stack model, this would require experimental data. The developed FC from section 3.3 was used to obtain the experimental data. The obtained data was used to calculate and

simulate for the predicted model. Table 3 above, gives the output voltage of the single cell PAFC at different currents.

The open circuit voltage (OCV) for this particular experiment was found to be 0.784 V. This is the output voltage of the FC when not producing any current (no load condition), and as soon as current is drawn, the OCV drops to a lower value.

In order for the voltage output equation (2.22) in section 2.4 to be used for predicting the characteristics for the 100 W model, it can be rewritten to accommodate N_C (number of identical cells). The parameters of this equation are then determined and N_C adjusted accordingly to predict the 100 W performance characteristics.

$$V_{STACK} = N_C E_{OC} - N_C ri - N_C A \ln(i) - N_C me^{ni} \quad \text{V} \tag{3.1}$$

In practice, the typical operating voltage of a FC is usually around 0.6 V. From the experiment, the power of the PAFC stack was found to be 3.3 W. In order to obtain a mathematical model for a 100 W stack, a value of N_C is required. Therefore:

$$N_C = \frac{100 \text{ W}}{3.3 \text{ W}} = 30.3 \text{ Cells} \tag{3.2}$$

The value is rounded to 30 cells.

The performance of the FC stack is determined by using equation (3.1). The value of N_C found in (3.2) is substituted into equation (3.1) and the values of r, A and m are calculated in order to reproduce the performance curve. The value of n is given typically as 0.008 cm^2mA^{-1} (Larminie and Dicks 2003:60). The values of r, A and m are solved using MATLAB and the following values were found:

r = -0.0041 $K\Omega cm^{-2}$
A = 0.2019 V
m = 0.0219 V

The mathematical model of a 100 W PAFC stack can therefore be represented from equation 3.1 with the obtained values and substituting for N_C = 30. This is shown in the equation below:

$$V_{STACK}=30(0.784)-30(-0.0041)i-30(0.2019)\ln(i)-30(0.0219)e^{0.008i}\ V$$

Therefore:

$$V_{STACK}=(23.52)-(0.123)i-(6.057)\ln(i)-(0.657)e^{0.008i}\ V \qquad (3.3)$$

The equation above (3.3) only holds true when i is expressed in terms of current density ($mAcm^{-2}$). The output curves are presented in Chapter 4.

3.4.2 Equivalent electronic circuit model

As discussed previously in 2.6, the equivalent electronic circuit model can predict the working of a PAFC. This model is evaluated below. The output voltage of the equivalent circuit model as given by equation 2.29 is:

$$V_O = V_S - V_{BE1} - I_O R_2 - nV_T \ln\left(\frac{I_O}{I_{SD}}\right) - R_1 I_S e^{\frac{I_O R_2}{V_T}} \quad V$$

Where:

$V_T \equiv$ thermal voltage = 25 mV at STP

$V_O \equiv$ output voltage in V

$I_O \equiv$ load current from stack in mA

To finalise the circuit model, the following values were determined by using equation 2.29.

$V_s \equiv$ battery voltage in V

$R_1 \_ R_2 \equiv$ resistance values in Ω

$n \equiv$ emission coefficient

$I_{SD} \equiv$ saturation current in mA

$I_S \equiv$ saturation current of the two transistors in mA

$R_D \equiv$ ohmic resistance of the diode in Ω

The maximum or higher current value from experimental data (Table 4 on page 75) together with the corresponding current density is substituted into equation 2.29 and hence the values of r and n can be calculated. The values of r and n have to be standardised to volts when the current density is given in mA. The resulting values of r and n can then be substituted into equation 3.3.

3.4.3 Modelling of performance curves in MATLAB

The output voltage of a FC is given in equation 2.22 in section 2.4. This equation forms the basis of all parameters that are analysed in MATLAB for a FC. An attempt was made to illustrate the schematic model in MATLAB used for performance simulation of a PAFC in Figure 35 below.

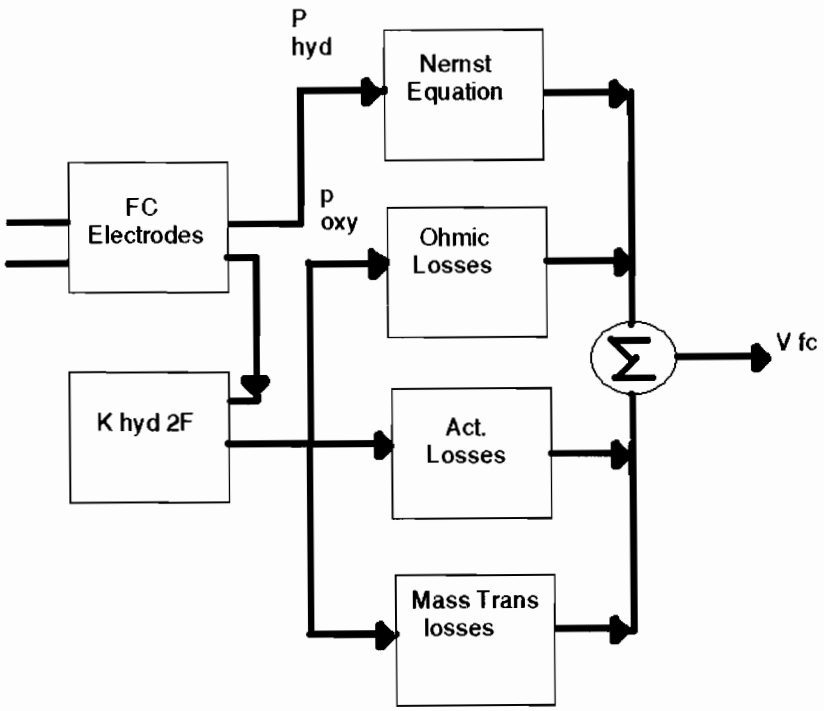

Figure 35 Schematic MATLAB model of PAFC

From this model, the output voltage of a FC (Vfc) is given by:

$$Vfc = E_{OC} - ir - A\ln(i) - m^{ni}$$

The simulation graphs for the above model and their interpretations are given in Chapter 4. The MATLAB program used for simulation is given in Annexure A.

3.5 Design of a DC-DC boost converter

A FC power system normally uses a power converter in order to deliver a regulated output voltage. The power converter used here is a DC-DC boost converter that converts the DC voltage output of a FC to a different and regulated DC voltage level.

The boost converter is a type of switching converter that operates by periodically opening and closing an electronic switch. It is called a boost converter because the output voltage is larger than the input. A typical circuit of a boost converter is shown below.

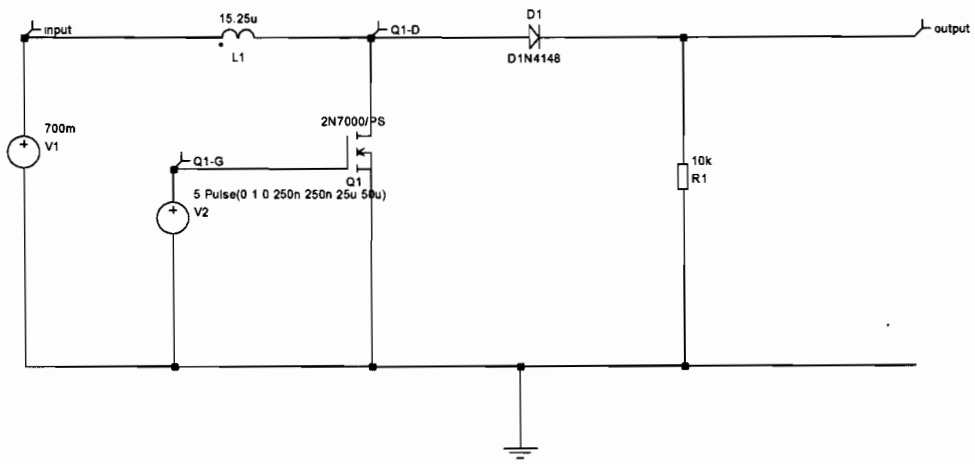

Figure 36 Boost converter circuit

3.5.1 Design considerations

The following discussion gives a typical example of the procedure to design a boost converter (Rashid 2004:190-194).

Firstly the desired parameters required for the design of the boost converter are stated:

Input voltage (V_S)

Average output voltage (V_a)

Average load current (I_a)

Switching frequency (f)

Output power (P_{out})

Output voltage ripple to 1%

Variable components:

Then if:

Inductance $L = 150\ \mu\text{H}$

Capacitance $C = 220\ \mu\text{F}$

The boost converter design:

$$D = 1 - \frac{v_{in}}{v_o} = 1 - \frac{5}{12} = 0.583(or\_0.6\_approx)$$

$$f_s = \frac{V_{out}(M-1)}{10(0.1I_{out})(L1)(M^3)} = \frac{(12)(1.4)}{10(0.1)(330\times10^{-6})(2.4)^3} = 3.68\times10^3 \quad \text{Hz}$$

Peak current through switch:

$$I_{sw\_peak} = I_{out}\left[M + \left(\frac{V_{out}}{2.f_s.I_{out}.L1}\right)\left(\frac{M-1}{M^3}\right)\right] = 2.5 \quad \text{A}$$

Peak voltage across switch:

$$V_{sw\_peak} = V_{in\_\max} + V_{out} = 7 + 12 = 19 \ \text{V}$$

$$C_1 = \frac{L1\left(I_{sw-peak}\right)^2}{2 \cdot \Delta V_{out} \cdot \left(V_{out} - V_{in\_min}\right)} = 1227\ \mu\text{F}$$

Finally the value of C_1 which is 1220 μF, can be chosen.

The following design can also be done to get the critical values of both inductance and capacitance.

Given:

$$(1-k) = \frac{V_s}{V_a}$$

$$12 = \frac{5}{(1-k)}; k = 0.5834 = 58.34\%$$

$$\Delta I = \frac{V_s(V_a - V_s)}{fLV_a}$$

$$\Delta I = \frac{5 \times (12-5)}{25 \times 10^3 \times \left(330 \times 10^{-6}\right)(12)}$$

$$\Delta I = 0.3535A$$

$$I_s = \frac{I_a}{1-k}$$

$$I_s = \frac{1}{(1-0.5834)}; I_s = 2.4\ \text{A}$$

$$I_2 = I_s + \frac{\Delta I}{2}; I_2 = 2.4 + \frac{0.3535}{2} = 2.577\ \text{A}$$

$$\Delta V_c = \frac{I_a k}{fC}$$

$$\Delta V_c = \frac{1 \times 0.5834}{25 \times 10^3 \left(220 \times 10^{-6}\right)} = 0.1061\ \text{V}$$

$$R = \frac{V_a}{I_a}; = \frac{12}{1} = 12\ \Omega$$

The critical value for inductance (L_c) and capacitance (C_c) are then:

$$L_c = \frac{(1-k)kR}{2f}; = \frac{(1-0.5834)\times 0.5834\times 12}{2\times 25\times 10^3} = 58.33\ \mu\text{H}$$

$$C_c = \frac{k}{2fR} = \frac{0.5834}{2\times 25\times 10^3\times 12} = 972\ n\text{F}$$

An attempt is made in Figure 37 below to illustrate a typical circuit of a DC-DC boost converter. This is drawn and simulated by using SIMetrix software. The circuit has three switches and the pulse wave modulation (PWM) signal is accomplished by employing a UC 3843 chip.

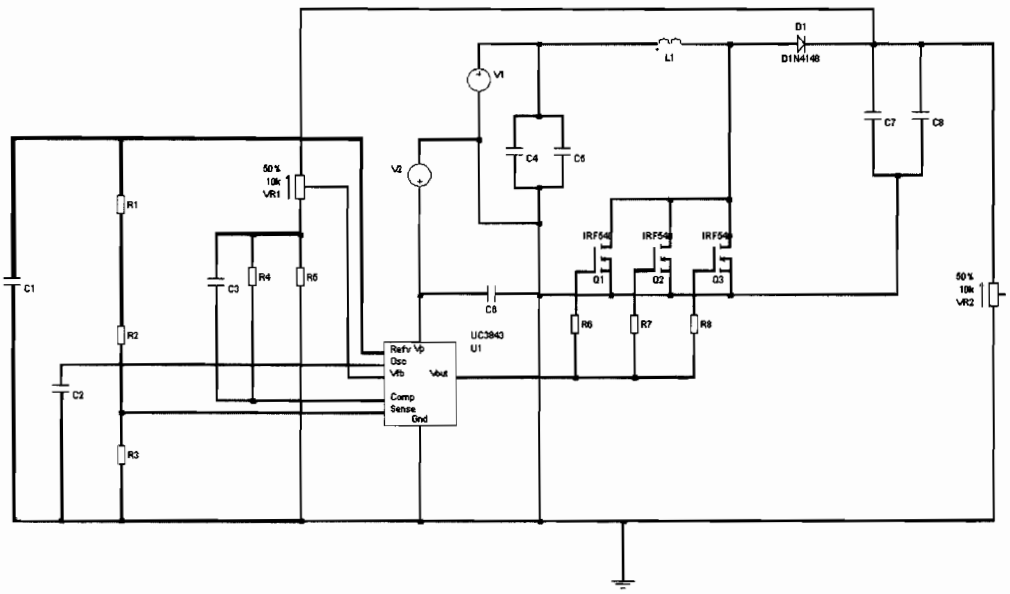

Figure 37 Schematic of a DC-DC converter

Figure 38 is a photo of the assembled DC-DC boost converter prototype. After being simulated, the converter circuit PCB was made using EAGLE software and machined at the Vaal University of Technology. The converter has an input of 5-8 Volts with an output of 25 Volts and a power of 10 W.

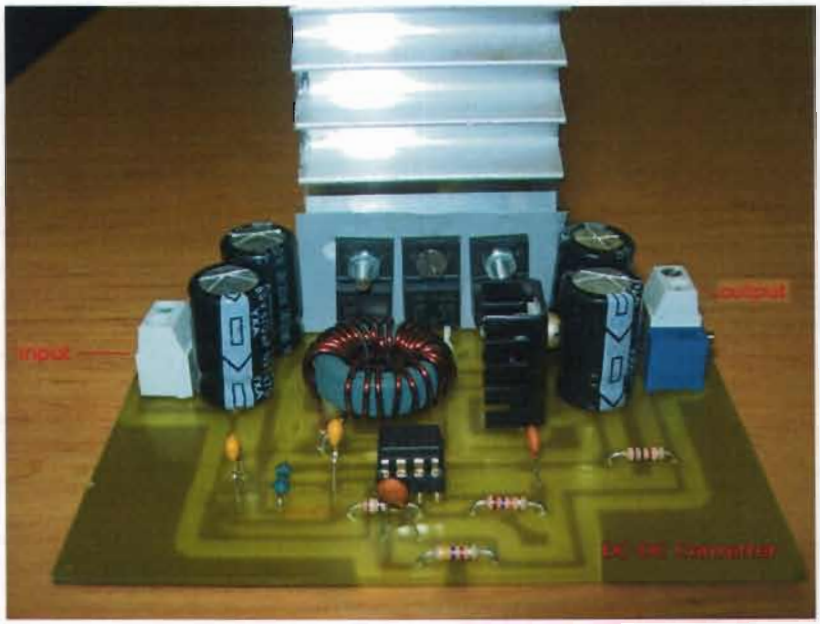

Figure 38 DC-DC converter

3.6 Summary

This chapter discussed the design and construction of a PAFC. This included the discussion of the individual components of the device. The design of the DC-DC converter was also presented. From the experimental data, the mathematical, equivalent electronic circuit and simulation models as discussed in Chapter 2 were constructed and validated. The models for a desired 100 W FC stack are adopted.

In Chapter 4, the experimental work and hardware setup of the PAFC is explained. The FC analysis and results are then presented. The simulation of the adopted 100 W FC stack concludes the chapter.

Chapter 4 Measurements and results

The previous chapter presented the designs of the PAFC unit cell through its various components, cell hardware, and electronic circuit model for optimisation to a 100 W FC stack and the DC-DC boost converter. Chapter 4 is devoted to the explanation of the experimental setup of the hardware and equipment used for the PAFC tests, results, and the interaction between various components and the performance of the unit cell as well as comparisons with the simulation models.

4.1 Experimental

All experiments were performed on a single cell and results were used to model a 100 W PAFC stack as previously stated. The experiments carried out show the potential of the PAFC and its prospects as an alternative power supply in a remote telecommunications system.

A 300 W digital electronic load from TTi allows operating the cell in constant current / voltage / resistance mode. The voltage of the cell was measured separately with a digital multimeter. Furthermore two thermocouples were connected to the data logger for the monitoring of system temperatures. All heaters were controlled by a temperature controller of the model Autonics TOS B4RJ3C (Korea).

The K-type (NiCr-Ni) and J-type (iron- copper/nickel) thermocouples were placed in the thermocouple wells on the side of the graphite block and the lead wire taken out to the data logger.

The FC was operated for eighteen hours continuously at a temperature of around 150 °C measured at the centre of the FC graphite block. The FC used hydrogen and air at less than 0.2 bars.

For data recording, all measuring devices were connected to the data logger (DAqpro). The flow rate and the pressure of the oxidant were manually controlled. The air (oxygen) pump is controlled by switching it on or off and its pressure and

flow is controlled by a digital mass flow controller. A detailed discussion on the setup and equipment is detailed below.

4.2 Fuel cell test equipment

The performance of the FC stack depends on the operating temperature, pressure of the inlet gas streams and the current. The experimental setup must be able to control the temperature and the mass flow of the reactant gases. Overall, the success of the PAFC test apparatus relies on the control of these parameters. The test apparatus is designed to control the operating variables that have an impact on the performance of the FC.

Ideally, all parameters would be automatically controlled and adjusted through the computer interface, but this would increase the complexity and cost of the test apparatus. Therefore, all parameters were manually controlled.

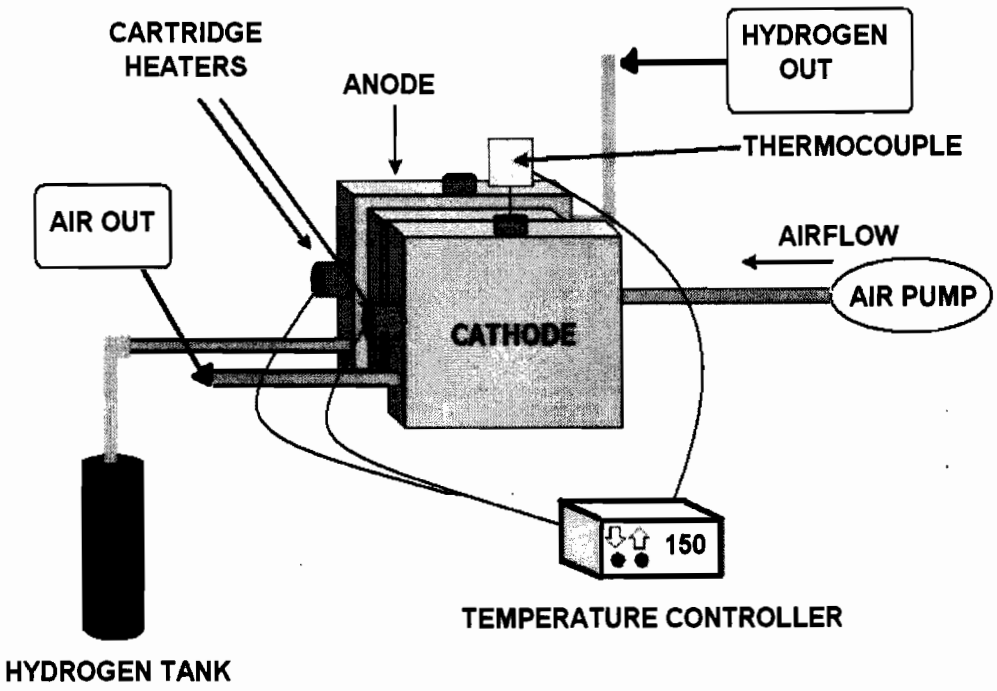

Figure 39 Fuel cell experimental setup

The devices that need to be precisely controlled include the mass flow controllers for the inlet gases, the electronic load, temperature controller and pressure regulators. The temperature of the FC will be controlled automatically, but the set points will be manually put into the heater control unit. The FC experimental setup is illustrated in Figure 39 and Figure 42 is a photograph of the experimental setup.

Air is supplied into the FC by means of an aerator. The advantages are its low cost and ability to maintain a low pressure of typically less than 2 bars needed for this particular FC. The aerator is also silent and can be operated for longer periods and is very efficient due to its low power consumption. The aerator must conform to strict standards in order to keep the air free of substances that could obstruct the matrix assembly or destroy the catalyst. In this way the aerator must be oil free. The commercial blowers and compressors have a large flow rate for the PAFC used in this study.

The use of hydrogen is due largely to the fact that it is the most electroactive fuel for use in FCs. It has exchange current densities for the cathodic reaction that are at least three to five orders of magnitude higher than any other fuel at low to intermediate temperatures (Srinivasan 2006:431).

Fuel (hydrogen) for the FC is supplied from a pressurized commercial cylinder through the pressure regulator. For better performance, hydrogen supplied should be pure (99.99 percent purity). This particular FC design is operated at low pressures and hence the hydrogen pressure should be less than 15 KPa. Hydrogen mass flow rate was measured using the digital mass flow meter (DMFM) and the flow was controlled using a ball valve.

The fuel pressure measurement in this research study was achieved by employing a PTX series pressure transmitter from Rototherm instrumentation. They employ a chemical vapour density sensing element and are therefore highly stable and accurate. These pressure transducers are a range of precision 2-wire pressure transmitters. They are factory calibrated for an excitation of 8 – 36 V DC to deliver an output of 4 mA at 0 pressure and 20 mA at full scale. Pressure ranges are from -1 bar to 600 bars.

The fuel and oxidant supply systems are similar in design. As stated above, the gases are supplied to the stack through components that regulate mass flow and pressure. The component designs are shown in Figure 40 and Figure 41 respectively. The connections between components for each system are made with PTFE tubing.

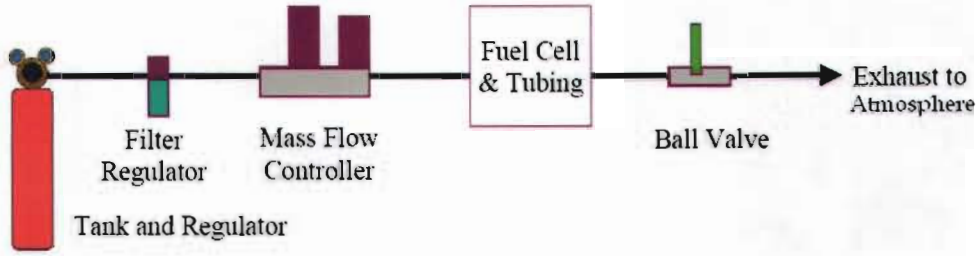

Figure 40 Hydrogen pressure regulation schematic

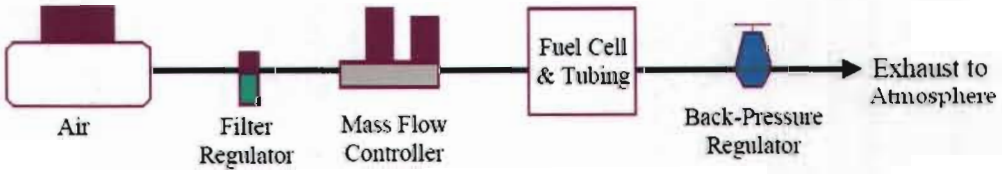

Figure 41 Air pressure regulation schematic

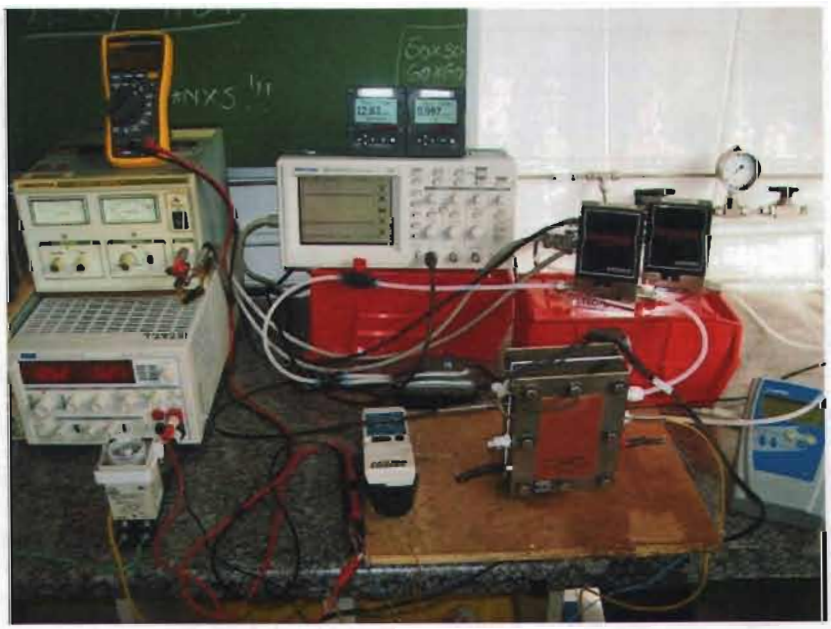

Figure 42 Experimental setup

The mass flow for the reactant gases, the fuel and the oxidant gas are dependant on the FC power. As the current is drawn by the load, hydrogen is reduced into protons and electrons at the reaction side (electrode-membrane interface) and because current is a measure of the flow of electrons, the hydrogen mass flow is directly related to the current. The actual mass flow of hydrogen depends on the current and the stoichiometry on the anode side of the FC. The test apparatus will typically run hydrogen dead-ended.

The mass flow of reactant gases was realised by employing the use of Smart-Trak Series 100 gas flow meters from Sierra Instruments Inc. Their operation is based on the heat transfer and the first law of thermodynamics. A small amount of the total gas is passed through a sensor tube which is maintained at a constant temperature and gas molecules carry heat from the sensor tube to the main flow tube so that the resulting temperature difference is linearly proportional to the mass flow (Sierra Instruments Inc.2005:1-4).

The DMFM is installed in series onto a hydrogen supply line. Mass flow meters require a provided power supply and output a voltage proportional to the mass flow of the reactant gases. The output of the mass flow is 6 standard litres per minute (SLPM) for each volt of the output.

The following calculation determines the maximum H_2 flow rate.

$$m_{H_2} = \frac{P\left(SR_{H_2}\right) \times M_{H_2}}{nFV_C} \tag{4.1}$$

Where:

$P \equiv$ the maximum power for the apparatus (4 W)

$SR_{H_2} \equiv$ the design stoichiometric ratio for hydrogen (2)

$M_{H_2} \equiv$ the molar weight of hydrogen (2 g/gmol)

$n \equiv$ the number of electrons (2)

$F \equiv$ Faraday's constant (96 484 C/mol)

$V_C \equiv$ the design cell voltage (0.5)

In this calculation, it is assumed that the minimum voltage at which a cell would operate is 0.5 V.

$$m_{AIR} = \frac{1}{2}\left(\frac{4.76 M_{AIR} P(SR_{AIR})}{nFV_C}\right) \tag{4.2}$$

Where:

$P \equiv$ the maximum power for the apparatus (4 W)

$SR_{H_2} \equiv$ the design stoichiometric ratio for air (2.5)

$M_{AIR} \equiv$ the molar weight of air (28.97 g/gmol)

$n \equiv$ the number of electrons

$F \equiv$ Faraday's constant (96 484 C/mol)

$V_C \equiv$ the design cell voltage

The minimum mass flow criteria are established by the range of the mass flow controllers. The controllers were capable of metering flows greater than 2 percent of full scale. This condition resulted in minimum flows of 0.8 SLPM for the fuel system and 2 SLPM for the oxidant system.

The pressure requirements of the FC test apparatus depend on the stack itself. Each FC stack and matrix has specific temperature limits which in turn have impacts on the type of material used in construction of the apparatus. The typical pressure limit for PAFC is approximately 400 KPa gauge. The minimum pressure is atmospheric pressure. However, the minimum working pressure is determined by the individual FC and the pressure drop associated with the gas streams flowing through the stack.

Owing to the difference in gas supplies, the pressure regulation will also be slightly different. The regulation of the hydrogen pressure was done by changing the pressure setting on the regulators. The air pressure is also controlled by the use of the regulator which is positioned before the mass flow controller.

Figure 43 Mass flow meter readings

The electronic load is the driving force for the entire FC testing. Applying the load to the FC at the wrong time can cause serious damage to the device. Because of this, the load applied to the stack must be adjustable and have the capability of being disengaged quickly.

As earlier stated, FCs are low voltage and high current devices, and the load must have the capability to measure and draw loads such as this. The electronic load used for the test is shown in Figure 44 below.

Figure 44 Electronic load showing output voltage and current

The test apparatus will have the ability to record data and in addition must be able to display the same data during testing. In any system, the output can only be as accurate as its least accurate component therefore the data needs to be as accurate as possible owing to the fact that it provides a clear picture of the system's efficiency and effectiveness as much as its overall performance.

4.3 Fuel cell testing

After assembling, the fuel cell was connected to the test set-up and was then ready for operation. The first task in the start-up sequence is checking for fuel leaks in the cell. There are a couple of tests that need to be run before and during operation so as to get all the required data for performance characteristics of the FC. The tests are described below:

- Cross-over test: this is the first test done after assembling the FC. The test is done in order to test for gas crossovers and can be done in many ways according to the size and type of fuel cell. In this study, the simplest cross-over test was done. The air supply is shut off, while maintaining a steady stream of hydrogen to the anode. Any hydrogen leak into the cathode chamber will result in the lowering of the pressure from the regulator, and hence indicating the gas cross-over. Note should be taken that all the open air channels are closed to prevent the entry of external air into the fuel cell.

- Open circuit testing: suffice to mention again here that this is the maximum possible voltage across the cell when no current is flowing. Most of the hydrogen-oxygen fuel cells have an OCV in the range of 0.8-1.0 V. When the FC has a lower value than this range, it may be due to either gas cross-over or electronic short circuit through the matrix or the poisoning of the catalyst or the electrolyte.

- Cell voltage as a function of current density: the FC is a device that produces voltage and hence the cell voltage test is the most important performance test for all FCs. The output cell voltage is obtained by continuously increasing the

current density starting from a lower value and in this particular study, from 5 $mAcm^{-2}$ to the maximum attainable value depending on the type and size of the cell (in this case 5 Acm^{-2}). Most of the researchers recommend 5 – 7 points per decade of current density to be collected. The important part in data collection with this test is to stay at each current value for several minutes to allow the voltage to reach a stable value (except in the case of quick screening).

- Reactant flow rates: the reactant flow rate has an influence on the performance of the matrix assembly. The flow rate can also provide diagnostic information on the status of the membranes. This is shown for example when the FC performance improves with higher flow rates of air, which implies a cathode-flooding problem. An increase in the air flow rate can help in removing the water in the form of water vapour thus providing for better access of oxygen to the cathode. Again, better cell performance with lower flow rates imply operating the matrix fairly wet and increased moisture retention arising out of lower gas flow rates improves cell performance.

- Effect of reactant pressure: the controlled increase and decrease of the reactant pressure helps in making sure that the matrix assembly gives the best performance and thus protects it from potential damage. The FC membranes are very delicate and too much reactant pressure can damage them. The increase in reactants gas pressure leads to the improvement in the FC performance as well as facilitating in the high temperature operation of the FC. However, the drawback of water balance still exists which has to be managed. With the use of air, the pressure effect is more pronounced due to the lower concentration of oxygen in air (Srinivasan 2006:296).

The FC was installed in the testing apparatus and was then ready for operation. At OCV, the supply of the reactants was at a temperature of about 150 °C and at ambient pressure. Hydrogen of 99.99 percent purity and air were used as the

reactants for the anode and the cathode respectively. The flow rate of hydrogen and airflow was kept constant.

The operation of the FC was characterized at the different operating conditions. Data of the polarisation curves were recorded starting from the OCV and continuously incrementing the current of the cell until the cell voltage dropped below a given cut-off value. Single cell operating parameters are summarized in Table 4 below.

Table 4 Operational parameters for the PAFC

Cell temperature	150 °C
Hydrogen stoichiometry	2
Air stoichiometry	2
Hydrogen flow (cm^3 min^{-1} A^{-1})	14
Air flow (cm^3 min^{-1} A^{-1})	33
Clamping bolt torque	2.5 Nm
Air pressure	0.2 KPa
Hydrogen pressure	0.2 KPa
Air flow rate	1.002 SLPM
Hydrogen flow rate	11.82 SLPM
Ambient temperature	18 ° C

4.4 Performance characteristics of a PAFC unit stack

The performance of a FC is determined by the use of a polarisation curve. Measuring polarisation curves is widely acknowledged and used in FC performance testing. Polarisation curves together with resistance measurements provide information on the polarisations incurred in FCs.

Polarisation curves are normally measured by generating a current sweep with a load unit and recording the cell voltage as a function of current density. The voltage is measured for a given time after each step so as to achieve a steady state operation. A polarisation curve in Figure 45 below presents the performance of the PAFC

designed in this research study. The parameters used for this stack are tabled in Table 4 section 4.3.

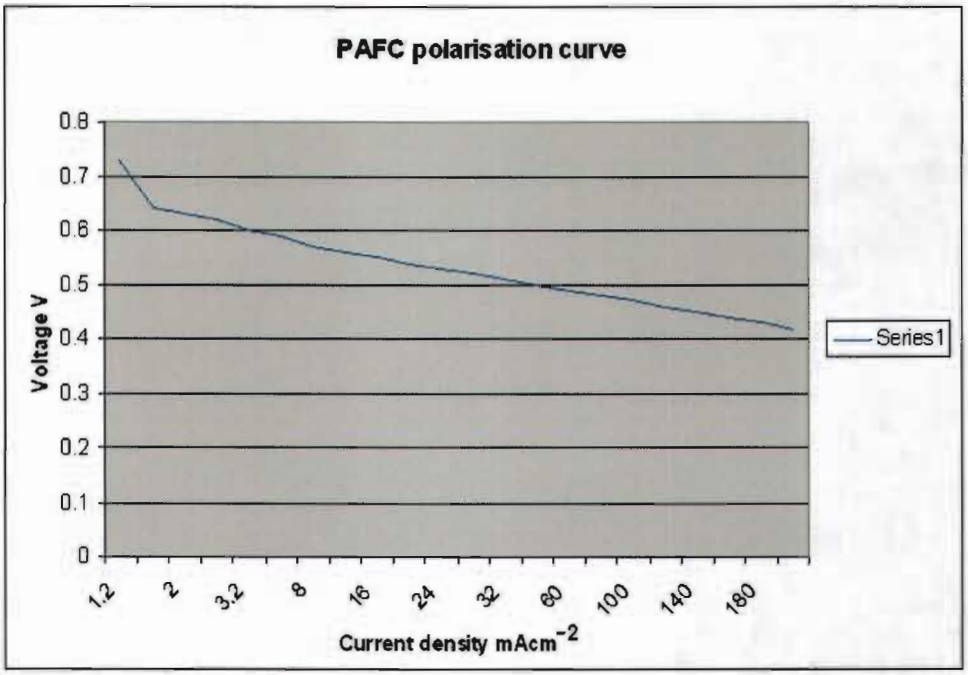

Figure 45 Performance curve for the PAFC stack

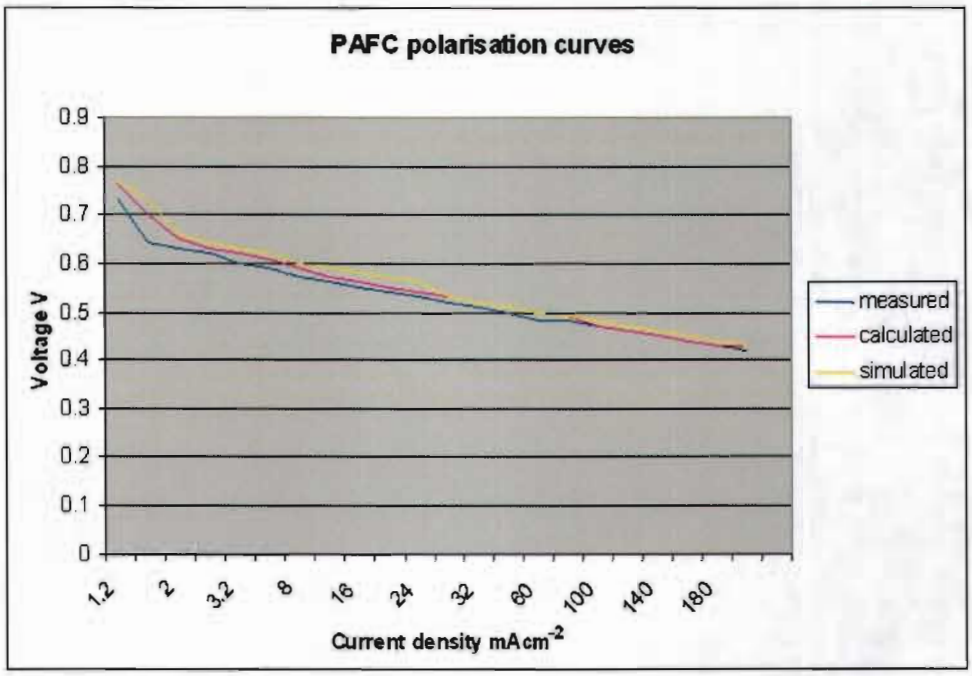

Figure 46 Performance curves for measured, simulated and calculated

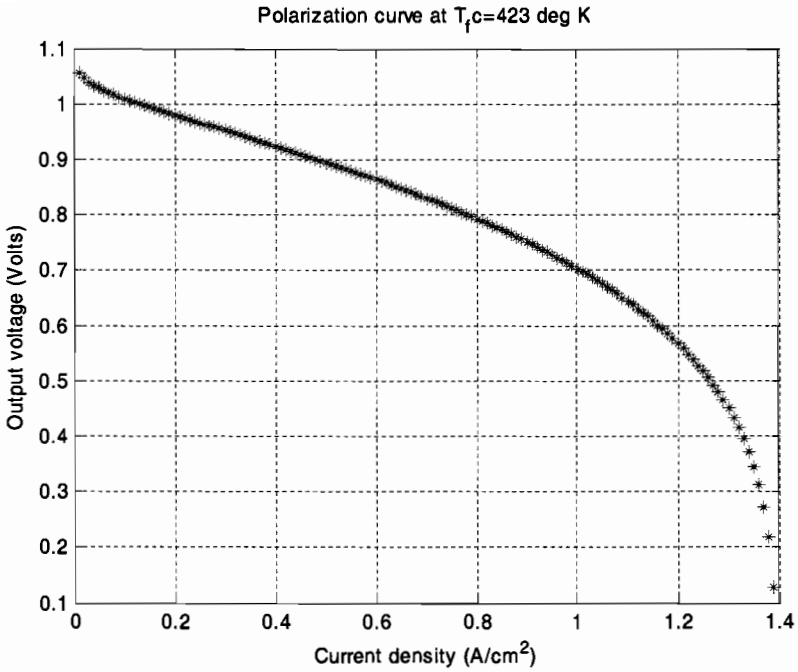

Figure 47 Polarisation curve for MATLAB simulation script in section 2.5

Figure 47 shows the simulated polarisation curve of the PAFC stack using MATLAB. The shape of the curve of the output voltage is in non-linear terms as activation loss occurs at low densities and mass transport loss at high current densities. Ohmic polarisation affects the fuel cell output voltage in the middle of current density.

The shape of the practical and the measured curve corresponds with the simulation curve and this shows that they can also be used in predicting the performance of any given size cell. The models can be used also for calculations on the performance of FC parameters when designing FC stacks. The simulation results and the experimental results confirm the feasibility of the proposed system.

The polarisation curves were subject to some experimental errors due to:

- variations in the fuel supply
- pressure fluctuations
- the precision of the temperature measurement
- the temperature difference between reactant gases and FC

While all of these errors are small, a way of estimating or calculating their impact on the polarisation curves quantitatively is beyond the scope of this study.

There are a number of aspects that contribute to the major differences between the simulated and the practical polarisation apart from the ones stated earlier in the preceding paragraphs in this section.

The use of air instead of pure oxygen and using humidified air and hydrogen instead of dry gases further reduces the maximum voltage obtainable from the FC to a lower value (Thomas and Zalbowitz 2000:13). Furthermore, Hirschenhofer *et al.* (1998:2-14), argue that the gas composition changes between the inlet and outlet of a FC caused by the electrochemical reaction, leads to the reduced cell voltages. This voltage reduction arises because the cell voltage adjusts to the lowest electrode potential given by the Nersnt equation for the various gas compositions at the exit of the anode and cathode chambers.

Another contributing factor is the impurities which could poison the catalyst and the electrolyte, thereby reducing the overall rate of reactions. Normally before the FCs are tested, the diffusion layers and the gas passages including the pipes are treated with nitrogen and are also nitrogen purged in an attempt to make sure they are free of impurities.

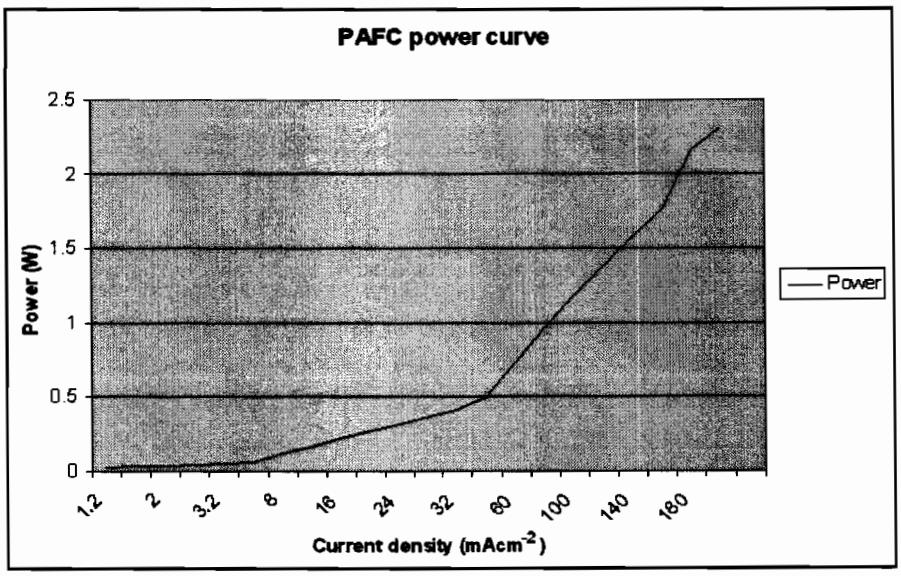

Figure 48 Power output of the PAFC

The output power of the FC increases as the pressure of the reactant gases is increased or the temperature of the FC is decreased. The power output of the FC is shown in Figure 48.

After continuous operation of the FC for almost eighteen hours, the output voltage did not show a significant decrease. However, the constraint was only due to the electrolyte reservoir. Owing to electrolyte leakages, the reservoir was partly sealed and the FC was not able to operate for longer hours because of the depletion of the electrolyte. After a number of trials, the membrane was checked and after a few hydrations it still operated efficiently.

One of the major problems encountered was the damage to the first membrane (anode-side) due to the high pressure of hydrogen which was applied only to the anode side and without any air supply to the cathode. This is observed owing to the rapid drop in the OCV. However, after extensive degradation of the matrix, more hydrogen and oxygen will mix, usually resulting in an open fire. Figure 49 below, shows a damaged membrane due to excessive pressure differences between the reactant gases. In this particular figure, the damaged part is circled in red.

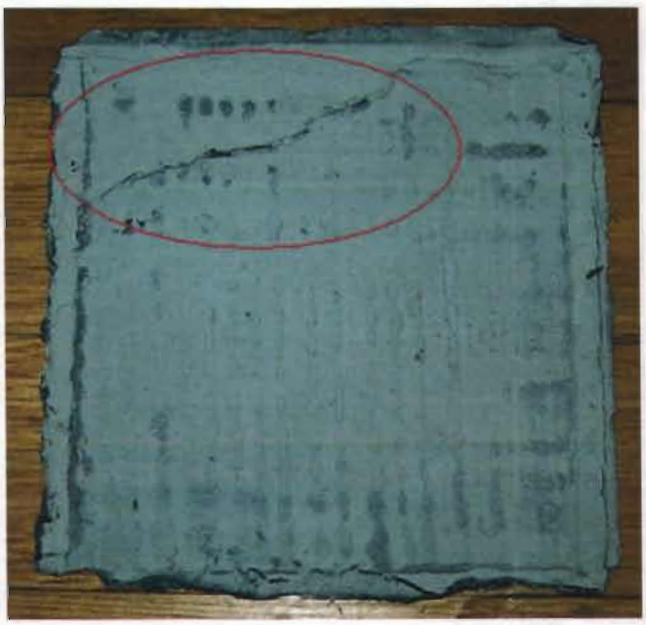

Figure 49 Damaged matrix assembly

The PAFC, as the name suggests, uses a liquid electrolyte in the form of concentrated H_3PO_4. Owing to the nature of the electrolyte, the FC needs greater care when assembling so that electrolyte leakages do not occur.

The start-up time was measured using a constant load of 0.5 A by means of an electronic load. The FC was heated to the operational temperature before the reactant gases were supplied to it. A current probe was used measure the current which is easily converted to voltage by means of an oscilloscope. Once the valves were opened, and the FC started producing voltage, the readings were taken simultaneously and recorded.

The start-up time was almost three seconds and it took the FC a further two seconds to stabilise. In order to measure the start-up time of the FC, the stack output voltage was measured by means of a data logger. Data were recorded from zero voltage when reactant gases are not supplied to the stack to a maximum stable voltage after the valves were opened. Results are shown in Figure 50.

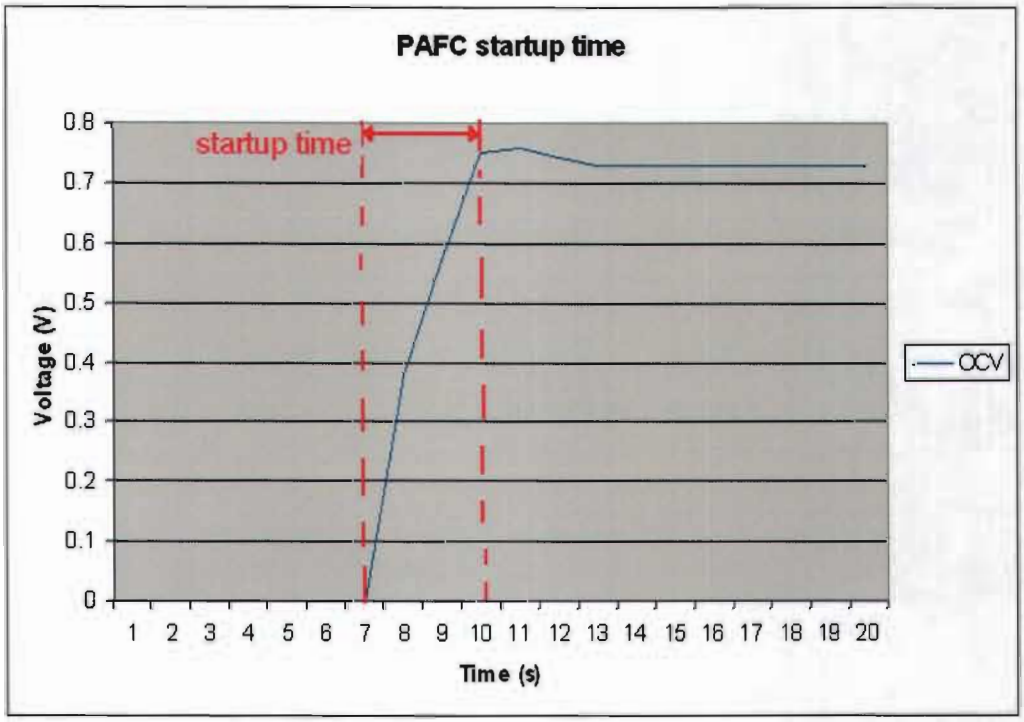

Figure 50 Startup time of the PAFC

From the graph in Figure 50, the zero voltage values depict the time when the data logger started logging in values whilst the reactant gases valves were still closed. After 6 seconds the valves were open and the FC started to give out voltage.

4.5 Performance characteristics of the power conditioning

Power conditioning is an important technology necessary for converting the DC electrical power generated by a FC into usable AC power for specific load requirements. However, as shown in Figure 11 on page 26, the electrical characteristic of a FC clearly shows that they are not an ideal electrical power source. A typical FC stack has a DC output voltage that varies widely with the load current and has a limited overload capability.

As stated earlier, a DC-DC converter stage is often required to increase and regulate the FC voltage to higher voltage levels for further processing into AC through a DC-AC inverter stage. Another characteristic of a DC-DC converter is the ability to provide a constant output voltage irrespective of the fluctuations in the input voltage, as long as the fluctuations are within the converter specification or input limits.

The design of the boost converter is discussed in section 3.5 in the previous chapter. The converter output characteristics are shown in Figure 54 on page 83. The output of the converter was connected to the electronic load and supplied with an input voltage of 5 V resembling an output voltage of the FC stack. The results as shown from the electronic load gives a good correlation with the converter output characteristics of a regulated 25 V DC output voltage. Even with a variation in the input voltage of between 4-7 V, the output remained at 25 V.

The setup of the test procedure is shown in Figure 51 overleaf. The first test on the converter was by varying the input voltage and then measuring the output voltage at full load. The results of this test as shown by the output voltage are depicted in Figure 54 on page 83. The second test was to reduce the input voltage at the same condition and observing the output voltage. These results are shown in Figure 55 on page 84. The graph shown in Figure 56 on page 84 gives the results of varying the input voltage up and down intermittently.

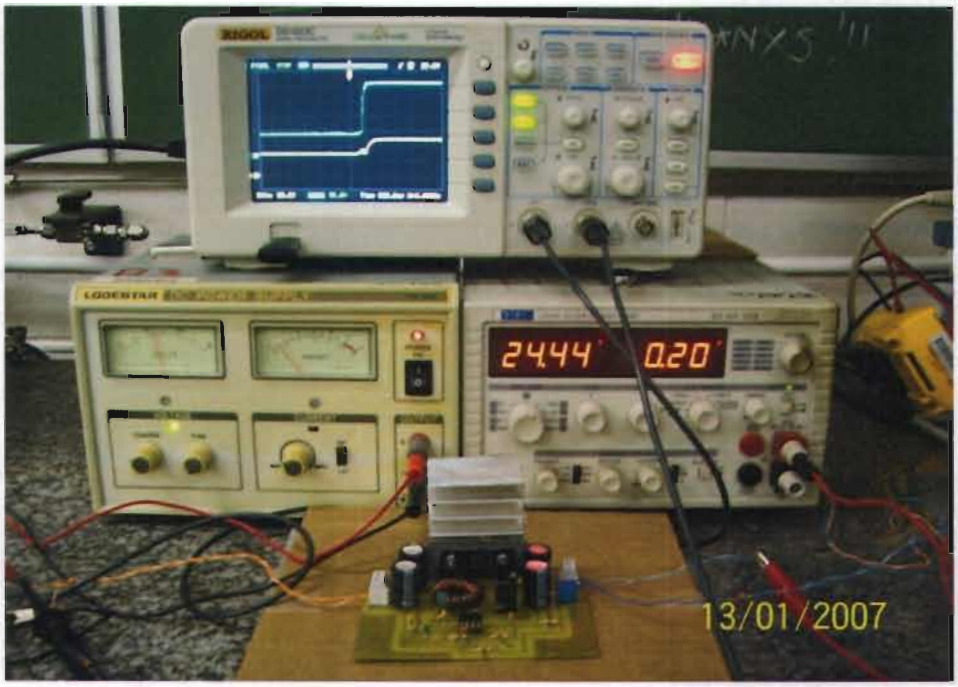

Figure 51 DC-DC converter under test

Figure 52 shows the output power delivered by the converter. However, the output power delivered by this particular converter was up to 10 W.

Figure 52 DC-DC converter showing power delivered by the converter

In spite of a change in input voltage to the converter, the output voltage stays at a constant voltage.

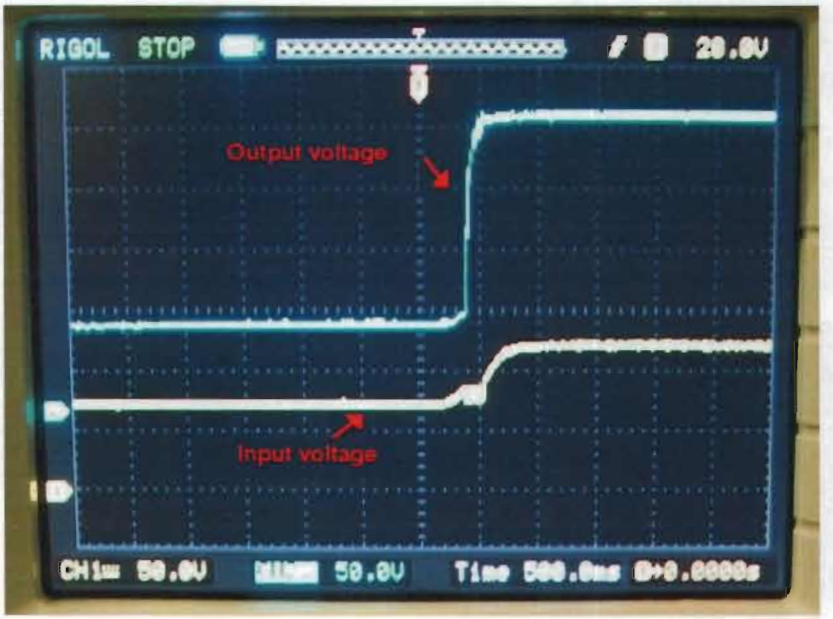

Figure 53 Output voltage of converter with input voltage from below limit

Figure 54 Output voltage of the converter with increasing input voltage

Figure 55 Output voltage of the converter with decreasing input voltage

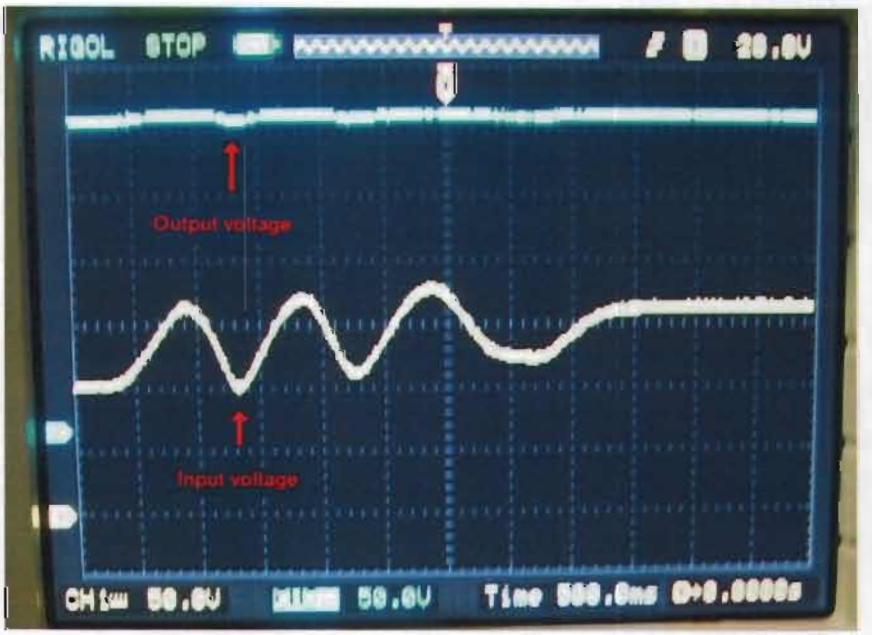

Figure 56 Output voltage of the converter with varying input voltage

The results in these graphs (Figures 53-57) shows that when the converter is connected to a FC stack and irrespective of the stack voltage variations, a constant output voltage will always be maintained.

Lastly, the input voltage was kept at a constant level whilst the load current was varied from a minimum value at almost 0 A to a maximum of 0.6 A. The output voltage was then measured. The resulting graph in Figure 57 shows that the output voltage stays the same even with the load current changes.

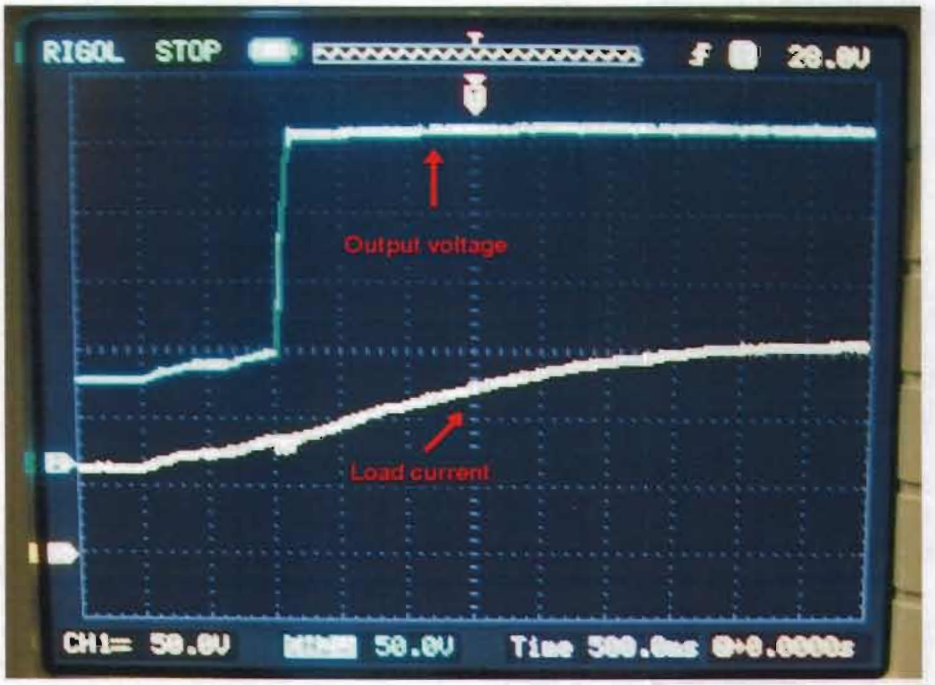

Figure 57 Output voltage of the converter with changing load current

4.6 Simulation of the 100 W stack system

Section 3.4.3 in the previous chapter outlined the discussion on the simulation procedure for the DC-DC boost converter. As stated again, the simulation is done using the MATLAB toolbox. The graph in Figure 58 shows the output of a simulation model of a FC output connected to a boost converter.

On the same Figure 58, the bottom graph shows the switching frequency and current while the middle graph is the input to the boost converter. The upper graph is the output voltage of the boost converter at a steady output voltage. The simulation graph also showed that even with variations in the input voltage within a specified voltage, the output will always be fixed at a specified level.

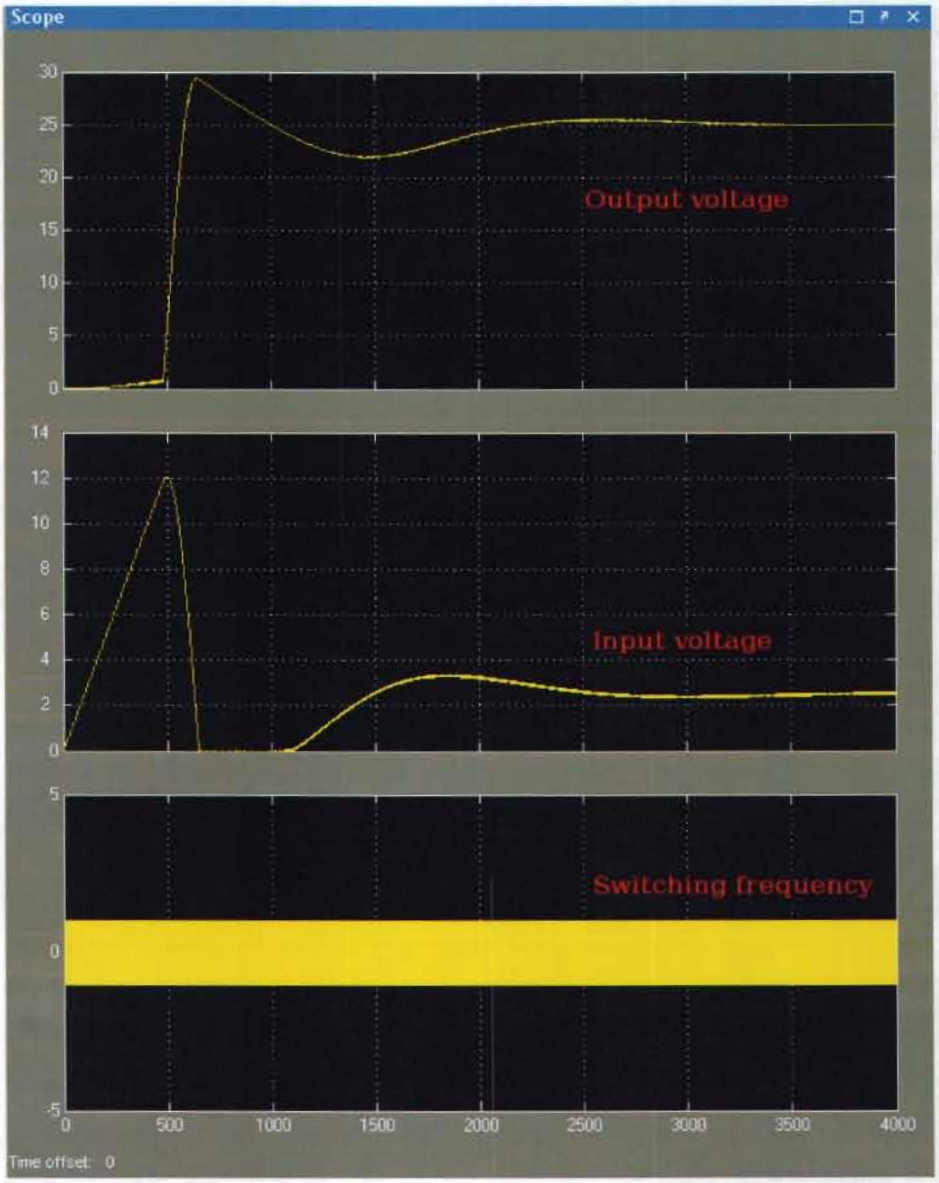

Figure 58 Simulation results of the DC-DC boost converter connected to a FC stack

4.7 Summary

The experimental description as well as the FC test setup equipment were presented. The performance characteristics of the PAFC unit stack and the power conditioning were also discussed. The correlation between the measured, calculated and simulation results yielded the final model of a 100 W FC system which was simulated and presented in this chapter.

The DC-DC converter under different input voltages was also discussed to ascertain its use in regulating the stack output voltage which is rendered useless without such regulation. Simulation results accompany the discussion.

In chapter 5, conclusions are drawn, suggestions for further improvements are also presented drawn from this research study and hence recommendations are made with regard to the research.

5 Conclusions and recommendations

5.1 Introduction

This chapter presents the conclusions drawn from this research document with regard to the design and development of a PAFC that can culminate in a 100 W stack for use as a stand-by power source in remote telecommunication sites. The topology for the use of power conditioning and regulation of the FC is also presented. Recommendations for future research will conclude this chapter.

5.2 Conclusions

The design and development of any FC is centred around the membrane. In this particular research study, the 'heart' of the FC is the electrolyte-retaining matrix. However, the research did not focus entirely on the actual manufacturing of the matrix. The electrode catalyst structure and the GDL together with the silicon carbide was built into one single structure – the electrolyte-retaining matrix. All major areas of the system performed their duties well except for the problem encountered with the leaking reservoir. A FC consisting of an electronic load, temperature controller, data logger and a separate power conditioner module (DC-DC converter) was integrated.

The thesis sets down some preliminary investigations that are useful in delivering a PAFC power system. Amongst the investigated items, the electronic circuit model of the FC was investigated. The model is simple and uses a diode and a pair of bipolar junction transistors (BJTs) for static conditions and a capacitor and inductor for dynamic conditions. The model is validated by comparing the simulation and experimental results.

The FC was modelled mathematically and the electrochemical model was established. The equivalent circuit models were discussed and used to model and implement the performance of the whole unit cell. This showed that the performance of a relatively small stack can be accurately scaled up to represent the performance of a larger stack.

Amongst the various flow field topologies described, it was found that the column flow topology was the best choice for the PAFC design as it had a low pressure drop from inlet to output resulting in lower auxiliary power and thus helping in preventing the build-up of water in the reactive areas of the flow fields.

The operating temperature of the FC was kept constant by using the temperature controller; however when the temperature was let to drift slightly from 150 °C to 180 °C with an increase in pressure, an effect on the output voltage of the FC was observed.

The fuel and oxidant were supplied at an acceptable temperature at relatively higher mass flow rates initially. A load was applied to the FC at the appropriate time after the OCV had stabilised and was at a correct value. Most importantly, the FC together with the test apparatus yielded a polarisation curve for the unit cell that was consistent with the curves found elsewhere in literature and also by other researchers.

It was also concluded that even though the theoretical output voltage of the PAFC as calculated in Chapter 2 was 1.23 V, the PAFC physically would give an E_{OCV} value of 0.784 V and would operate at between 0.6 V and 0.7 V. The output voltages are tabled in Table 3 on page 57.

A common safety concern for FC systems is hydrogen leaks. In order to curb this, different torques were implemented until the satisfactory torque was achieved. However, the used torque should be in agreement with the contact pressure exerted on cell components and on the membrane. It was found that the required torque should be sufficient for avoiding gas leaks and also not damage the matrix assembly.

A simulation of the performance of the FC feeding a boost converter was also studied. The values of the components of the converter were calculated based on the presented design specifications. It was observed that with varying input voltages, the boost converter always produced a regulated output voltage. The experimental results were in close agreement with the simulation results and showed that the system produces a good performance.

The use of the power-conditioning devices was found to be influenced by the non-linearity of the stack output voltage so that the power of the FC can be useful. The start-up time of the PAFC was also investigated even though it was started only after the cell had maintained its operational temperature of 150 °C. This may yield a higher value than the 2 seconds if determined at a lower temperature.

5.3 Recommendations

This project has laid groundwork for more complex research work in this area of the PAFC. However, it leaves a lot of possibilities to be explored, some of which are listed here:

- The performance of the stack voltage under varying conditions: For example, the performance of the stack voltage with and without the temperature effect and its overall effect on the load can be ascertained.

- The operation of the FC under different atmospheric conditions: pressure, temperature and humidity.

- The use of different materials for flow field plates or bipolar plates other than graphite and the effect of different flow field topologies other than the column flow topology on the output voltage.

- To implement the control scheme and simulate the complete system in FClib, MATLAB and or PSpice.

- Although the test apparatus was able to acquire a polarisation curve relatively easily, there are significant modifications and improvements that could strengthen its abilities. This include the acquisition and use of a FC test bench where the use of programs such as LABVIEW would simply send a set point signal to controllers and everything would be automated.

BIBLIOGRAPHY

ACHARYA, P.R. 2004. *An advanced fuel cell simulator*. Texas: Texas A&M University.

ACRES, G.J.K. 2001. Recent advances in fuel cell technology and its applications. *Journal of Power Sources*, 100: 60-66.

ADAMS, A.M., BACON, F.T. and WATSON, R.G.H. in: MITCHELL. W. Ed. 1963. *Fuel cells*. New York: Academic Press.

ALCOCK, J., SHIRVILL, L. and CRACKNEL, R. 2001. *Compilation of existing safety data on hydrogen and comparative fuel*. Deliverable report, EIHP 2, May.

AMPHLETT, J.C., BAURNERT, R.M., MANN, R.F., PEPPLEY, B.A. and ROBERGE, P.R. 1995. Performance modelling of the Ballard Mark IV solid polymer electrolyte fuel cell, empirical model development ii. *Journal of the Electrochemical Society*, 142:9-15.

APPLEBY, J. and FOULKES, F.R. 1993. *Fuel cell handbook*. New York: Van Nostrand.

ARCHANT REGIONAL. The future of windfarms. 2004. [Online]. Available at: < http: // www.edp24.co.uk/windfarms/asp/Why/Glogal_B2iii.asp>. Accessed: 20/02/2007.

ASCOLI, A., PANDYA, J.D. and REDAELLI, G. 1989. Modelling of an electrolyte matrix for a phosphoric acid fuel cell. *Energy*, 14:875.

BARBIR, F. 2005. *PEM fuel cells theory and practice*. New York: Academic Press.

BELL, S. 2001. An assessment of PAFC for distributed power generation. *Journal of Power Sources,* 108: 69-80.

BLOMEN, L.J.M.J. and MUGERWA, M.N. 1993. *Fuel cell systems*. New York: Plenum Press.

BRANDON, N. and THOMPSETT, D. 2005. *Fuel cells compendium*. Oxford: Elsevier.

BROWN, S.L. and HOLME, A.T. 2006. *Chemistry for engineering students*. California: Thomson Brooks/ Cole.

BRUCE, P. G. 1995. *Solid state electrochemistry*. Cambridge: Cambridge University Press.

CARRETTE, L., FRIEDRICH, K.A. and STIMMING, U. 2001. *Fuel cells fundamentals and applications*. New York: Springer.

COUNIHAN, M.A. 1981. *Dictionary of energy*. London: Routledge and Kegan Paul.

DACHUAN, Y. and YUVARAJAN, S. 2004. Electronic circuit model for proton exchange membrane fuel cells. *Journal of Power Sources*, 142: 238-242.

DYER, C.K. 2002. Fuel cells for portable applications. *Journal of Power Sources*, 106: 31-43, April.

EG & GT TECHNICAL SERVICES INC. 2002. *Fuel cell handbook*. 6th edition. United States Department of Energy publication.

ERDC. Phosphoric acid fuel cell (PAFC) demonstration program. 2007. [Online]. Available at: <http://www.erdc.army.mil/pls/erdcpub/!www_fact_sheet.research_page?ps_rp_numb=58854&tmp_Main_Topic=51586&page=BENEFITS>. Accessed: 23/03/2007.

ERICKSON, R.W. and MAKSIMOVIC, D. 2001. *Fundamentals of power electronics*. 2nd edition. Colorado: Kluwer Academic Publishers.

FERET, J. M. 1990. Air cooled PAFC technology. *Journal of Power Sources*, 180:29

GROVE, W.R. 1839. The first fuel cell.*Philosophical Magazine*. 14:127. [Online]. Available at:<http://chem.ch.huji.ac.il/history/grove.htm> Accessed: 15/06/2007.

HEINZEL, A., HEBLING, C., MULLER, M., ZEDDA, M. and MULLER, C. 2002. Fuel cells for low power applications. *Journal of Power Sources*, 105(2): 250-255, March.

HIRSCHENHOFER, J.H. 1992. Latest progress in fuel cell technology. IEEE-*Aerospace and Electronics Systems Magazine*, 7 Nov.

HIRSCHENHOFER, J.H. and McCLELLAND, R.H. 1995. The coming of age of fuel cells. *Mechanical Engineering,* vol.117, 10: 84-88.

HIRSCHENHOFER, J.H., STAUFFER, D.B., ENGELMAN, R.R. and KLETT, M.G. 1998. *Fuel cell handbook.* 4th edition. Published under contract. United States Department of Energy.

HIRSCHENHOFER, J.H. and STAUFFER, D.B. 2004. *Fuel cell handbook.* 5th edition. Published under contract. United States Department of Energy.

HOOGERS, G. 2003. *Fuel cell technology handbook.* Florida: CRC Press LLC.

KAYASHIKI, T. and YOTSUMOTO, K. 1992. Advanced fuel cell energy system for telecommunication use. *Telecommunications Energy Conference,* IEEExplore 1-2: 4-11.

KING, A. and ISHIKAWA, L. 1996. *Fuel cells for direct generation.* New York: CRC Press.

KORDESCH, K. and SIMADER, G. 1996. *Fuel cells and their applications.* Germany: VCH Weinheim.

LARMINIE, J. and DICKS, A. 2000. *Fuel cell systems explained.* New York: John Wiley and Sons.

LARMINIE, J. and DICKS, A. 2003. *Fuel cell systems explained.* 2nd edition. Chichester, England: John Wiley and Sons.

LAUGHTON, M.A. 2002. Fuel cells. *Power Engineering Journal*, February.

LINDEN, D. 1984. *Handbook of batteries and fuel cells.* New York: McGraw-Hill.

LOVERING, D.G. 1990. *Fuel cells.* Barking, U.K: Elsevier.

MENCH, M.M. 2008. *Fuel cell engines.* New Jersey: John Wiley.

MIYAKE, Y., AKIYAMA, Y., HAMADA, A., ITOH, Y., ODA, K., SUMI, S., NISHIO, K. and NISHIZAWA, N. 1996. Status of fuel cells R & D activities at Sanyo. *Journal of Power Sources*, 61: 153-160.

O'HAYRE, R., WON CHA, S., PRINZ, F.B. and COLELLA, W. 2005. *Fuel cell fundamentals.* New York: John Wiley and Sons.

PALM, W.J. 2004. *Introduction to Matlab 7 for engineers.* New York: McGraw-Hill.

PASRICHA, S. and SHAW, S.R. 2006. A dynamic PEM fuel cell model. *IEEE Transactions on Energy Conversion*, Vol 21, 2: 484-490.

PUKRUSHPAN, J.T., STEFANOPOULOU, A.G. and PENG, H. 2005. *Control of fuel cell power systems – principles, modelling, analysis and feedback design.* London: Springer-Verlag London.

RASHID. M. H. 2004. *Power electronics circuit devices and applications.* 3rd edition. New Jersey: Prentice Hall.

SAKAI, T., ITO, T. and TAKESUE, F. 1992. Portable power source with low temperature operated PAFC. *International Power Sources Symposium*, IEEE 18: 49-52.

SAMMES, N., BOVE, R. and STAHL, K. 2004. Phosphoric acid fuel cells: Fundamentals and applications. *Journal article, Current Opinion in Solid State and Materials Science*, Vol 8. 5: 372-378.

SCOTT, D.S. 2004. Inside fuel cells. *International Journal of Hydrogen Energy*, 29: 1203-1211.

SHIBATA, K. 1992. Tokyo electric company (TEPCO) fuel cell evaluation program. *Journal of Power Sources*, 37: 81-99.

SORENSEN, B. 2005. *Hydrogen and Fuel cells - Emerging technologies and applications.* Oxford: Elsevier.

SRINIVASAN, S. 2006. *Fuel cells, from fundamentals to applications*: New York. Springer Science + Business Media.

STEELE, H., BRIAN, C. and HEINZEL, A. 2001. Materials for fuel-cell technologies. *Nature*, 414: 345-352.

THOMAS, S. and ZALBOWITZ, M. 2000. *Fuel cells green power*. New Mexico: Los Alamos National Laboratory.

TODOROVIC, M.H. 2004. *Wide input range DC-DC converter with digital control scheme*. Texas: Texas A&M University.

TODOROVIC, M.H., PALMA, L. and ENJETI, P.N. 2008. Design of a wide input range DC-DC converter with a robust power control scheme suitable for fuel cell power conversion. *Industrial Electronics, IEEE transactions,* vol. 55, 3:1247-1255.

VIELSTICH, W., LAMM, A. and GASTEIGER, A. 2003. *Handbook of fuel cells*. West Sussex: John Wiley and Sons.

WARSHAY, M. and PROKOPIUS, P.R. 1990. The fuel cell in space, yesterday today and tomorrow. *Journal of Power Sources*, 29: 193-200.

WEIDLICH, E. 1989. *Constructional features and operating characteristics of fuel cells*. New Delhi: Wiley Limited.

YANG, J.C., PARK, Y.S., SEO, S.H., LEE, H.J. and NOH, J.S. 2002. Development of a 50KW PAFC power generation system. *Journal of Power Sources*, 106: 68-75.

YERRAMALLA, S., DAVARI, A., FELIACHI, A. and BISWAS, T. 2000. Modelling and simulation of the dynamic behaviour of polymer electrolyte membrane fuel cell. *Journal of Power Sources*, 124: 104-113.

YOON, K.H., JANG, J.H. and CHO, Y.S. 1998. Impedance characteristics of a phosphoric acid fuel cell. *Journal of Materials Science Letters*, 17: 1755-1758.

YU, D. and YUVARAJAN, S. 2005. Electronic circuit model for proton exchange membrane fuel cells. *Journal of Power Sources*, 142: 238-242.

ANNEXURE A MATLAB program script for simulation

```
clear all;

clf;
prompt = {'Enter temperature in celsius (range 150):',
'Enter air pressure in atm (range 1.00-6.00):'
'Enter hydrogen pressure in atm (range 1.00-6.00):'
'Enter cell area in cm2:'...
'Enter number of cells:'
'Enter charge transfer coefficient (range 0.1-0.5):'
'Enter resistance (ohm/cm^2) (range 0.190-0.275):'
'Enter exchange current density (A/cm^ 2) :',}


dlg_title = 'PAFC MODELING/Part-1';
num_lines= 1.0;
def = {'150','3.0','2.0','25','2','0.5','0.80','0.190','10^-6.912'};

ans = inputdlg(prompt,dlg_title,num_lines,def);
ans1=ans{1};ans2=ans{2};ans3=ans{3};ans4=ans{4};ans5=ans{5};ans6=ans{6};
ans7=ans{7};ans8=ans{8};ans9=ans{9};

Tc=str2num(ans1);P_air=str2num(ans2);P_hyd=str2num(ans3);
A_cell=str2num(ans4);N_cells=str2num(ans5);Alpha=str2num(ans6);
UF=str2num(ans7);r=str2num(ans8);io=str2num(ans9);


prompt = {'Enter amplification constant:'
'Enter the limiting current density (A/cm2):'
'Enter constant k used in mass transport:'
'Gibbs function in liquid form (J/mol):'
'Fuel cell voltage based on higher heating value:'
'Molar gas constant in (J/mol K):'
'Faradays constant (Coulombs) :',};


dlg_title = 'PAFC MODELING/Part-2';
num_lines= 1.0;
def = {'0.085','1.4','1.1','-228170','1.48','2.016*10^-3','18.016*10^-3','8.1345','96485'};

ans = inputdlg(prompt,dlg_title,num_lines,def);
ans1=ans{1};ans2=ans{2};ans3=ans{3};ans4=ans{4};ans5=ans{5};ans6=ans{6};
ans7=ans{7};ans8=ans{8};ans9=ans{9};

Alpha1=str2num(ans1);il=str2num(ans2);k=str2num(ans3);Gf_liq=str2num(ans4);
E_HHV=str2num(ans5);Mm_H2 = str2num(ans6);Mm_H2O=str2num(ans7);
```

```
R=str2num(ans8);F=str2num(ans9);
Tk=Tc+273.15;
loop=1;
i=0;
for N=0:150
i=i+0.01;

% Calculations of voltage losses

% Calculations of activation loss

b=R.*Tk./(2.*Alpha.*F);
V_act=-b.*log10(i./io);

% Calculation of ohmic loss

V_ohmic=-(i.*r);

% Calculation of mass transport loss

term=(1-(i./il));
if term>0
V_mt=Alpha1.*(i.^k)*log(term);
else
V_mt=0;
end

% Calculation of Nernst voltage

E_nernst=-Gf_liq./(2.*F)-((R.*Tk).*log(P_H2O./(PP_hyd.*(PP_oxy.^0.5)))./(2.*F);

% Calculation of output voltage

V_out=E_nernst+V_ohmic+V_act+V_mt;
if term<0
V_mt=0;
break
end
if V_out<0
V_out=0;
break
end

figure(1)

title('Polarisation curve at T_fc=353 deg K')
xlabel('Current density (A/cm^2)');
ylabel('Output voltage (Volts)');
plot(i,V_out,'*')
grid on
hold on
disp(V_out)
```

```
% Calculation of power

P_out=N_cells.*V_out.*i.*A_cell;


figure(2)

title('T_fc=353 deg K')
xlabel('Current density (A/cm^2)');
ylabel('Power(Watts)');
plot(i,P_out,'*');
grid on
hold on
disp(P_out);



% Calculation of efficiency (HHV)

if V_out<=0
Efficiency_HHV=0;
else
Efficiency_HHV=(UF.*V_out.*100)./(E_HHV);
end

figure(4)

title('Fuel cell efficiency at HHV T_fc=353 deg K')
xlabel('Current density (A/cm^2)');
ylabel('Efficiency (%)');
plot(i,Efficiency_HHV,'*');
grid on
hold on
disp(Efficiency_HHV);
```

ANNEXURE B Calculations for r, A and m using matrices

From Table 3, in page 57, six points were taken:

Voltage (V)	Current (A)	Current density ($mAcm^{-2}$)
0.73	0.03	1.2
0.63	0.05	2
0.52	0.7	28
0.48	2	80
0.43	4.5	180
0.42	5.5	200

From the output stack voltage of the cell:

$$V_{Stack} = N_C E_{OC} - N_C ri - N_C A\ln(i) - N_C me^{ni} \quad \text{V} \qquad N_C = 1 \tag{G1}$$

$$0.73 = 0.784 - \text{r}\,(1.2) - \text{Aln}\,(1.2) - \text{me}^{(0.008)(1.2)}$$

$$0.054 = 1.2\text{r} + 0.1823\text{A} + 1.0096\text{m} \qquad [1]$$

$$0.63 = 0.784 - \text{r}\,(2) - \text{Aln}\,(2) - \text{me}^{(0.008)(2)}$$

$$0.154 = 2\text{r} + 0.6931\text{A} - 1.0161\text{m} \qquad [2]$$

$$0.52 = 0.784 - \text{r}\,(28) - \text{Aln}\,(28) - \text{me}^{(0.008)(28)}$$

$$0.264 = 28\text{r} + 3.3322\text{A} + 1.2511\text{m} \qquad [3]$$

$$0.48 = 0.784 - \text{r}\,(80)\ \text{Aln}\,(80) - \text{me}^{(0.008)(80)}$$

$$0.0304 = 80\text{r} + 4.3820\text{A} + 1.8965\text{m} \qquad [4]$$

$$0.43 = 0.784 - \text{r}\,(180) - \text{Aln}\,(180) - \text{me}^{(0.008)(180)}$$

$$0.354 = 180\text{r} + 5.1930\text{A} + 4.2207\text{m} \qquad [5]$$

$$0.42 = 0.784 - \text{r}\,(200) - \text{Aln}\,(200) - \text{me}^{(0.008)(200)}$$

$$0.364 = 200\text{r} + 5.29883\text{A} - 4.9530\text{m} \qquad [6]$$

These result in:

$$1.2\text{r} + 0.1823 + 1.0096 = 0.054$$
$$2\text{r} + 0.6931 + 1.0161 = 0.154$$
$$28\text{r} + 3.3322 + 1.2511 = 0.264$$
$$200\text{r} + 5.2983 + 4.9530 = 0.364$$

The above equations can be written in matrix form:

$$Ax = b \qquad \text{(G2)}$$

And this will yield:

$$A = \begin{matrix} 1.2 & 0.1823 & 1.0096 \\ 2 & 0.6931 & 1.0161, \\ 28 & 3.3322 & 1.2511 \\ 200 & 5.2983 & 4.9530 \end{matrix} \quad x = \begin{matrix} r \\ A \\ m \end{matrix} \quad \text{and} \quad b = \begin{matrix} 0.054 \\ 0.154 \\ 0.264 \\ 0.364 \end{matrix}$$

In order to solve for the solution matrix, x, equation G2 can be written in the form:

$$X = A^{-1}b$$

Where x was solved using MATLAB in order to obtain the values of r, A and m for simulation of polarisation curve, the values are:

$$r = -0.0041$$
$$A = 0.2019$$
$$m = 0.0219$$

The output voltage of the stack (G1) then becomes:

$$V_{Stack} = 23.52 + 0.123i - 6.057 \ln i - 0.657e^{0.008i}$$

ANNEXURE C **Graphite bipolar block drawing**

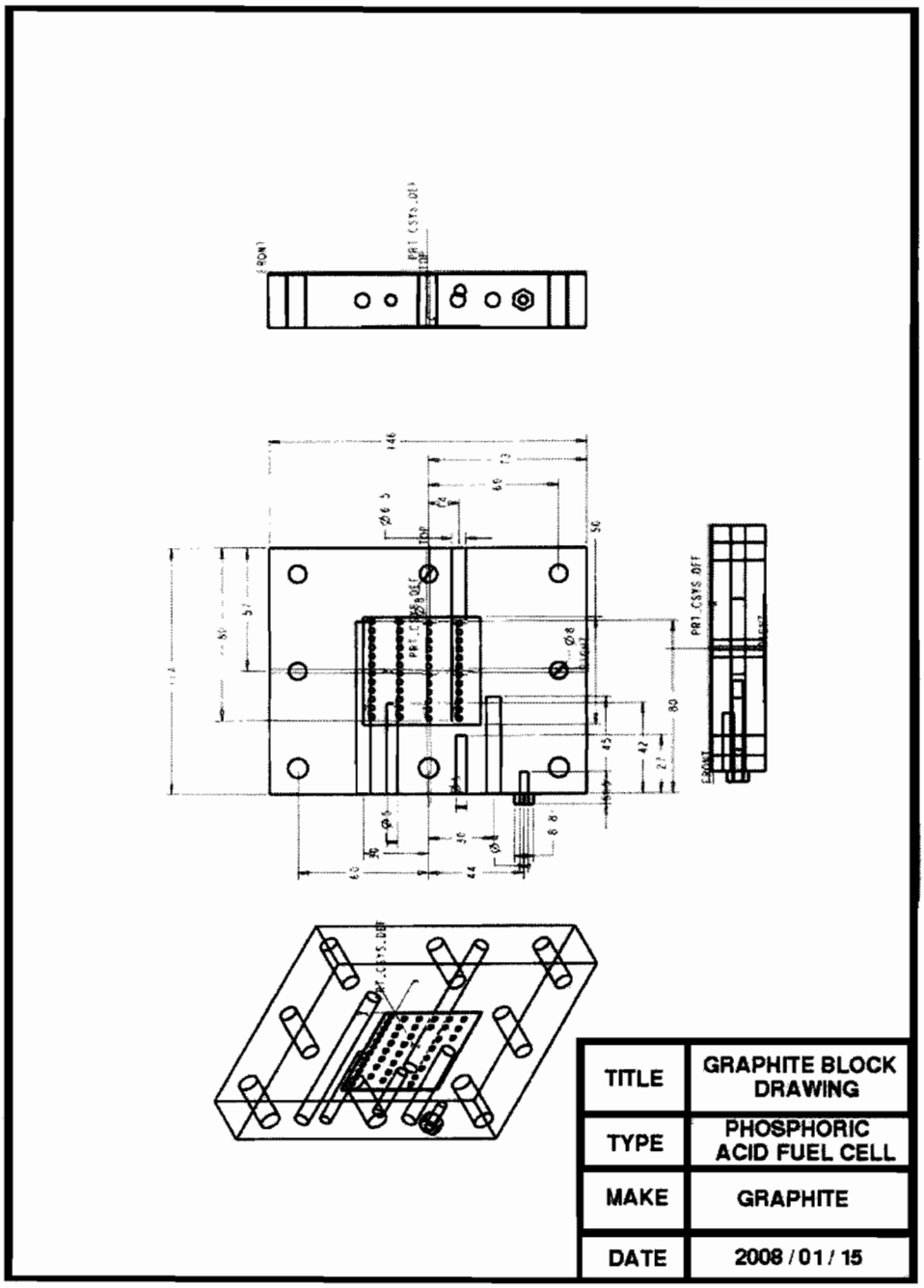

TITLE	GRAPHITE BLOCK DRAWING
TYPE	PHOSPHORIC ACID FUEL CELL
MAKE	GRAPHITE
DATE	2008 / 01 / 15

ANNEXURE D 3D diagram of graphite block

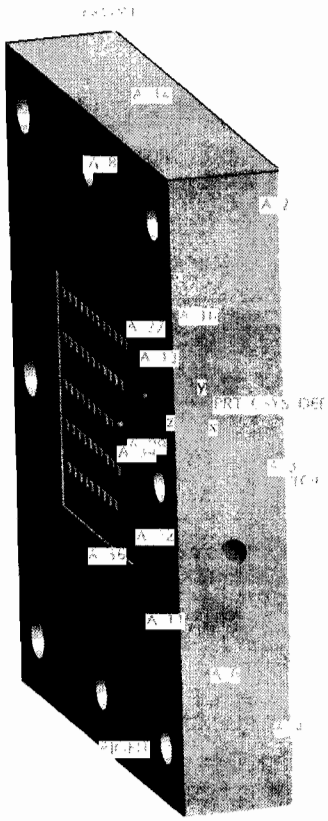

TITLE	GRAPHITE BLOCK WITH FLOW FIELD PATTERN
TYPE	PHOSPHORIC ACID FUEL CELL
MAKE	GRAPHITE
DATE	2008 / 01 / 15

ANNEXURE E **Side view of graphite block**

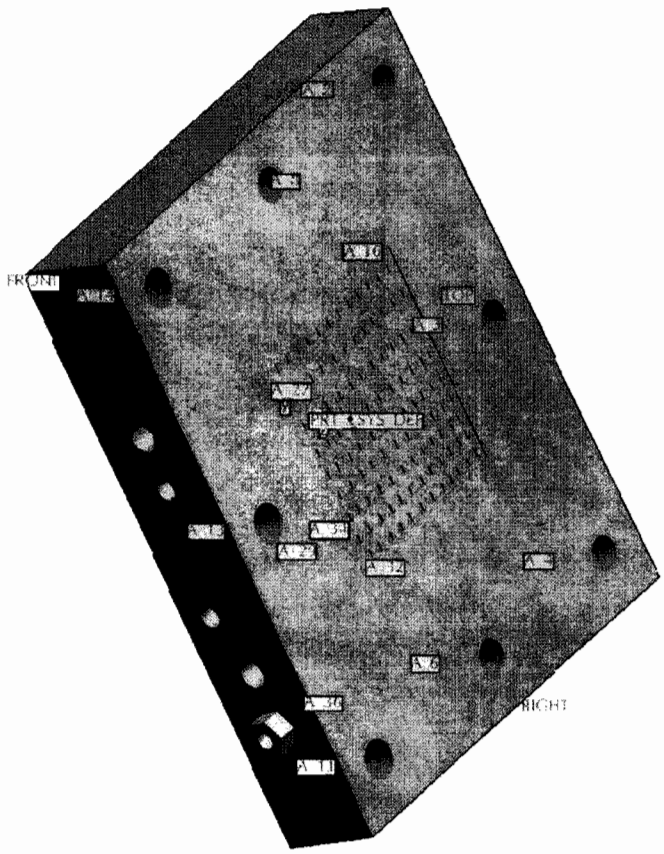

TITLE	GRAPHITE BLOCK WITH FLOW FIELD PATTERN
TYPE	PHOSPHORIC ACID FUEL CELL
MAKE	GRAPHITE
DATE	2008 / 01 / 15

PTx Series Pressure Transmitters

PTx Series Pressure Transmitters

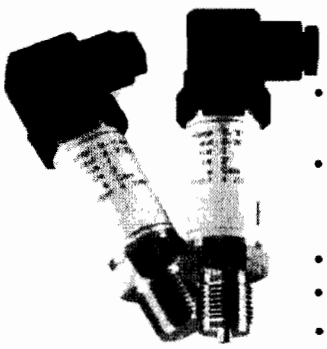

Application Examples

Monitoring product, process and hydraulic pressures and triggering safety shutdowns when hazardous conditions are detected.

- **Mining Industries** - Monitoring of hydraulic pit props to indicate condition of the prop and ground strata.
  Monitoring of hydraulic pressure on cutting machinery using hydraulic systems.
- **Oil Rigs** - Monitoring ballast tanks levels and hydraulic pressure on jack-up drilling rigs.
  Monitoring pressure on platform flowlines.
  Monitoring pressure on additive metering pumps.
  Monitoring pressure on sub-sea injection valves / well cleancuts.
- **Refrigeration** - Monitoring compressor pressure of both low and high pressure sides.
- **Heavy Industry** - Modern industrial gas turbines use pressure transmitters for control and automatic start-up.
- **Electrical Industry** - Monitoring of steam pressures and distribution pressures within the generating station.
  Oil and nitrogen gas cooled systems are used on high voltage three phase cables. Local and telemetry monitoring of the coolant pressures are often required.

Features

- Accuracy to better than 0.5%FS (including linearity and repeatability).
- Transducer rated at 50 million cycles.
- Metalwork made of Type 316 Stainless Steel.
- Protected against reverse voltage and overvoltage.
- Protected against noise on the supply line.
- Wide supply range, 8 to 36V DC - allows a wide range of load resistance.
- Transducer is temperature compensated by means of laser-trimmed resistors.
- Operating temperature range from 0°C to +85°C.

Description of Operation

The **PTx** series are a range of precision 2-wire pressure transmitters.
These units are factory calibrated to deliver an output of 4mA at 0 pressure and 20mA at full scale.
If necessary, the units can be calibrated in the field. Pressure Ranges are from vacuum (-1 Bar) to 600 Bar.

Description of Controls

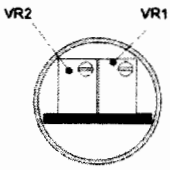

Connect as shown below and carefully remove the electrical connector, exposing the controls.

VR1: Set pressure to 0 Bar. Adjust for a reading of 4mA. Turning the control counterclockwise increases the reading and clockwise reduces the reading.

VR2: Set pressure to Full Scale. Adjust for a reading of 20mA. Turning the control counterclockwise reduces the reading and clockwise increases the reading.

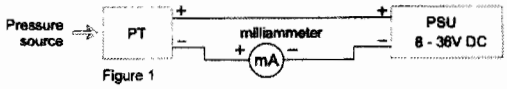

Figure 1

Note:
Precision of calibration is determined by the accuracy of the pressure source and the accuracy of the millammeter.

Rototherm
instrumentation and control

PTx Series Pressure Transmitters

Specifications

Output	4 to 20 mA
Excitation	8 to 36V DC
Accuracy	<0.5% FS
Compensated Temp. Range	0° to 85°C
Temperature error zero	<-0.02% FS / K
Temperature error span	<-0.01% FS / K (0 to 70°C)
Ingress Protection	IP65
Burst Pressure	2.5 x FS (except where indicated)

Ranges (Bar)

-1	1.6	2.5	4	6	
10	16	25	40	60	
100 (175)	160 (280)	250 (400)	400 (700)	600 (1050)	( ) = Burst Pressure

Wiring Connections

1 Red	+ Us
2 Black	- Vs
⏚ Yellow	GND

Dimensions

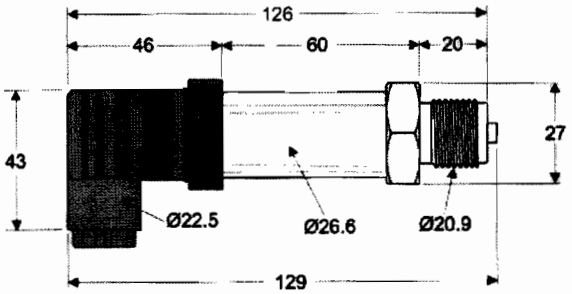

NOTE: All measurements in mm

BS En ISO9001 2000
Certificate No FM11958

British Rototherm Co. Ltd.
Kenfig Industrial Estate, Margam,
Port Talbot, SA13 2PW
United Kingdom

Telephone : +44 (0) 1656 740 551
Facsimile : +44 (0) 1656 745 915
E-Mail : sales@rototherm.co.uk
Web Site : www.rototherm.co.uk

Rototherm
instrumentation and control

ANNEXURE H **Temperature controller**

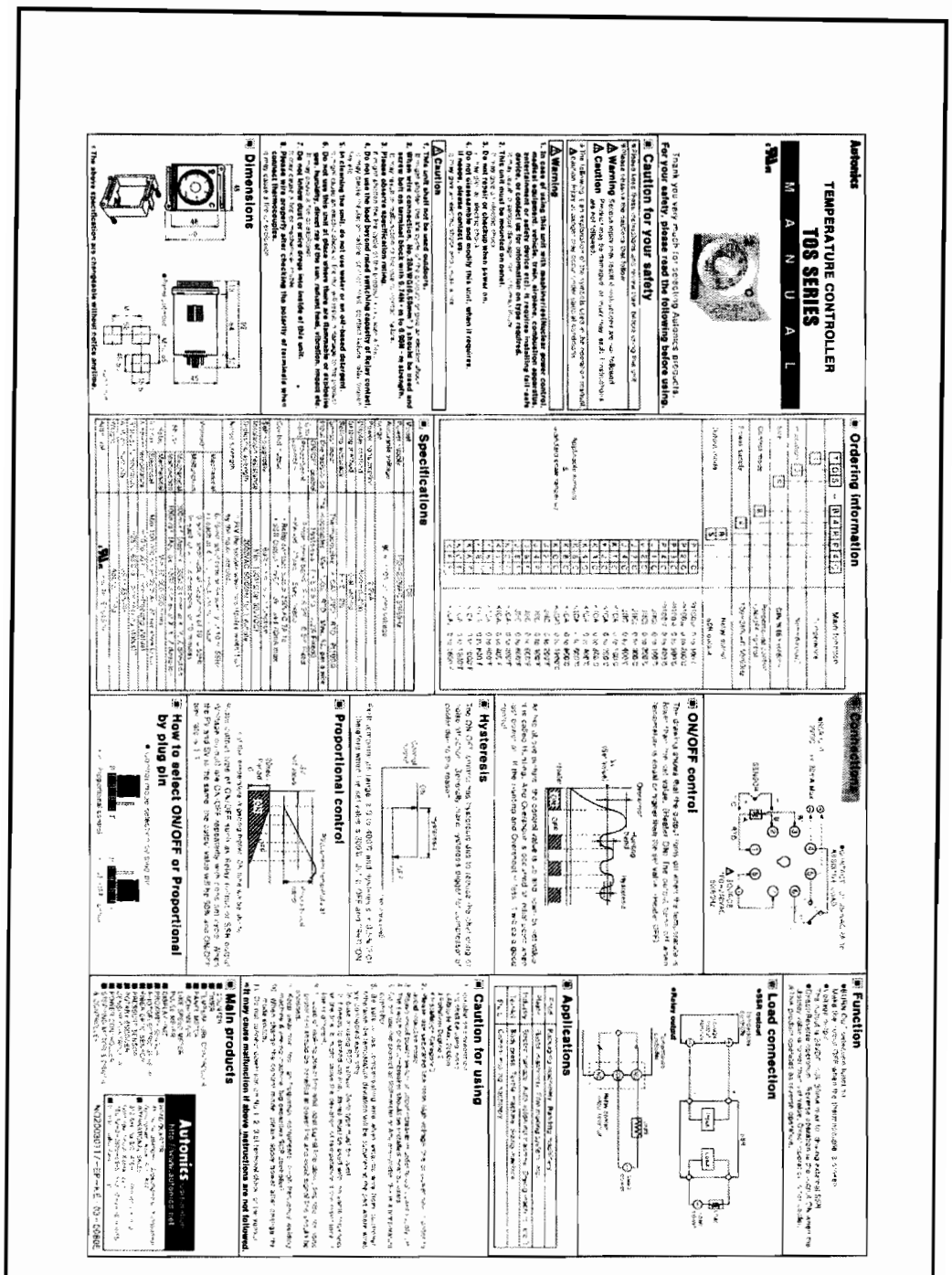

Autonics

TEMPERATURE CONTROLLER

TOS SERIES

M A N U A L

Caution for your safety

Ordering information

Specifications

Dimensions

Connections

Function

Load connection

ON/OFF control

Hysteresis

Proportional control

How to select ON/OFF or Proportional by plug pin

Applications

Caution for using

Main products